

CRANFIELD UNIVERSITY

EWA MOCZKO

NEW APPROACH IN MULTIPURPOSE OPTICAL DIAGNOSTICS:
FLUORESCENCE BASED ASSAY FOR SIMULTANEOUS
DETERMINATION OF PHYSICOCHEMICAL PARAMETERS

CRANFIELD HEALTH

PhD THESIS

CRANFIELD UNIVERSITY

CRANFIELD HEALTH

PhD THESIS

ACADEMIC YEAR 2009-2010

EWA MOCZKO

NEW APPROACH IN MULTIPURPOSE OPTICAL DIAGNOSTICS:
FLUORESCENCE BASED ASSAY FOR SIMULTANEOUS
DETERMINATION OF PHYSICOCHEMICAL PARAMETERS

Supervisor: Dr Igor V. Meglinski, Prof. S. Piletsky

September 2009

This thesis is submitted in partial fulfilment of the requirements for the degree of
Doctor of Philosophy

Abstract

The development of sensors assays for comprehensive characterisation of biological samples and effective minimal-invasive diagnostics is highly prioritised. Last decade this research area has been actively developing due to possibility of simultaneous, real-time, *in vivo* detection and monitoring of diverse physicochemical parameters and analytes.

The new approach which has been introduced in this thesis was to develop and examine an optical diagnostic assay consisting of a mixture of environmental-sensitive fluorescent dyes. The operating principle of the system has been inspired by electronic nose and tongue devices which combine nonspecific (or semispecific) sensing elements and chemometric techniques for multivariate data analysis. The performance of the optical assay was based on the analysis of the spectrum of selected dyes with discreet reading of their emission maxima. The variations in peaks intensities caused by environmental changes provided distinctive fluorescence patterns, which could be handled similar to the signals collected from nose/tongue devices.

The analytical capability of the assay was engendered by changes in fluorescence signal of the dye mixture in response to changes in pH, temperature, ionic strength and the presence of oxygen. Further findings have also proved the ability of optical assay to estimate development phases and to discriminate between different strains of growing cell cultures as well as identify various gastrointestinal diseases in human.

This novel fluorescence-based diagnostic tool offers a promising alternative to electrochemical systems providing high sensitive measurements with broad dynamic range, easy, inexpensive measurements and the possibility of remote sensing and extreme assay miniaturisation. Additionally it does not require reference signal.

This new approach can impact on a number of applications such as routine minimal-invasive diagnostics for medical samples, biomedical analysis, pharmaceutical or cosmetic research, quality control and process monitoring of food or environmental samples.

Acknowledgements

I would like to express my considerable gratitude to all the people who helped me throughout the time working on this thesis.

I am sincerely grateful especially to my both supervisors Prof. Sergey Piletsky and Dr Igor Meglinski for giving me the opportunity to pursue the project, benefit from their criticism, guidance and constant support.

My special thanks go also to Dr Conrad Bessant and Dr Michael Cauchi whose expertise in Bioinformatics contributed significantly to the performance of my research experience.

I would also like acknowledge my appreciation to the institutional support provided by the Cranfield University, which includes the generous Vice- Chancellor Trans-School/Campus Initiative Award.

And last but never the least warm thanks and a lot of hugs to everyone from my family, especially to my mum for her great love, encouragement throughout my studies, listening and understanding me like no one else.

Table of content

Abstract.....	i
Acknowledgements	ii
Table of content.....	iii
List of figures	vii
List of tables	xiii
Abbreviations	xv
1. Motivation and research objectives	1
1.1 Motivation of the study	1
1.2 State of art in multisensing technology	6
1.2.1 Sensor arrays	6
1.2.2 Electronic nose system	8
1.2.3 Electronic tongue system.....	10
1.2.4 Optical multisensing approach	12
1.2.4.1 Fluorescence-based assay.....	14
1.2.5 Multivariate approach - chemometrics	18
1.2.5.1 Pattern recognition: Principal Component Analysis (PCA).....	19
1.2.5.2 Multivariate calibration: Artificial Neural Network (ANN).....	21
1.3 Analytical characterisation of samples	24
1.3.1 pH	24
1.3.2 Dissolved oxygen	25
1.3.3 Temperature.....	25
1.3.4 Buffer composition.....	26

1.4	Thesis statement	27
1.5	Aims of the research	27
2.	First objective: selection of commercially available fluorescent dyes	30
2.1	Introduction	30
2.2	Selection criteria for single fluorescent dyes.....	31
2.3	Results and Discussion	32
2.3.1	pH sensitive fluorescent dyes	34
2.3.2	Temperature sensitive fluorescent dyes.....	40
2.3.3	Oxygen sensitive fluorescent dyes	43
2.3.4	Glucose sensitive fluorescent dyes	47
2.4	Conclusions	51
3.	Second objective: optimisation of fluorescent dye mixtures	52
3.1	Introduction	52
3.2	Selection criteria for a mixture of fluorescent dyes.....	52
3.3	Experimental section	53
3.3.1	Chemicals	53
3.3.2	Sample preparation	53
3.3.3	Fluorescence measurements	54
3.3.4	Three-dimensional data display.....	55
3.4	Results and Discussion	56
3.4.1	Choice of fluorescence dyes	56
3.4.2	Excitation/emission spectra of selected fluorescent dyes.....	58
3.4.3	Hypothetical mixtures of environmentally sensitive fluorescent dyes... 64	
3.4.4	Experimental examination of fluorescence dye mixtures.....	71
3.5	Conclusions	73

4.	Third objective: investigation of analytical capability of suitable optical assay	74
4.1	Introduction	74
4.2	Experimental section	75
4.2.1	Composition of fluorescent dye mixture	75
4.2.2	Buffer solutions	75
4.2.3	Instrumentation	76
4.2.4	Data evaluation	77
4.3	Results and Discussion	78
4.3.1	Dyes assay characterisation	78
4.3.2	Investigation of analytical capability of the optical assay engendered by changes of single parameter	79
4.3.3	Investigation of analytical capability of the optical assay engendered by changes of several parameters.....	86
4.4	Conclusion	100
5.	Fourth objective: testing optical assay with biological samples	101
5.1	Introduction	101
5.2	Identification of growing phases of cell cultures.....	102
5.2.1	Experimental part	102
5.2.2	Results and discussion	104
5.3	Discrimination between cell strains using mixture of fluorescent dyes	108
5.3.1	Experimental part	108
5.3.2	Results and discussion	110
5.4	Recognition of various gastrointestinal diseases in human.....	111
5.4.1	Experimental part	112
5.4.2	Results and Discussion	113
5.5	Conclusions	115

6. Overall discussion and conclusions	117
6.1 Dyes selection.....	117
6.2 Quantitative and qualitative analysis.....	118
6.3 Suggestions and future work	121
7. References.....	124
Appendix A: Matlab pseudo-codes	146
Appendix B: Code of practice and content forms	149
Appendix C: Human skin properties	163
Appendix D: List of publications and awards	171

List of figures

Figure 1.1: Shift towards different causes of a number of human deaths worldwide.....	2
Figure 1.2: Schematic illustration of multispot optical dual sensor assay used to measure CO ₂ and O ₂	15
Figure 1.3: The illustration of PCA performance when the original high-dimensional data space (e.g. three dimensions) is projected onto a two dimension principal component space that maintains the largest variance in the data	19
Figure 1.4: Graphical illustration of PCA model	20
Figure 1.5: Schematic illustration of a single neuron: biological neuron (A), artificial neuron (B).....	22
Figure 1.6: Schematic representation of fully connected nodes layers.....	23
Figure 1.7: Schematic representation of sensing systems: human olfactory system (A), electronic analogue (B) and our optic analogue (C).....	29
Figure 3.1: The spectrofluorometer capable of acquiring three-dimensional excitation–emission matrix (EEM) fluorescence spectra.....	54
Figure 3.2: Schematic illustration of three-dimensional spectrofluorometry with CCD detection	55
Figure 3.3: Three-dimensional colour mapped surface diagram of FL (0.004 μM) in 50 mM PB buffer (pH 7.4).	58
Figure 3.4: Three-dimensional colour mapped surface diagram of HPTS (0.03 μM) in 50 mM PB buffer (pH 7.4)	58
Figure 3.5: Three-dimensional colour mapped surface diagram of OG514 (0.006 μM) in 50 mM PB buffer (pH 7.4)	59

Figure 3.6: Three-dimensional colour mapped surface diagram of OG488 (0.01 μM) in 50 mM PB buffer (pH 7.4)	59
Figure 3.7: Three-dimensional colour mapped surface diagram of TAMRA (0.02 μM) in 50 mM PB buffer (pH 7.4)	60
Figure 3.8: Three-dimensional colour mapped surface diagram of FITC (0.02 μM) in 50 mM PB buffer (pH 7.4)	60
Figure 3.9: Three-dimensional colour mapped surface diagram of R101 (0.02 μM) in 50 mM PB buffer (pH 7.4)	61
Figure 3.10: Three-dimensional colour mapped surface diagram of RB (0.02 μM) in 50 mM PB buffer (pH 7.4)	61
Figure 3.11: Three-dimensional colour mapped surface diagram of RuBpy (2.8 μM) in 50 mM PB buffer (pH 7.4)	62
Figure 3.12: Three-dimensional colour mapped surface diagram of THA (2 μM) in 50 mM PB buffer (pH 7.4)	62
Figure 3.13.1: Three-dimensional colour mapped surface diagrams (right) and colour filled contour diagrams (left): HPTS (A), mixture of HPTS and FITC (B). Measurements of single dyes were performed in 50 mM PB buffer at pH 7.4.....	65
Figure 3.13.2: Three-dimensional colour mapped surface diagrams (right) and colour filled contour diagrams (left): mixture of HPTS, FITC and RB (C), mixture of HPTS, FITC, RB and RuBpy (D), mixture of HPTS, FITC, RB, RuBpy and THA (E). Measurements of single dyes were performed in 50 mM PBS buffer at pH 7.4.....	66
Figure 3.14.1: Three-dimensional colour mapped surface diagrams (right) and colour filled contour diagrams (left): HPTS (A), mixture of HPTS and OG514 (B), mixture of HPTS, OG514 and RB (C). Measurements of single dyes were performed in 50 mM PB buffer at pH 7.4.....	67

Figure 3.14.2: Three-dimensional colour mapped surface diagrams (right) and colour filled contour diagrams (left): mixture of HPTS, OG514, RB and RuBpy (D), mixture of HPTS, OG514, RB, RuBpy and THA (E). Measurements of single dyes were performed in 50 mM PBS buffer at pH 7.4..... 68

Figure 3.15.1: Three-dimensional colour mapped surface diagrams (right) and colour filled contour diagrams (left): HPTS (A), mixture of HPTS and FL (B), mixture of HPTS, FL and RB (C). Measurements of single dyes were performed in 50 mM PB buffer at pH 7.4..... 69

Figure 3.15.2: Three-dimensional colour mapped surface diagrams (right) and colour filled contour diagrams (left): mixture of HPTS, FL, RB and RuBpy (D), mixture of HPTS, FL, RB, RuBpy and THA (E). Measurements of single dyes were performed in 50 mM PBS buffer at pH 7.4..... 70

Figure 3.16: Three-dimensional colour mapped surface diagrams (right) and colour filled contour diagrams (left): mixture of HPTS, FITC, RB, RuBpy and THA. Measurements were performed in 50 mM PBS buffer at pH 7.4..... 71

Figure 3.17: Three-dimensional colour mapped surface diagrams (right) and colour filled contour diagrams (left): mixture of HPTS, OG514, RB, RuBpy and THA. Measurements were performed in 50 mM PBS buffer at pH 7.4..... 71

Figure 3.18: Three-dimensional colour mapped surface diagrams (right) and colour filled contour diagrams (left): mixture of HPTS, FL, RB, RuBpy and THA. Measurements were performed in 50 mM PBS buffer at pH 7.4..... 72

Figure 4.1: Cuvettes containing solutions of five selected fluorescent dyes and their mixture: HPTS (A), RB (B), OG514 (C), RuBpy (D), THA (E) and mixture of five selected dyes (F)..... 75

Figure 4.2: Three-dimensional colour mapped surface diagram of 5 fluorescent dyes: Dye 1 is HPTS, Dye 2 is OG514, Dye 3 is RB, Dye 4 is RuBpy, Dye 5 is THA. Measurements were performed in 3 ml of 50 mM PB buffer at pH 7.5..... 78

Figure 4.3.1: Three-dimensional colour mapped surface diagrams (left) and colour filled contour diagrams of the fluorescence signal of dyes mixture at pH 9 (A), pH 8 (B) and pH 7 (C) in 50 mM borate buffer (pH 9.0) and phosphate buffer (pH 8.0 and pH 7.0).....	80
Figure 6.3.2: Three-dimensional colour mapped surface diagrams (left) and colour filled contour diagrams of the fluorescence signal of dyes mixture at pH 6.0 (D), pH 5.0 (E) and pH 4.0 (F) in 50 mM phosphate buffer and acetate buffer	81
Figure 4.4: Change in fluorescence intensity of dyes mixture as a function of pH. Dye 1 is HPTS, Dye 2 is OG514, Dye 3 is RB, Dye 4 is RuBpy, Dye 5 is THA. Measurements were performed in 50 mM acetate (pH 4.0-5.0), phosphate (pH-5.0-8.0) and borate (pH 9.0) buffers	82
Figure 6.5: Change in fluorescence intensity of dyes mixture as a function of temperature. Dye 1 is HPTS, Dye 2 is OG514, Dye 3 is RB, Dye 4 is RuBpy, Dye 5 is THA. Measurements were performed in 50 mM phosphate buffer at pH 7.5.....	83
Figure 6.6: Change in fluorescence intensity of dyes mixture as a function of buffer concentration. Dye 1 is HPTS, Dye 2 is OG514, Dye 3 is RB, Dye 4 is RuBpy, Dye 5 is THA. Measurements were performed in 50 mM phosphate buffer at pH 7.5.....	84
Figure 4.7: Correlation between actual (measured) and determined by ANN values of pH (A), temperature (B)	86
Figure 4.8.1: The effect of momentum on ANN learning in the estimation of pH.....	93
Figure 4.8.2: The effect of learning rate on ANN learning in the estimation of pH.....	93
Figure 4.9.1: The effect of momentum on ANN learning in the estimation of temperature	94
Figure 4.9.2: The effect of momentum on ANN learning in the estimation of temperature	94

Figure 4.10.1: The effect of momentum on ANN learning in the estimation of DO concentration	95
Figure 4.10.2: The effect of momentum on ANN learning in the estimation of DO concentration	96
Figure 4.11.1: The effect of momentum on ANN learning in the estimation of PB concentration	97
Figure 4.11.2: The effect of momentum on ANN learning in the estimation of PB concentration	97
Figure 4.9: Correlation between actual (measured) and determined by ANN values of pH (A), temperature (B), DO concentration (C) and PB concentration (D)	99
Figure 5.1: <i>E. coli</i> growing on the nutrient agar plate.....	103
Figure 5.2: Growth curve of <i>E. coli</i> culture showing exponential and stationary phase of bacteria growth.....	104
Figure 5.3: Changes in fluorescence intensity of five dyes of the mixture vs. time of bacteria growth. Dye 1 is HPTS, Dye 2 is OG514, Dye 3 is RB, Dye 4 is RuBpy, Dye 5 is THA. Measurements were performed in bacterial supernatant obtained from growing <i>E.coli</i>	105
Figure 5.4: Control measurements of fluorescence intensity of the mixture of five dyes in LB broth. Dye 1 is HPTS, Dye 2 is OG514, Dye 3 is RB, Dye 4 is RuBpy, Dye 5 is THA	106
Figure 5.5: Correlation between actual (measured) and determined by ANN time of growth of bacteria culture.....	107
Figure 5.6: White yeast (left) and pink yeast (right) growing on nutrient agar plate..	109
Figure 5.7: PCA score plot showing distinction between two different strains of yeasts	110

Figure 5.8: Ability of the ANN to discriminate the three diseases from the healthy controls: % Overall means the overall success of discrimination; % Specificity means the success of distinguishing the healthy controls; % Sensitivity means the success of distinguishing the disease.	114
Figure C.1: Three-dimensional, schematic drawing of the skin structure; thin hairy skin of the forearm	164
Figure C.2: Layer structure of the epidermis	164
Figure C.3: Structure of the dermis: a) layers of the dermis, b) the papillary layer, made of loose tissue, forms dermal papillae, c) the reticular layer, dense irregular connective tissue	165
Figure C.4: Structure of the hypodermis.....	166
Figure C.5: Schematic drawing of optical pathway in the skin	167

List of tables

Table 1.1: Classification of chemical sensors based on the type of transducer.....	8
Table 1.2: Advantages and disadvantages of optical sensors.....	13
Table 2.1: List of pH sensitive fluorescent dyes. They are listed by increasing emission wavelengths	34
Table 2.2: List of temperature sensitive fluorescent dyes. They are listed by increasing emission wavelengths	40
Table 2.3: List of oxygen sensitive fluorescent dyes. They are listed by increasing emission wavelength	43
Table 2.4: List of glucose fluorescent dyes. They are listed by increasing emission wavelengths	47
Table 3.1: List of excitation and emission maxima of selected fluorescent dyes.....	63
Table 4.1: List of fluorescent dyes selected for the assay	74
Table 4.2: Effect of the number of neurons in the hidden layer and training algorithm on ANN performance for pH.....	88
Table 4.3: Effect of the number of neurons in the hidden layer and training algorithm on ANN performance for temperature	89
Table 4.4: Effect of the number of neurons in the hidden layer and training algorithm on ANN performance for DO.....	90
Table 4.5: Effect of the number of neurons in the hidden layer and training algorithm on ANN performance for buffer concentration	90
Table C.1: Mean values for full epidermal thickness.....	165

Table C.2: Main chromophores found in human skin.....	167
Table C.3: The relationship between depth of penetration of incident light and wavelength in the case of caucasian skin	168

Abbreviations

ANN	Artificial neural network
BAW	Bulk acoustic waves
CD	Crohn's disease
CP	Conductometric polymer
COP	Code of practice
DNA	Deoxyribonucleic acid
DO	Dissolved oxygen
EEM	Excitation and emission matrix
FITC	Fluorescein isothiocyanate
FL	Fluorescein
HPTS	Hydroxypyrene-1,3,6-trisulfonic acid trisodium salt
LR	Learning rate
IBS	Irritable bowel syndrome
MU	Momentum
MOS	Metal-oxide semiconductors
MOSFET	Metal-oxide silicon field-effect transistors
NIR	Near-infrared
OG488	Oregon green 488
OG514	Oregon green 514
PB	Phosphate buffer
PC	Principal components
PCA	Principal component analysis

PHC	Primary health care
R6G	Rhodamine 6G
R101	Rhodamine 101
RB	Rhodamine B
RMSE	Root means square error
ROS	Reactive oxygen species
RuBpy	Tris(2,2'-bipyridine) dichlororuthenium(II) hexahydrate
SAW	Surface acoustic waves
TAMRA	5(6)-carboxytetramethylrhodamine
UC	Ulcerative colitis
VIS	Visible
WHO	World Health Organisation

1. Motivation and research objectives

1.1 Motivation of the study

Each year the World Health Organisation (WHO) provides a detailed report on major concerns of the international public health, performance of the research and strategic approaches to improve health and health quality. The recent report issued in 2008 covers the information on current health facilities and highlights the importance of increasing needs and demands to renew primary health care (PHC) systems (WHO, 2008). It emphasises one of the key aspects for the urgent discussion which are chronic and non-communicable diseases.

Different from unintentional injuries (e.g., road-traffic accidents) and infection diseases (e.g., tuberculosis, HIV/AIDS), which has been reported the frequent cause of human deaths in low income countries during the recent past, chronic and non-communicable diseases are the major cause of deaths in middle and high income countries including The United Kingdom (The World Bank, 2009). They are long duration and often slow progression diseases, such as cardiovascular diseases, cancers or diabetes, which may result from genetic or lifestyle factors (Kotze *et al.*, 2005). The WHO data has indicated that about 75 % of the total population suffers at least one chronic condition which certainly becomes a worldwide issue. Furthermore, chronic diseases have been projected to cause the highest impact on a number of mortality over the present and coming years (see Figure 1.1) and spread across the world, irrespectively of the country income level (Abegunde *et al.*, 2007; Beaglehole *et al.*, 2008).

The global call for action highlights the essential role of researchers and modern technologies in finding an effective way to improve healthcare facilities and detection of illness before it might become critical or life threatening (Beaglehole *et al.*, 2007). This requires new developments and implementation of suitable indicators to estimate potential risk factors and their effects on health, identification of early symptoms of diseases or monitoring the progress of treatment (Danaei *et al.*; 2009; Genuis, 2008).

Additionally, the examination should be possible to perform in any environment, including natural conditions, outside the controlled hospital or laboratory environment. Advantageous would also be the simplicity and high speed of measurements and data analysis.

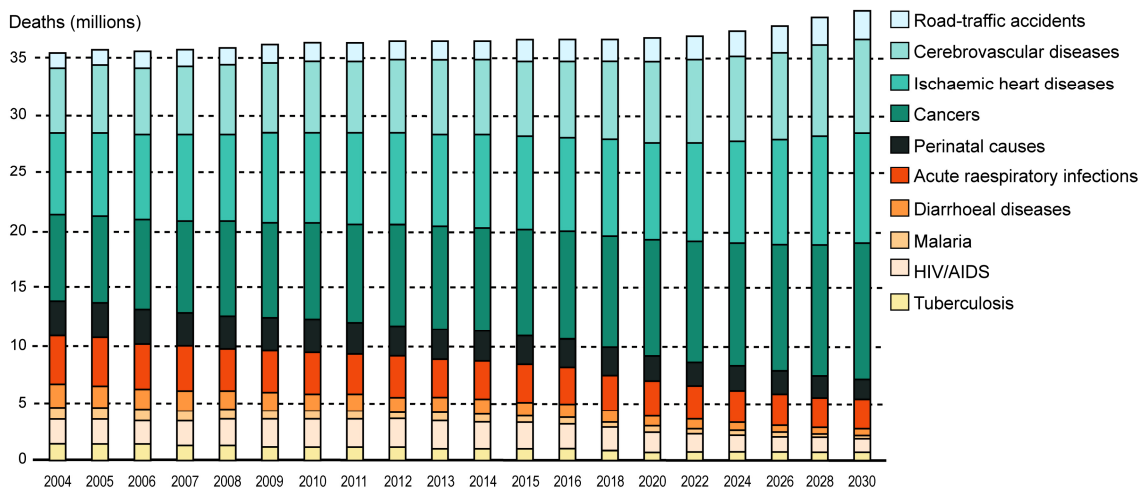


Figure 1.1: Shift towards different causes of a number of human deaths worldwide. Figure adopted from (WHO, 2008).

The ideal approach would be to develop a versatile and portable sensing device with the ability to measure simultaneously as many metabolites and parameters as possible in a single sample (LaFratta *et al.*, 2008; Palacios *et al.*, 2007; Paolesse *et al.*, 2008). The use of such an intelligent device with the capability of accurate and reliable diagnosis could help to decrease probability of harm, minimise clinical intervention, costs of medical treatment and as a consequence improve long-term public healthcare. This has found great interest in many academic and industrial sectors. Particularly medical or biochemical, for monitoring glucose concentration or biochemical reactions in patients (Castillo *et al.*, 2004; Moczko *et al.*, 2008; Rock *et al.*, 2005; Shepard *et al.*, 2005), healthcare and food industries estimating and modifying inappropriate diet (reduction of a consumption of certain substances, e.g. salt, cholesterol, sugars, caffeine (Asaria *et al.*, 2007; Ordovas *et al.*, 2008)), monitoring of blood gases and other cardiovascular parameters (Daar *et al.*, 2007; Ganter *et al.*, 2003; Perez-Guisado *et al.*, 2008), testing

quality of food and reformulation when it is high in salt, sugar or fat, controlling drinking water (Brettar *et al.*, 2008; Prüss-Üstün *et al.*, 2008; Thompson *et al.*, 2008), environmental pollutions (Hassing *et al.*, 2009; Rodriguez-Mozaz *et al.*, 2006; Rogers, 1995; Wanekaya *et al.*, 2008), or bioprocess control (Esbensen *et al.*, 2004; Rudnitskaya *et al.*, 2008).

Presently a wide number of analytical strategies for sensitive detection and monitoring of various biochemical components and physical parameters of a sample have been constantly developed. They are often combined with different techniques to generate the signal and process output data more rapidly and effectively. Distinct progress in this area is related to the approach of sensor arrays. Differing from former research and developments in sensor technology, which were focused on obtaining analytical device with the highest possible selectivity to specific analyte (Cammann *et al.*, 1991), sensor arrays have been proposed to identify multitude components in a single sample. They have revolutionised the traditional way of samples examination, usually improved by accuracy of particular sensor but always limited to real-time monitoring of only one analyte at a time, this remaining impractical for diagnostic purposes.

Further development in multisensing began with the use of diverse chemically selective single sensors with appropriate transducers for multicomponent measurements and data analysis (Collison *et al.*, 1989; Frost *et al.*, 2002). They enabled examination and provided additional information about analysed samples but often involved large amounts of reagents and sampling materials, resulting in more complicated, lengthy and costly measurements. Although such systems are able to identify several parameters, they detect and analyse each compound separately. This, however, could be optimised by measuring only a few key parameters, but clearly this proves to be impractical especially in studies of complex environmental and biological samples (Careri *et al.*, 2009). The natural environment may in fact be very demanding and it is not possible to predict an importance of the impact of all potential external conditions on the diagnosis.

Current trends toward rapid, simultaneous measurements of several metabolites and parameters in a single sample and real time have encouraged analytical researchers to

create new, more sophisticated, selective (and partially selective), versatile sensing devices for identification and quantification of multiple analytes (Codinachs *et al.*, 2008; Luong *et al.*, 2008; Seidel *et al.*, 2008). These devices combine an array of cross-sensitive chemical receptors with statistical techniques for multivariate interpretations of composite signals collected from different sensing units (Cai *et al.*, 2008; Janzen *et al.*, 2006; Lawrence *et al.*, 2002). The specificity of a device is related to recognition of response patterns that originate from the interface between components of a sample and all sensing elements. The obtained patterns are unique to particular conditions and can be considered similar to fingerprints identification. Using sensor arrays and multivariate statistical techniques for interpretation allows qualitative analysis of samples in a relatively short time (Olivieri, 2008).

This approach of multianalyte detection compared to single analyte methods or the use of selective sensors is attractive due to its lower sample consumption, higher efficiency, and shorter analysis time. The possibility of simultaneous detection and determination of several compounds in a single measurement reduces the overall cost of the assay and increases the number of potential applications. Additionally, the analytical capability of an assay may not always lie in measurements of precise analyte concentration, but rather to provide profiling of the chemical or biological processes (Bachinger *et al.*, 2000). It is of the great advantage for qualitative analysis of samples.

The majority of such multidetection systems have been developed for odour characterisation, so-called electronic noses consisting of an array of gas sensors combined with statistical techniques for multivariate interpretation of signals (Gopel, 1998; James *et al.*, 2005; Pravdova *et al.*, 2002). More recently, a similar operating principle has been applied to sensor arrays for liquid analysis, known as electronic tongues, which are used of qualitative samples analysis (Ciosek *et al.*, 2007; Gutierrez *et al.*, 2008; Gutierrez *et al.*, 2008). Although both devices are currently commercially available, they suffer from significant limitations, such as poor stability, limited selectivity, low reproducibility, demand for frequent calibration, complexity of generated information, and high fabrication costs of sensor arrays (del Valle, 2008; Pearce *et al.*, 2003; Rock *et al.*, 2008).

Lately there has been a surge of attention to optical diagnostics and has been projected to expand tremendously in the future, especially in the field of real-time detection *in vivo*. This is explained by the facts that optical techniques are often non-destructive, do not require physical contact with a sample during analysis and enable rapid response (DTI, 2006; Jokerst *et al.*, 2009; Lee *et al.*, 2007; Tanev *et al.*, 2008). They are able to provide information at the molecular level through tissues and living organs to animals or human bodies. Light can also be used as a tool for manipulating or modifying living cells and can be focused at a tiny spot, which allows precise localised and minimal invasive treatment (Duckett, 2009). By providing a more effective, cheaper and easy accessible service, biophotonics and optical diagnostic technology can have huge and crucial impact on health care facility (Pereira *et al.*, 2009).

In this thesis the development of a novel fluorescence-based assay which offers a promising alternative to electrochemical systems is described. The proposed assay benefits from numerous studies and analytical ability provided by optical chemical multisensors, particularly fluorescence-based sensors (Dickinson *et al.*, 1996; Nagl *et al.*, 2007; Wang *et al.*, 2008; Wolfbeis, 1985). Among these are high selectivity and sensitivity. Optical systems are often reversible and do not require a reference signal. They require low fabrication costs and offer rapid response, which makes them a promising tool for simultaneous real-time detection of multiple analytes and complex sample characterisation (Baleizao *et al.*, 2008; Kocincova *et al.*, 2008). Another advantage of this sensing system also lies in the possibility of extreme assay miniaturisation.

Present chapter emphasises the importance of multisensing approach, which is described in this thesis. Specific aspects of development, technical demands and improvements in multisensing technology have been described in following section (Chapter 1.2).

1.2 State of art in multisensing technology

In the last several decades, the area of research in the development of sensor arrays to detect multiple analytes has been growing intensively. They have become crucial for analytical examination and used more and more frequently for quantitative analysis of samples. While improving sensors functionality, researchers have also worked actively on their physicality to minimise their sizes.

1.2.1 Sensor arrays

Sensor arrays are an assembly of several chemical, physical or biochemical sensing elements designed for simultaneous, multitarget detection (Price, 2001) (Alegret, 2006). Although work in this area continues for many years already, there is still a lack of robust, versatile devices for multianalyte characterisation of a single sample.

Similar to conventional selective sensors, arrays should operate continuously or in repeated cycles (Gründler, 2007). The efficiency of the systems can be characterised by their reproducibility, stability, sensitivity, accuracy, response time, detection limit, miniaturisation, portability, simplicity and production costs (Diamond, 1998; Orsini *et al.*, 2005). An important feature for clinical sensors is that their operation should adhere to the policy and standards of health care. A significant attribute that distinguishes array systems from conventional sensors is that sensors merged in an array do not need to be highly selective toward given analytes. The specificity of a device is related to recognition of response patterns of all sensing elements (Srivastava *et al.*, 2006). The patterns obtained are unique to particular conditions and can be recognised similar to fingerprints identification.

The existing multisensor devices typically consist of chemical and/or physical sensors that are well established, and commonly available in a wide range of applications. Sensors can be classified depending on their two main functional units, either the receptor (recognition element), or the type of transducer for signal processing

(Cammann *et al.*, 1991; Fraden, 2003; Hulanicki *et al.*, 1991). Based on receptors and different mechanisms of an operation, sensors are organised into several groups:

- PHYSICAL, applied to measure physical variables of the system. These sensors do not require a chemical reaction to take place, but use physical effects in the recognition and transduction processes (e.g. optical, thermal, motion sensors);
- CHEMICAL, utilise chemical reactions for identification and quantification of specific analytes or monitoring various chemical events (e.g. electrochemical, optical, electrical sensors);
- BIOCHEMICAL, also called biosensors. They may be included in a group of chemical sensors that employ particular classes of biological or biochemical recognition/transduction processes (e.g. immunosensors, microbial, enzyme sensors).

Chemical sensors that depend on the various operating principles of transducers are listed in Table 1.1 (Collings *et al.*, 1997; Fraden, 2003).

The most frequently used sensors for physicochemical and biochemical analysis are electrochemical sensors (Janata *et al.*, 1994; Wang *et al.*, 2008). They have been employed in a wide variety of analytical applications including well-known electronic nose and tongue systems (Gründler, 2007). Both devices are currently commercially available devices, which are based on chemical multicomponent characterisations of gas and liquid samples. They combine an array of various non-specific chemical sensors with subsequent chemiometric techniques in order to simulate human olfactory and taste perceptions (Vlasov *et al.*, 1997). These two systems are chemical in nature and therefore it is possible to create their artificial analogues.

Table 1.1: Classification of chemical sensors based on the type of transducer.

Sensor type	Detection principle or property measured	Operating mechanism
Optical	Fluorescence Absorbance Reflectance Light scattering Luminance Refractive index (surface Plasmon resonance, SPR) Optothermal effect	Transformation of changes of electromagnetic radiation caused by the interaction between the analyte and receptor
Electrochemical	Voltametry Amperometry Potentiometry Impedometry Conductometry	Transformation of the effect of electrochemical interaction of the analyte with sensing surface of the electrode (chemical reaction or charge transport modulated by the reaction)
Electrical	Surface conductivity Electrolyte conductivity Capacitance	Transformation of changes of electrical properties caused by the interaction of the analyte
Thermal	Calorimetry Thermistors Pyroelectric Thermopile	Transformation of changes of internal energy of a system that involve the analyte (heat effects of specific chemical reaction or adsorption)
Mass Sensitive	Piezoelectric Surface acoustic wave (SAW) Bulk acoustic wave (BAW)	Transformation of the mass changes at a specially modified surface. The mass changes are caused by adsorption of the analyte
Magnetic	Paramagnetism	Transformation of the change of paramagnetic properties of a gas being analysed

1.2.2 Electronic nose system

The electronic nose is an artificial sensing system based on the same principles as human olfaction. A schematic illustration of the biological mechanism, followed by its electronic analogue is shown in Figure 1.7. Figure 1.7-A indicates the mechanism of the human olfactory system which is composed of three main parts: olfactory receptor, responsible for the detection of odours; olfactory bulb that transports the detected signal from the nose to the brain; and olfactory cortex, where the information is processed.

This mechanism and the main stages of the human olfactory system are possible to simulate within an artificial olfactory device - an electronic nose (Figure 1.7-B) (Haddad *et al.*, 2008). The idea behind it is that the sensor array consists of different sensor types, equivalent to the olfactory receptor, with high sensitivity to a variety of odours. This is followed by complex signal collection and data processing using adequate pattern recognition technique, such as artificial neural network (ANN) (Scott *et al.*, 2006).

Electronic noses may utilise different types of chemical gas sensors. Typically these are conductometric sensors (metal-oxide semiconductors (MOS), and conductometric polymers (CPs)), potentiometric sensors (metal-oxide silicon field-effect transistors (MOSFETs)), mass sensitive surface acoustic waves (SAW) or bulk acoustic waves (BAW) coated with different odour sensitive polymer membranes (Fernandes *et al.*, 2008; Garcia-Gonzalez *et al.*, 2002). These sensors, when combined with signal processing systems for odour classification and identification, have been frequently used for food processing (e.g., testing for food freshness) (Casalinuovo *et al.*, 2006; Pioggia *et al.*, 2007), biomedical applications (breath analysis, volatile compound analysis of body fluids) (D'Amico *et al.*, 2008; Penn *et al.*, 2007), cosmetics evaluation, atmospheric or military applications (detection of pollutants, explosives, fuel dumps) (Distante *et al.*, 2009; Srivastava *et al.*, 2006).

In recent years, one of the most studied and extensively used components of electrochemical gas sensors and their arrays are CPs deposited on the sensor surface (Bai *et al.*, 2007; de Leon *et al.*, 2008; Rahman *et al.*, 2008). Some of these sensors have been employed in the development and optimisation of commercially available devices. CPs and their composites display a number of unique conducting, optical, mechanical, electric and chemical features when they are in contact with various gases, organic molecules, inorganic ions, and changes in pH, which means that they are very useful in a variety of applications (Rajesh *et al.*, 2009). However, despite a number of advantages (Lange *et al.*, 2008; Rahman *et al.*, 2008), polymers are often highly sensitive to even small variations in procedure during synthesis and treatment, which is crucial for

reproducibility of sensor manufacturing and commercialisation. They can also be very sensitive to thermal and environmental changes affecting their stability during storage.

Additionally, the efficiency of devices used for gas detection is also decreased by humidity, temperature and base line drift that can result in unstable sensor response over time (Pan *et al.*, 2007; Turner *et al.*, 2007). Some major challenges related to the utilisation of these devices also include improvements involving their simplicity, long term stability, recalibration, and successful operation for real-time measurements in natural environments (outside controlled laboratory conditions) (Chang *et al.*, 2008; Lieberzeit *et al.*, 2009).

1.2.3 Electronic tongue system

An electronic tongue or taste sensor, combines an array of chemical sensors and data processing system for operation in liquid samples. This sensing system has been used for discrimination of different taste groups in a manner similar to biological taste perception. It has been used in the analysis of food products (sauces, soups) or drinks (water, wines, milk). The analysis is based on the taste being determined by five elementary flavour qualities and their combinations: sourness, saltiness, sweetness, bitterness and umami. The first, sourness, is determined by the presence of hydrogen ions of HCl, acetic acid, citric acid, etc. Saltiness depends on the presence of NaCl, bitterness - quinine, caffeine and MgCl, sweetness - sucrose, glucose, aspartame, etc. The last, umami is a Japanese term referring to deliciousness and implies for e.g., monosodium glutamate (MSG) contained mainly in seaweeds, disodium inosinate (IMP) in meat and fish and disodium guanylate (GMP) in mushrooms (Toko, 1998). More recently, electronic systems (so-called taste sensors) have been used as general analytical instruments, based on the principle of taste recognition (Ciosek *et al.*, 2008; Citterio *et al.*, 2008; Lopez-Feria *et al.*, 2008).

Due to well known operating principles of electrochemical techniques, the majority of electronic tongue systems rely on arrays of electrochemical sensors of a common type, in particular potentiometry and voltammetry (Ciosek *et al.*, 2007; Winquist, 2008), with

different polymeric membranes and electrode coating. Developments of novel sensors are focused on the utilisation of various polymeric membranes, which leads to a number of possible modifications of working electrodes. This can result in greater sensor selectivity and sensitivity towards different species (Pioggia *et al.*, 2008) (Ciosek *et al.*, 2007; Citterio *et al.*, 2008).

The electronic tongue system in combination with odour sensors has also been used for gaseous analytes. The ability to integrate both liquid and gaseous sensors, and also the possibility of using a combination of different sensors (not only those chemical in nature) is an essential advantage of these devices and has led to an improvement in the performance of artificial sensing.

Despite the wide variety of chemical sensors that can be used for electronic tongue array construction and the possibility of tuning the mode of device operation to the desired application (multicomponent analysis, discrimination, classification, recognition, estimation), the number of commercially available systems is still low (Krantz-Rulcker *et al.*, 2001; Pioggia *et al.*, 2007; Twomey *et al.*, 2006). Major technical challenges facing electronic tongue manufacturing are data handling (massive database), system optimisation towards a specific given application, and requirements of the system such as frequent recalibration. Common problems are also reproducibility and signal drift of sensors (Gutierrez *et al.*, 2008).

The electronic tongue can be compared to the electronic nose, with regards to them both via a similar mechanism. They both combine an array of non selective (or partially selective) sensors with multivariate data processing using pattern recognition. However, electronic noses are still better developed for analyte recognition, samples classification, or multicomponent quantitative analysis (Chang *et al.*, 2008; Gutierrez *et al.*, 2008; Vlasov *et al.*, 2008) taste sensors enable analysis of liquid samples or solids dissolved in liquids. Despite a number of limitations relating to artificial systems, electronic nose and tongue systems offer significant advantages over the natural receptors of taste and smell, including better selectivity, objectivity, and the possibility of detecting some substances not detectable by natural systems. Furthermore, electronic systems do not

become tired, overworked or infected and their performance is not affected by previous valuations. Using electronic devices it is also possible to analyse toxic or uneatable samples.

Artificial systems are very promising for the future but there are still a number of applications where their use is insufficient and can often cause problems. This includes commonly employed electrochemical sensors. They are well-established and popular but not always easy to operate, which is important, e.g. during routine handling. Additionally, they are invasive, limited to single-point valuation and are unable to analyse analytes distribution. The development of an analytical tool that enables detection or differentiation among a wide range of analytes and microorganisms is urgently required, especially for testing real food or medical samples. The aim is to detect and quantify analytes and physical parameters in real-time, at low cost, with high reproducibility, specificity and sensitivity. Ideally the device should be prompt for automatisisation, allowing routine handling and minimising the risk of contamination and human error during measurements (Ahmed *et al.*, 2008). These requirements could possibly be met by using mentioned alternative system based on optical sensing.

1.2.4 Optical multisensing approach

While the concept of multivariate analysis as an approach for examination of sensor array data and detection of analytes in complex samples has been explored mainly for electrochemical, electrical or piezoelectric sensors (Fernandes *et al.*, 2008; Rudnitskaya *et al.*, 2008; Steen *et al.*, 2008), only limited efforts have been put into the development of equivalent optical sensors.

Optical methods when compared to electrochemical techniques, represent one of the oldest and most widespread methods for chemical, biochemical or physical examination (Mendelson, 2000). Optical sensing systems are based on light–matter interactions in order to obtain required information.

Currently, optical sensing and imaging techniques have experienced increased attention, especially in the field of *in vivo* measurements, since they do not require physical contact with a sample during analysis. Other specific advantages compared to electrochemical sensors are included in Table 1.2, along with a few less essential limitations.

Table 1.2: Advantages and disadvantages of optical sensors.

Advantages	Disadvantages
<ul style="list-style-type: none"> - do not require an additional reference signal as electrodes do - offer greater flexibility with design - enable more efficient and easier remote sensing (long-distance transition of light) - provide real-time analysis of complex samples - enable monitoring or probing of a wide range of analytes and parameters (chemical, biochemical, physical) - do not consume an analyte (non destructive) - offer lower cost and time of measurements - measurements are less invasive and harmless for the system, far less so than electrochemical devices - transmit more information than an electrical signal - do not suffer from electrical interferences - allow possibility of wide-range temperature control, smaller temperature dependence 	<ul style="list-style-type: none"> - interference of ambient light - limited dynamic range, smaller compared to electrochemical sensors - dependence on concentration of indicator and analyte - signal dependency on ionic strength, solvent - require immobilisation for better sensitivity and selectivity - as a result smaller slope of response curve - possess limited long-term stability due to photobleaching or leaching of the indicators - higher power consumption

Optical sensing is a very attractive alternative to state-of-the-art sensing technology since they often provide simple, user friendly, real-time, continuous monitoring of analytes and environmental parameters. Different from other techniques, optical examination enables multimode measurements. It enlarges the number of output parameters including intensity, spectral shape, wavelengths, decay time, energy transfer, quenching efficiency, and polarisation providing collective information on a sample thereby simplifies and reduces cost and time of measurements. The application of available mechanisms and outputs of optical signal can be specified according to the actual requirements.

The most common optical techniques applied in sensing systems are absorption, fluorescence, reflection and light scattering (Baldini *et al.*, 2006). Recent advances in technology and development highlighted a focus on fluorescence-based methods.

1.2.4.1 Fluorescence-based assay

Among these optical techniques, fluorescence spectroscopy appears to be particularly promising for chemical and biochemical sensing technology as it contains most of the advantages listed for optical sensors (Lakowicz *et al.*, 1999). This includes high sensitivity, ability to monitor several analytes with a single instrument at very low concentrations, and detection of real-time responses for a target. An additional advantage is versatility, possibility of system miniaturisation, speed and compared to others low cost (Basabe-Desmonts *et al.*, 2008). Fluorescence spectroscopy has become favourable especially in the areas of medical, cosmetic or biochemical science as they allow contactless sensing. This is of great advantage over other sensing methods for diagnostic and analytical proposes if the non-invasive *in-vivo* measurements (or sterile conditions) are an essential requirement (Kocincova *et al.*, 2007; Öberg, 2003). Optical assessment and data collection can be performed directly from the sample, thus a sample extraction is not necessary (Wolfbeis, 2008). Also they are not limited by area (monitoring of distribution of oxygen and pH in human skin, seawater). A further advantage is that fluorescence measurement does not consume analytes, does not require a reference signal or any physical waveguide for the light. These significant

features facilitate technical requirements and devices handling, and greatly increase the potential of fluorescence-based optical sensing from a technical point of view. Fluorescent sensors also prompt to miniaturisation (Nagl *et al.*, 2005).

Considering the possibilities of an optical multisensing approach, the strategies of using a number of optical sensing elements (biochips, micro-, nanobiosensors or probes) employed in high-density sensing arrays for multiplex screening and biochemical analysis have already been reported (Bally *et al.*, 2006; Basabe-Desmonts *et al.*, 2008; Basabe-Desmonts *et al.*, 2007; Lee *et al.*, 2008). One very attractive concept that has been described is the implementation of fluorescence-based sensor arrays, so-called multispot sensors that involve each single sensing spot to yield distinctive optical information including analytical information for chemical, biochemical or physical species in the sample (Demchenko, 2005; Nagl *et al.*, 2007; Thete *et al.*, 2009). This approach is illustrated in Figure 1.2.

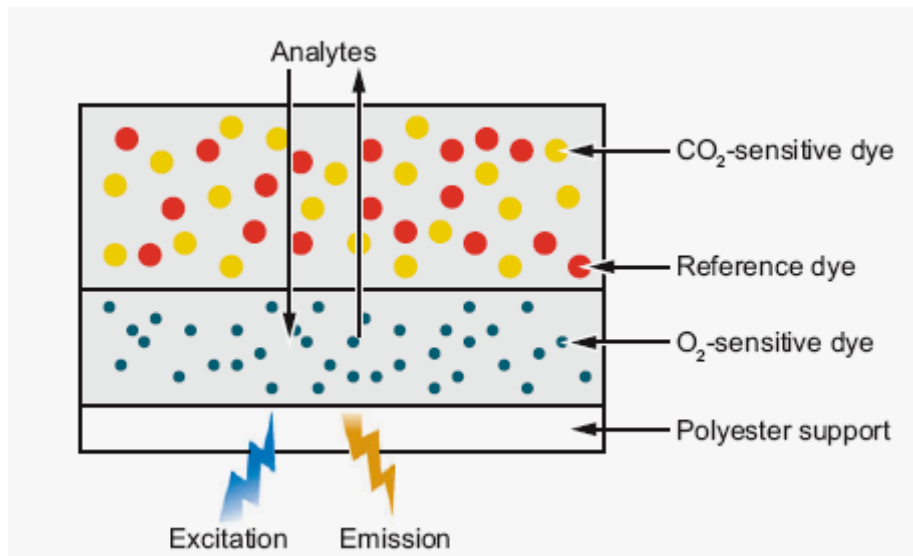


Figure 1.2: Schematic illustration of multispot optical dual sensor assay used to measure CO₂ and O₂. Figure adopted from (Bake *et al.*, 2008).

Dye indicators are deposited on the surface of the analysed sample and they are allowed to diffuse inside the sample. Excitation and emission collection are performed from the bottom. However, it gives multiplex information about the analysed media, but it does

not allow truly simultaneous measurements. These spots are separated from each other and therefore cannot measure several analytes at the same point and time.

The best solution for this limitation would be to use a single spot that consists of several fluorescence-based sensors combined together. It would minimise the size of the sensing system and enable all sensors of the array to be placed in the one, exact place in the sample allowing local and simultaneous measurements of numerous of parameters. It could also be very useful for controlling different factors that cause interferences in measurements, such as temperature, pH, humidity, etc. So far, the multisensors based on this approach were limited to the detection of only two parameters in a single measurement (Baleizao *et al.*, 2008; Borisov *et al.*, 2006; Kocincova *et al.*, 2007).

Currently, numerous studies have proven the advantages and great potential of fluorescence-based chemical multisensing. A large group of optical sensors use fluorescent dyes for the identification of different physicochemical, biochemical or biological species (Wolfbeis, 2005, 2008). Fluorescent dyes often provide high sensitivity and selectivity for the analytes of interest. Molecular information about the media is contained in their spectral behaviour (Nagl *et al.*, 2009). The relationship between spectral characteristics of a free fluorophore, and changes caused by interactions with its surroundings, can provide significant information about a sample. It makes a great tool for fast, easy monitoring of the environmental conditions.

The nature of the fluorophore spectra are usually analysed based on the fluorescence intensity, lifetime, energy distribution or anisotropy (Lakowicz, 2006; Valeur, 2001). The fluorescence intensity is related to the changes in emission of the fluorophore in response to interactions or binding with analytes. Fluorescence lifetime is defined as the time when molecules stay in its excited state before returning to the ground state (Valeur, 2001). This parameter is important because it determines the time available for fluorophores to interact with the environment. Energy distribution is analysed based on the shape or shift of fluorescence spectra and fluorescence anisotropy on the polarisation, that provides information on the size and shape of fluorescent molecules, and examines binding interactions with other species (McCarroll *et al.*, 2001).

A variety of fluorescent probes is known from the literature and is commercially available (Haugland, 1996). In addition, they are not expensive and so cost of the measurement is minimal. The principal demands on fluorescent probes are for high fluorescence quantum yields, selectivity, long-wave excitation and emission, and a high excitation coefficient at the excitation wavelength (Kemnitzner *et al.*, 2002). Further requirements are lack of toxicity, photochemical and chemical stability, and the presence of functional groups for suitable immobilisation on the rigid support without any changes in the physicochemical constant of the indicator.

Considering all these requirements, the first important step for the successful design of a fluorescent sensing scheme is the selection of the most suitable fluorescent probes for the recognition of particular target analytes (Basabe-Desmonts *et al.*, 2007). Additionally in the multisensing approach, the selected fluorescent dyes should possess various sensitivities and substantially different emission spectra so they can be combined together in order to enable the monitoring of the contribution from the individual dyes in the total fluorescent spectrum of their mixture. Such a system might offer a promising optical equivalent to electronic noses and tongues that use fluorescence spectroscopy and a mixture of environment-sensitive fluorescent dyes (where each dye of the mixture represents a different indicator). If the intensity spectrum of the suitable dyes allows discreet reading of emission maxima of all dyes, the intensity variations in response to environmental changes might provide distinctive patterns, which can then be analysed in the same way as complex signals collected by an electronic nose/tongue electrochemical or piezoelectric array. The analytical information about a sample coded in the fluorescence pattern can be decoded using multivariate data analysis by transformation of an optical system response into the actual physicochemical parameters and target analytes.

The use of a mixture of fluorescent dyes for optical sensing could have a number of advantages, including easy application, high speed and low cost of measurements. It might also resolve one of the main problems associated with electronic nose technology, wherein a sensor array has to be calibrated each time it is used. The proposed assay does not have this limitation and the mixture of fluorescent dyes can be perceived as an

analytical reagent that can be tuned for various specific analytical tasks. Since the proposed assay includes only a small spot of all dyes, it opens the possibility of extreme system miniaturisation and application to a very small volume of sample. The utilisation of a mixture of fluorescent dyes is very promising for simultaneous measurements of several physicochemical, biochemical or chemical properties of analytical species that has not been documented before.

1.2.5 Multivariate approach - chemometrics

A large number of multicomponent sensing systems consist of cross-reactive chemical non-specific sensor arrays that generate a complex pattern as a response. The outcome signal is less specific, but distinctively different for each sample. The challenge is to process the obtained patterns in order to understand the meaning of the outcomes. Therefore, the success of sensing technology depends not only on accurate analytical measurements and technology developments, but also on chemometrics applications which help to process the data. Nowadays, the multivariate approach is commonly used by scientists and plays a major role in interpretation of sensor array responses. This includes different fields of science, starting from environmental, food, biological, chemical, physicochemical, forensic and geochemical, up to areas of sociology or marketing.

The multivariate outputs can be evaluated by several chemometric methods depending on the purpose. This includes four main approaches, such as pattern recognition, multivariate calibration, experimental design and signal processing (Brereton, 2007). In this study the first two methods have been briefly described and used in further experiments. The pattern recognition technique has been employed by performing Principal Component Analysis (PCA) for discrimination between different samples and multivariate calibration applied Artificial Neural Network (ANN) for quantitative analysis of specific compounds as well as qualitative analysis of samples (Gutes *et al.*, 2007).

1.2.5.1 Pattern recognition: Principal Component Analysis (PCA)

Among chemometric and multivariate analysis one of the most recognised disciplines is pattern recognition technique. It aims at uncovering information contained within the raw data (patterns in data) through identification, extraction and conversion of this data into more understandable format to allow easier analysis.

A standard pattern recognition technique and probably the most widespread statistical approach for multivariate data analysis is PCA (Otto, 2007). The key idea of PCA is to reduce the large original dataset to a smaller matrix by highlighting similarities and differences within the data. As a consequence, redundant and noisy information can be eliminated, which helps to improve visualisation and simplify analysis of the data pattern without essential information being lost. Performing PCA, the large number of variables in raw data (the dimensionality of the data) is reduced to a lower number of significant factors, so-called principal components (PCs) (Malecha *et al.*, 2002). They are determined from a linear projection of the original data. This approach is illustrated for three dimensions in Figure 1.3.

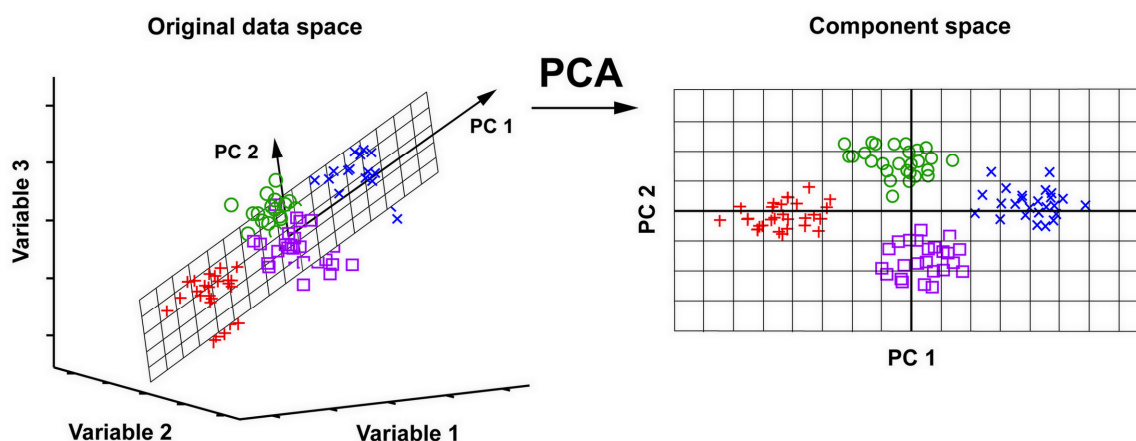


Figure 1.3: The illustration of PCA performance when the original high-dimensional data space (e.g. three dimensions) is projected onto a two dimension principal component space that maintains the largest variance in the data. The illustration is adopted from (Lobanov *et al.*, 2001; Scholz, 2006).

The selected PCs indicate the most variance that has been found in the original data. The first PC is evaluated based on the maximal variance in the data, the second PC results from the maximal variance in the direction that is orthogonal to the first one. Other components can be defined in different dimensions followed by the most variance of observations (Rencher, 2002). Two dimensional visualisation of the presented example (Figure 1.3) reveals qualitative information about four experimental conditions of the analysed system.

Mathematically, the input data matrix X ($M \times N$) is decomposed into two matrices: scores matrix T ($M \times K$) and loading matrix P ($N \times K$) and residual, noisy part E ($M \times N$) according to (Esbensen *et al.*, 2002):

$$X = t_1 p_1^T + t_2 p_2^T + \dots + t_k p_k^T + E$$

$$X = TP^T + E$$

Where, matrix T describes the spread of samples within the PCA model space (TP^T). M is the number of rows of matrix X and indicates the number of samples or measurements. Matrix P defines the relationships between variables, where N is the number of columns and indicates the number of variables. K defines the number of PCs and the symbol T is a transpose of the matrix.

The graphical interpretation of the decomposition of the original dataset X is illustrated in Figure 1.4.

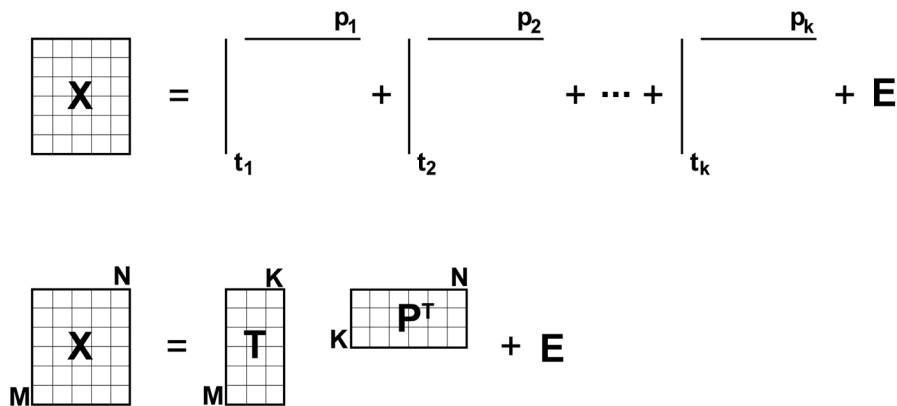


Figure 1.4: Graphical illustration of PCA model. Adopted from (Esbensen *et al.*, 2002).

PCA performance has been appreciated especially for the interpretation of sensor arrays responses when many variables have to be analysed simultaneously. It can be a very useful tool to sort out acquired data, recognise similarities and differences in the samples (Palacios *et al.*, 2007) and also to pre-process response datasets that can be later used for quantitative analysis of target compounds as well as qualitative samples evaluation (Raykov *et al.*, 2008; Siripatrawan, 2008). Additionally, PCA does not require any prior information other than the original data.

1.2.5.2 Multivariate calibration: Artificial Neural Network (ANN)

Along with PCA, ANN is another chemometric technique extensively used by scientists. While PCA has been frequently applied for processing large amounts of data or qualitative analysis, ANN allows quantitative analysis of a particular species and samples classification. The origin of the artificial neural network concept has a biological nature. Inspired by the mammalian neural system, ANN forms a model of human brains and imitates some of its functions. This includes information processing, such as function approximation (prediction of behaviour and properties of a system), pattern classification (identification and assignation of data to a class), or clustering (recognition clusters in data) (Samarasinghe, 2007). ANN aims at following the ability of the human brain and learning this information over a period of time to allow the drawing of the conclusions, and making reliable predictions. It should be accomplished despite complexity, and irrelevant or partial information on the environment.

Based on the structure of a biological system, ANN consists of nodes/neurons connected together forming an artificial neural net to process information. A biological neuron structure and its artificial representation are presented in Figure 1.5.

A biological cell (Figure 1.5-A) contains three basic components: dendrites, cell body and axons. Dendrites lead the input signals to the cell body, where these signals are accumulated, processed and then sent further to axons, which channel the information to other neurons of the net. This process is imitated by nodes that apply mathematical models for biological neurons (Figure 1.5-B). The input information (x_n) is weighted

(w_n) and transferred to the cell body of the artificial neuron. Further, two actions are performed: the weighted inputs are summed (Σ) and then the sum is processed through a transfer function ($f(\Sigma)$) to produce an output signal (y). The outcome is moved forward to neighbouring units. Weights form connections between nodes and they are adjustable during the network learning process. Their estimation is crucial to the network performance and error minimisation. Finding the appropriate weights leads to the smallest network error.

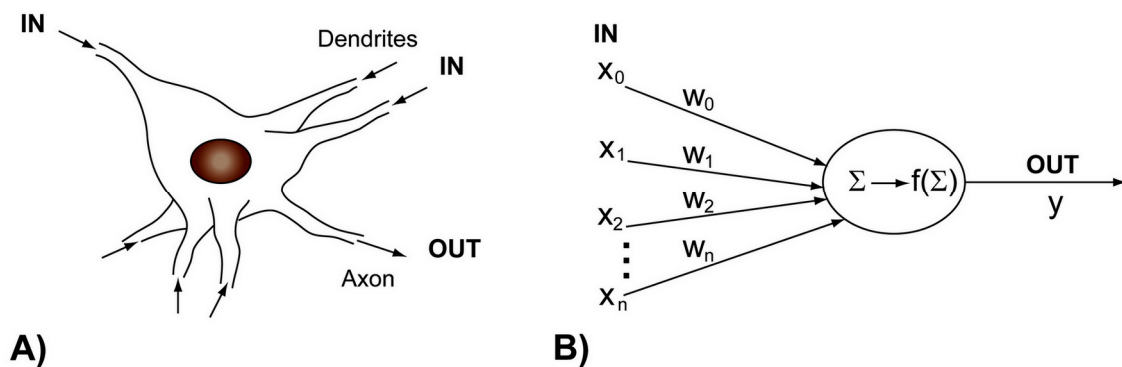


Figure 1.5: Schematic illustration of a single neuron: biological neuron (A), artificial neuron (B). Illustration adopted from (Lobanov *et al.*, 2001; Samarasinghe, 2007).

Artificial neurons are organised in layers, and most artificial neural networks have a multilayered architecture (see Figure 1.6). The first layer, input layer consists of independent variables. The last layer is the output layer, which projects the outcome of the dependent variables. The middle layer is called the hidden layer, which provides interconnections between the input and output layers. There can be one or more hidden layers, usually depending on the complexity of the problem. Commonly used models contain one hidden layer with a varying number of nodes. Additional hidden layers are often used for more complicated applications (Huang *et al.*, 2007).

The network learning process can be either supervised with knowing target outputs as a guide, or unsupervised (self-organising) when targets are not required and by application of different mathematical methods, data organise themselves.

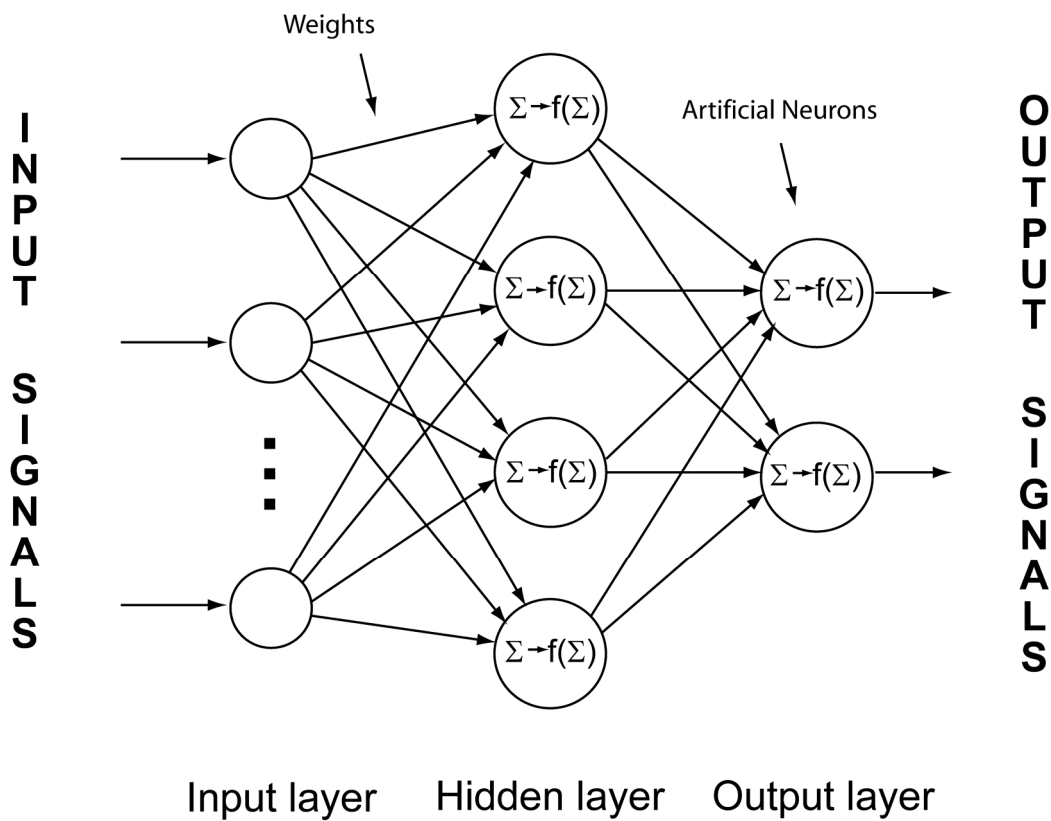


Figure 1.6: Schematic representation of fully connected nodes layers.

ANN is a powerful advanced tool in analysing different linear and non-linear systems with or without knowing the underlying characteristics of the complex problems. The main advantage of ANN over conventional statistical techniques is that once the network is trained and the model is evaluated, the same network can be applied to solve analogous problems (adaptive learning). It gives the possibility of real-time operations on numerous multicomponent systems.

1.3 Analytical characterisation of samples

The approach of multidetection has become crucial in analytical laboratories for routine measurements of physicochemical parameters and metabolites in complex samples and constant real-time bioprocess monitoring (Schroder *et al.*, 2007). The list of required analytes is lengthy and continuously expands. Therefore, it is extremely critical to improve sensing tools for multiple analyte detection and quantification, which would allow rapid diagnosis. The development of the assay presented in this work involves analytical characterisation of samples including simultaneous measurements of several critical parameters (Ferguson *et al.*, 1997; Krommenhoek *et al.*, 2008; Lieberzeit *et al.*, 2008), such as pH, temperature, level of oxygen and salinity. For a number of applications these parameters should be monitored continuously.

1.3.1 pH

The determination of pH is essential in many areas of research and industry. The pH is one of the commonly measured parameters e.g. in clinical analysis of blood samples and other physiological fluids (Baldini *et al.*, 2007; Medlock *et al.*, 2007) for diagnostic purposes, tissues engineering as an important physicochemical control factor for tissues regeneration and functioning (Mano, 2008; Starly *et al.*, 2008). It is also used as a crucial chemical stimulus in studies of smart materials for drug delivery applications (Ju *et al.*, 2009). Furthermore it can be used as a quality indicator to regulate the condition of drinking water, determine the freshness of food and monitor growth of cell cultures (Krommenhoek *et al.*, 2007; Wu *et al.*, 2009). The pH also plays an important role in environmental examination by investigation of an industrial waste water treatment, characterisation of soil condition (Unger *et al.*, 2009) or the level of the air pollution by analysing acidity of rain (Badugu *et al.*, 2008). Along with oxygen concentration, information on pH is also required in marine research and seawater analysis (Schroder *et al.*, 2005; Vasylevska *et al.*, 2006).

1.3.2 Dissolved oxygen

Besides pH, oxygen is one of the most important and essential for life chemical species. The determination of the oxygen concentration is constantly required in medicine, cell biology, biotechnology, marine science or environmental analysis (Borisov *et al.*, 2009). Dissolved oxygen (DO) is the key parameter that refers to liquid systems, which describes the amount of gaseous form of oxygen dissolved in aquatic media. It is an important factor often referred as the quality of water (Xu *et al.*, 2008) but also applied in clinical research, as a key physiological parameter in monitoring of the oxygen level in blood samples (Baldini *et al.*, 2007; Jiang *et al.*, 2008) or internal oxygen concentration of tissues (Amao, 2003; Schmalzlin *et al.*, 2005). In fermentation and other biological, chemical or biotechnological processes, it is used to control and optimise microenvironment and growth of bacteria or yeasts (Funfak *et al.*, 2009; Mehta *et al.*, 2007). It can also be used as a guide for ecology condition of waste or territorial waters analysis (Amao, 2003).

1.3.3 Temperature

Temperature is an important factor in medical, pharmaceutical applications and bioprocess control. Different temperatures of environmental conditions can radically change cell metabolism and further process efficiency (Vojinovic *et al.*, 2006), therefore the microenvironment of cell cultivation must be carefully adjusted and controlled to ensure effective productivity of the process. This is also related to the pharmaceutical industry and metabolic engineering, which utilises plants and microorganisms for production of drugs such as antibiotics or extraction of valuable natural pharmaceutical compounds (Lee *et al.*, 2009). The examination of temperature changes is also essential for material science and drug delivery purposes (Bawa *et al.*, 2009). Of great importance is that drugs are encapsulated and carried to the desired place within the body where it can be safely released. This process is often controlled by temperature of phase transition of thermo-responsive materials (Bhattarai *et al.*, 2005). Additionally, temperature is a basic parameter that can influence sensors outputs, synthesis,

measurements, production, and storage, transport of different compounds or substances. Therefore it requires constant attention.

1.3.4 Buffer composition

The effect of changes in buffer composition similar to fluctuations in real samples has a significant impact on the sensor outputs. One of the factors which can be rather variable and influence the analysis of biological samples, is their ionic state (Chow *et al.*, 2009; Weidgans *et al.*, 2004). The presence of different salts and their various concentrations might change processes that occur in the environment (Cortez *et al.*, 2006), therefore it is essential to test the efficiency of sensing system in response to varying ionic strength or a presence of different ions in the samples. This can be simulated by preparing different buffers with adjusted proprieties and desired parameters, which has been done in presented experiments (Ahmad *et al.*, 2009).

1.4 Thesis statement

This thesis describes the work which has been done to prove the validity of following hypotheses:

- possibility to develop and examine novel fluorescence based diagnostic assay as an optical equivalent to electronic nose and tongue systems (Figure 1.7);
- application of fluorescence spectroscopy and a mixture of environment-sensitive fluorescent dyes instead of electronic sensor arrays to monitor changes in the sample;
- evaluation of acquired by the assay data base on chemometric methods, similarly to electronic nose/tongue sensors;
- using the assay for qualitative and quantitative analysis of complex samples.

1.5 Aims of the research

Following the approach of a new multipurpose fluorescent based assay, the research aims were focused on characterisation of the assay and testing its diagnostic potential. In particular, several tasks have been performed:

- (A) One of the major aims of this study was to design the recognition element for an optical assay consisting of a mixture of fluorescent dyes. Based on available information in the literature, lists of commercially available fluorescent dyes have been chosen and dyes were classified regarding their sensitivities, optical and chemical properties and prices.

Selection criteria for fluorescent dyes, their lists and required information are described in Chapter 2.

- (B) Collected information and lists of dye-indicators has been used to select the favoured ones. These dyes were later acquired and their optical properties were examined experimentally in order to test which of them could be mixed together in one solution. Based on the results, suitable mixtures of selective dyes have been defined, where each dye representing distinct unit of specific indication, and combined with chemometric techniques for fluorescence data processing.

The selection criteria and optimisation of fluorescent dye mixture are described in Chapter 3.

- (C) The next aim of this study was to investigate the analytical capability of the proposed assay engendered by changes in fluorescence signal in response to changes in environment such as pH, temperature, ionic strength and the presence of oxygen. It has been done to validate its potential for simultaneous identification and measurements of several physicochemical parameters, thus quantitative analysis of samples.

Testing of the analytical capability of the assay for multiply parameters of a sample is described in Chapter 4.

- (D) A further major aim was to investigate the possibility of using the assay for qualitative analysis of biological samples. The feasibility of this approach has been tested for the identification of development phases of growing bacterial cultures, discrimination between two different strains of yeast and urine samples from subjects with several gastrointestinal diseases.

The optical approach for diagnose of biological samples is described in Chapter 5.

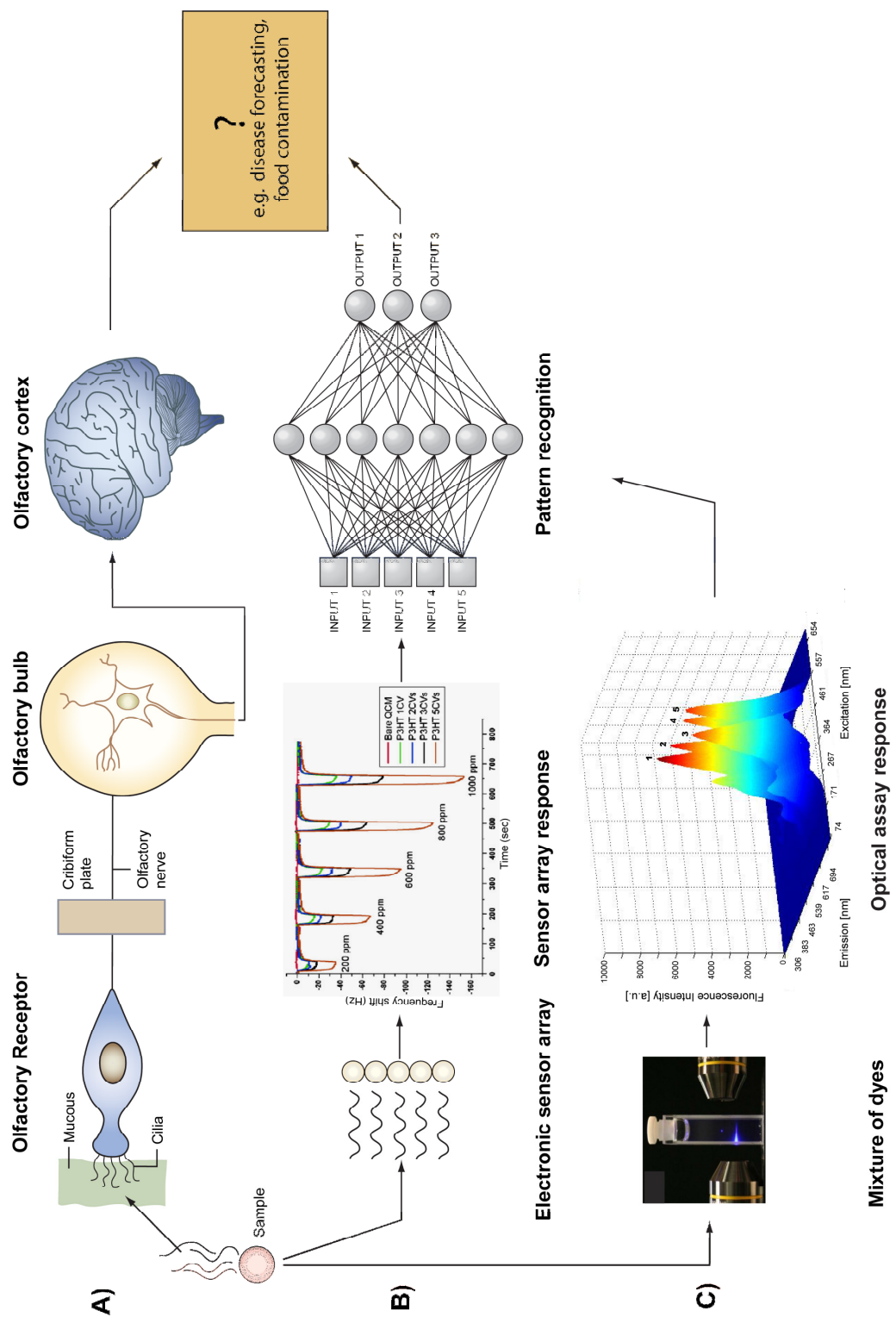


Figure 1.7: Schematic representation of sensing systems: human olfactory system (A), electronic analogue (B) and our optic analogue (C). Principle adopted from (Turner *et al.*, 2004)

2. First objective: selection of commercially available fluorescent dyes

2.1 Introduction

Considering the great potential of fluorescent dyes, their high sensitivity and specificity in measurements of wide range physicochemical and biochemical analytes, the first task of the project was to collect a number of well-characterised and commercially available fluorescent probes, which allow measurements of three physicochemical parameters, namely: pH, temperature and oxygen concentration. These parameters were chosen for the first instance since their regular examination is required in many areas including medicine, biotechnology or environmental diagnostics. The distinctive functions of these parameters were described in Chapter 1.3.

Later, the sensitivity of the assay was expanded to determine the ionic strength of a solution, which however was based not on the sensitivity of the particular dye but was related to recognition of response fluorescence pattern that originated from interferences between buffer concentration and all dyes included in the assay (see Chapter 4.3.3).

Taking also into account the future improvements and the application of the assay involving the development of a smart vanishing ‘tattoo’ (similar to kids temporal tattoos) (see Chapter 6 and (Moczko *et al.*, 2008)) the selection of dyes has been performed also for glucose concentration. The vanishing ‘tattoo’, consisting of a mixture of environmental-sensitive fluorescence dyes can be used for an *in-vivo* real-time clinical monitoring of physiological parameters and metabolite concentrations in human skin. Among other key parameters to control glucose concentration is crucial especially for diabetics. Diabetes affects the ability of the body to produce or respond to insulin, the hormone that allows glucose to enter the body’s cells and to be stored or used for energy (Bronzino, 2000). Most diabetics require insulin injections, and most of the time they have to carefully monitor and manage their blood glucose levels themselves. Because glucose levels can fluctuate widely throughout the day, for optimal control they have to do the blood test several times a day (usually from finger pricks).

Consequently, novel, rapid and minimal-invasive method for measurements of glucose level could have a significant impact on new developments in medicine.

Even though the actual measurements of glucose have not been attempted yet, the idea of vanishing 'tattoo' is still under development.

2.2 Selection criteria for single fluorescent dyes

Lists of suitable fluorescent dyes for the optical assay were prepared according to following criteria:

- Dyes should have the ability to change their optical prosperities in response to suitable changes of an environment (pH, temperature or oxygen).
- They should be commercially available and preferably inexpensive.
- For the minimum interference with biological samples, fluorescent dyes should be responsive in VIS-NIR (~400~1600 nm).
- Considering future immobilisation of dyes onto rigid support, they should contain functional chemical groups allowing binding to occur.

Other major factors which should be taken into account during a selection are also the molar excitation coefficient of the dyes (the ability of a dye to absorb light at a particular wavelength), fluorescence quantum yield (the efficiency of the fluorescence process) or photostability (quality of a dye to retain resistant to light exposure) (Singer, 1997).

A variety of fluorescent dye indicators have been reported and their susceptibility to different environmental effects have been characterised in a number of journals, handbooks of fluorescent probes and research chemicals (Haugland, 1996; Sabnis, 2008). The lists of suitable fluorescent dyes were prepared on the basis of this information and in respect to above specifications.

Additional requirements for the combination of favourable fluorescence dyes are described later, in Chapter 3.2.

2.3 Results and Discussion

The suggested indicators which allow qualitative and/or quantitative detection of different chemical or physicochemical analytes along with their spectral characteristics (excitation and emission maxima and spectra) were listed and reported in the earliest phase of this study on the optical assay development. This included pH, temperature, oxygen, which were considered in this study (see Table 2.1, 2.2, 2.3 for pH, temperature and oxygen respectively). Indicators for glucose detection are listed in Table 2.4.

The first table (see Chapter 2.3.1) consists of pH indicators which can change fluorescence spectra by shifting their fluorescence maxima, or changing the intensity at the certain range of pH. It can be also the combined influence of both these features. Dyes which have been chosen, are sensitive to pH within relatively wide range. Most of them are highly sensitive within physiological and higher pH, such as fluorescein and fluorescein derivatives and some of them, e.g. Oregon green 480 and Oregon green 514 have been reported very sensitive at lower pH. This gives the possibility of integrating the system of dyes with high sensitivity in different ranges of pH.

Regarding temperature (see Chapter 2.3.2), it is well known that the majority of fluorescent dyes change their spectral characteristics at different temperatures, however these changes may not be correlated with the influence of this one parameter only, but can be driven by the presence of other variables of the system. They can not therefore be used as reliable indicators to measure the actual temperature of the sample. Moreover, they are less sensitive to temperature than some fluorescent probes presented in the literature as accurate indicators for temperature and less or not sensitive to others. The fluorescence intensity of these dyes can therefore be proportional to temperature. Depending on the sensitivity range for temperature, several suitable probes have been selected for the consideration of their implementation in the optical assay.

The third table includes oxygen sensitive probes (see Chapter 2.3.3). The measurement of oxygen concentration in a sample is based on the principle of collisional quenching of certain fluorophores by the presence of oxygen (Lakowicz, 2006). First the

fluorophore absorbs certain energy, produces excited electrons, which then comes back to the original energy state. This is associated with emitting energy. When oxygen molecules are present, the amount of fluorescence intensity is reduced because the excited state of the fluorophore is deactivated upon diffusive encounter with a quencher molecule. By measuring the amount of quenching, it is possible to map the real concentration of oxygen in the sample.

The last table (see Chapter 2.3.4) includes glucose receptors that have been employed in fluorescence based sensing. Many of them involve measuring of changes in fluorescence resonance energy transfer (FRET) between fluorescence donor and the acceptor based on competitive binding to the lectin concavalin A (Con A) of either labelled carbohydrate derivative such as dextran, mannoside or glucose. FRET might occur only when the emission spectrum of the donor overlaps with absorption spectrum of the acceptor and when these molecules are placed in approximately 20-100 Å from each other (Fröster distance) (Lakowicz, 2006). This results in promotion of energy transfer and increases the fluorescence intensity. When glucose is introduced to the system, it replaces the donor, e.g. dextran from the Con A and increases the separation distance between two acceptor and donor, which leads to a loss of energy transfer and fluorescence decrease. Widely employed in glucose sensing has also been enzymatic assays such a one involving, e.g. glucose oxidase (GOx) as a catalyst and hydrogen peroxide (HRP) as a product of the reaction. The concentration of HRP is correlated with glucose levels in the sample and therefore dye sensitive to HRP can be use for this indication.

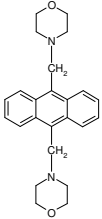
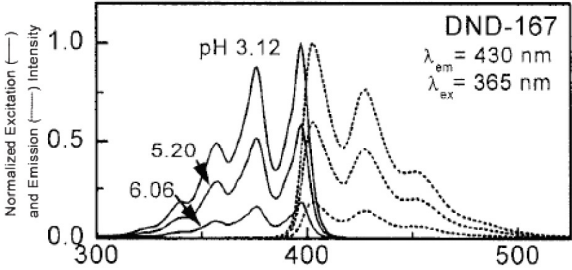
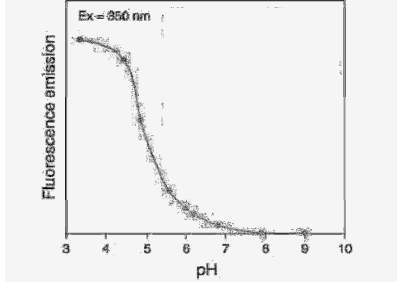
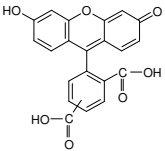
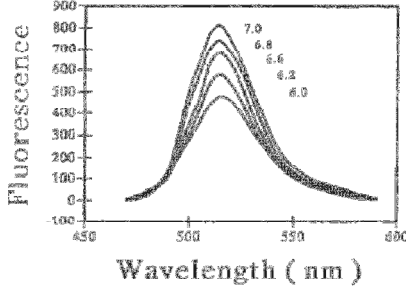
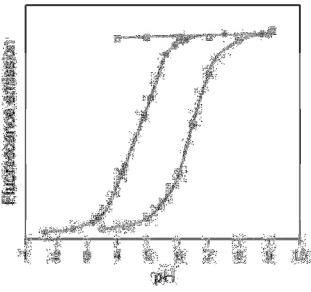
All dyes listed in following tables were considered as potential indicators for different parameters that can be combined and used in the optical assay.

The most challenging criterion was to choose dyes sensitive to specific parameters at the suitable range and their emission at the longer wavelengths of light spectrum. This property makes them advantageous for many biological applications.

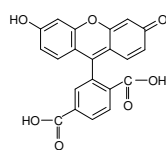
The lists of fluorescent dye indicators considered in this research are presented below in respect to their different sensitivities (pH, temperature, oxygen and glucose).

2.3.1 pH sensitive fluorescent dyes

Table 2.1: List of pH sensitive fluorescent dyes. They are listed by increasing emission wavelengths.

Indicator Name	Chemical Structure	Sensitivity	Excitation / Emission [nm]	References Supplier/Price		
LysoSensor blue DND-167		pH 4.0-7.0	365 / 430	(Lin <i>et al.</i> , 2001) Molecular Probes Unit Size: 20 × 50 µl Price: 194.00 GBP		
					Figure. Excitation and emission spectra of LysoSensor DND-167	Figure. Fluorescence of LysoSensor Blue DND-167 as a function of pH.
5(6)- carboxyfluorescein 5,6-CF		pH 4.5-7.0	490 / 517	(Mordon <i>et al.</i> , 1992) (Begu <i>et al.</i> , 2005) (Manconi <i>et al.</i> , 2007) (Lee <i>et al.</i> , 1998) Molecular Probes Unit Size: 100 mg Price: 92.00 GBP		
					Figure. Emission spectra of 10-5 5,6-CF in phosphate buffer saline (pH 6-7). (Ex = 490 nm)	Figure. Comparison of fluorescence of Oregon Green 488 5,6-CF and Alexa Fluor 488 fluorophores. (equal concentrations, ex/em at 490/520 nm)

6-carboxyfluorescein
6-CF



pH 5.0-7.5 492 / 517 (Aschi *et al.*, 2008)
(Thomas *et al.*, 1979)
(Cohen-Kashi *et al.*, 1997)

Molecular Probes
Unit Size: 100 mg
Price: 97.00 GBP

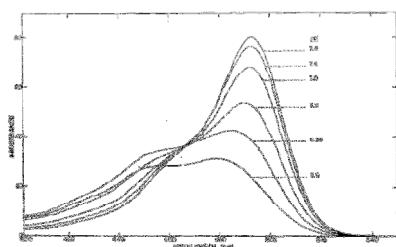


Figure. pH dependence of 6-CF spectra in 100 mM Mops buffers.

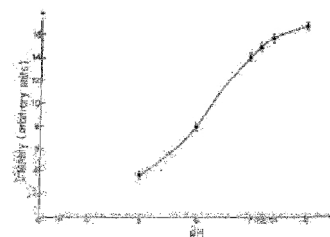
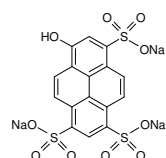


Figure. Fluorescence intensity of 6-CF in PBS as a function of pH (at 20°C).

8-hydroxypyrene-
1,3,6-trisulfonic acid
trisodium salt



pH 6.0-11.0 460 / 518 (Lakowicz, 2006)
(Oter *et al.*, 2006)
(Agostiano *et al.*, 2004)
(Hulth *et al.*, 2002)

HPTS

Molecular Probes
Unit Size: 1g
Price: 110.00 GBP

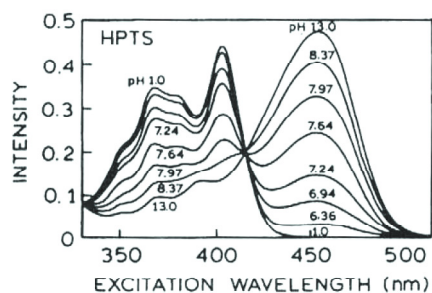


Figure. Excitation spectra of HPTS in 0.007 M phosphate buffer at various pHs.

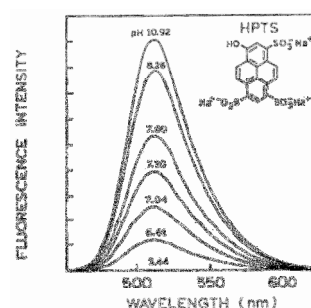
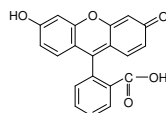


Figure. Emission spectra of HPTS in 0.007 M phosphate buffer at various pHs. (Ex = 404 nm)

Fluorescein
FL



pH 5.0-8.0 494 / 510 (Lakowicz, 2006)
(Sjoback *et al.*, 1995)
(Fisher *et al.*, 2003)
(Ge *et al.*, 2008)
(Baker *et al.*, 1999)

Molecular Probes
Unit Size: 1 g
Price: 67.00 GBP

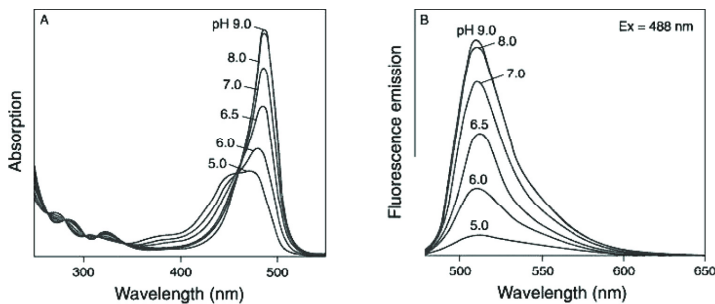


Figure. The pH-dependent spectra of fluorescein: A) absorption spectra, B) emission spectra.

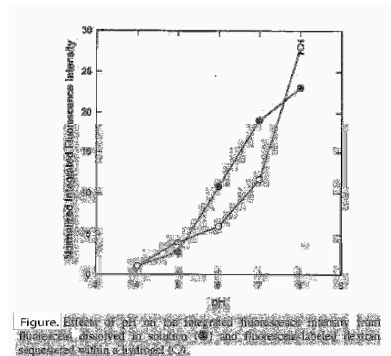
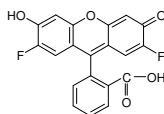


Figure. Effect of pH on the measured fluorescence intensity from fluorescein, dissolved in solution (○) and fluorescein labeled within a hydrogel (●).

Oregon green 488
carboxylic acid



pH 3.5-5.7

490 / 520

(Orte *et al.*, 2005)

OG488

Molecular Probes
Unit Size: 10 mg
Price: 36.00 GBP

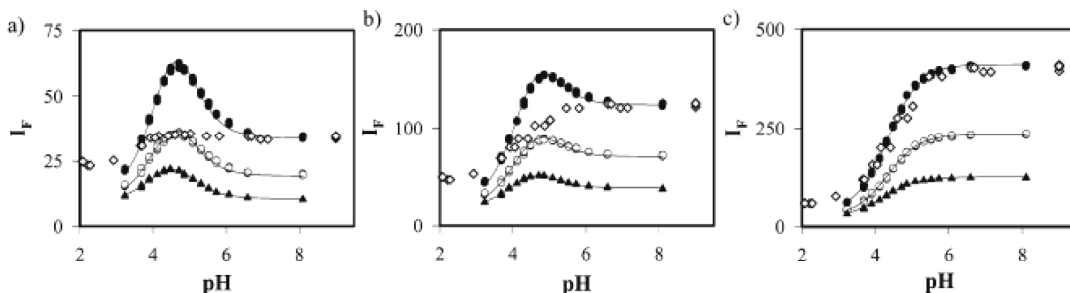
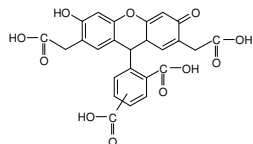


Figure. Emission intensity vs pH of 2.5×10^{-6} OG488 aqueous solutions in the presence of 1 M acetate buffer: ex = 420 (a), 440 (b), and 460 nm (c), and em = 500 (○), 515 (●), and 550 nm (▲). For comparison, intensity of solutions in the absence of buffer at em = 515 nm are also shown (◇).

2',7'-bis(2-carboxyethyl)-5(6)-carboxyfluorescein



pH 5.0-8.0

505 / 528

(Hanson *et al.*, 2002)
(Russell *et al.*, 1995)
(Rochon *et al.*, 2007)
(Boens *et al.*, 2006)

BCECF

Molecular Probes
Unit Size: 1 mg
Price: 96.00 GBP

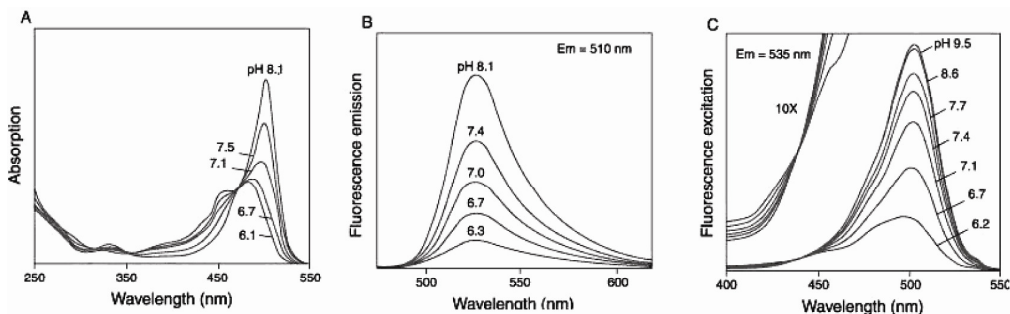
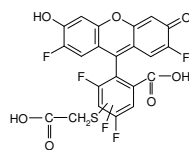


Figure. The pH-dependent spectra of BCECF: A) absorption spectra, B) emission spectra and C) excitation spectra.

Oregon green 514
carboxylic acid



pH 3.0-8.0

510 / 530

(Delmotte *et al.*, 1999)
(Lin *et al.*, 1999)

OG514

Molecular Probes
Unit Size: 5 mg
Price: 116.00 GBP

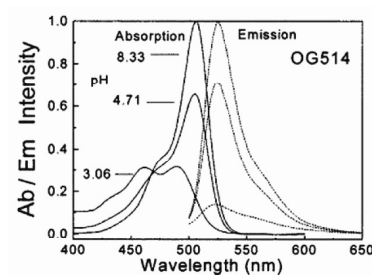
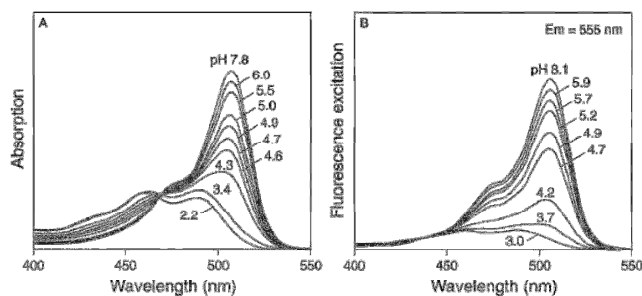
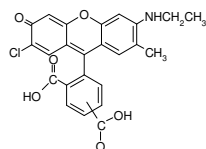


Figure. The pH-dependent absorption and emission spectra of OG514. The excitation wavelength was 488 nm.

Figure. The pH-dependent spectra of Oregon Green 514 carboxylic acid:
A) absorption spectra and B) excitation spectra.

DM-NERF



pH 5.0-7.0

488 / 536

(Lin *et al.*, 1999)
(Li *et al.*, 2008)

Molecular Probes
Price: N/A

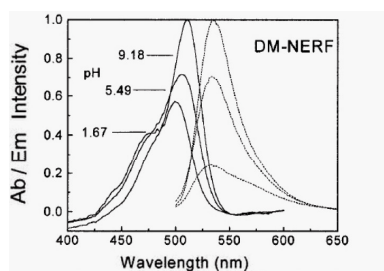


Figure. The pH-dependent absorption and emission spectra of DM-NERF. The excitation wavelength was 488 nm.

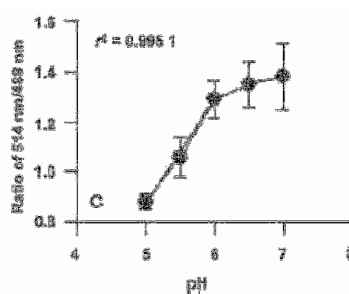
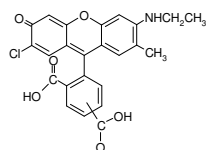


Figure. In vitro calibration of DM-NERF (pH indicator).

CI-NERF



pH 3.0-5.5

488 / 540

(Lin *et al.*, 1999)
(Slivka *et al.*, 2001)
(Coskun *et al.*, 2001)

Molecular Probes

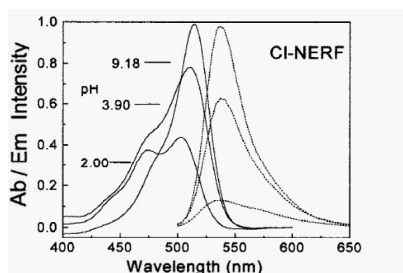


Figure. The pH-dependent absorption and emission spectra of CI-NERF. The excitation wavelength was 488 nm.

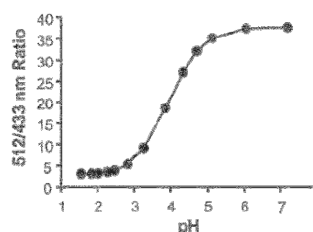
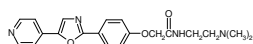


Figure. CI-NERF as on-line pH sensor. Calibration curve of 512- to 433-nm fluorescence excitation ratio of CI-NERF vs. pH. CI-NERF (0.1 mM) added to perfusate solution was measured at the indicated pH values.

LysoSensor
yellow/blue DND-160



pH 3.0-8.5
pressure

384 / 540

(DePedro *et al.*, 2009)
(Lin *et al.*, 2001)

Molecular Probes
Unit Size: 20 × 50 µl
Price: 190.00 GBP

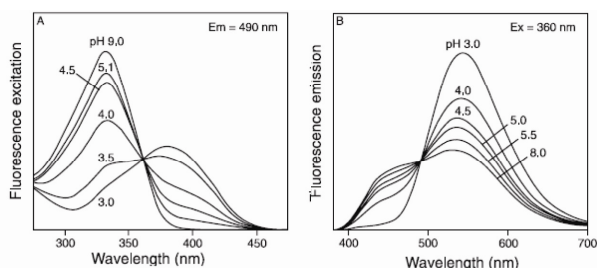


Figure. The pH-dependent spectral for LysoSensor™ Yellow/Blue DND-160 A) fluorescence excitation B) fluorescence emission spectra.

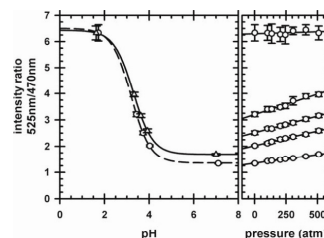
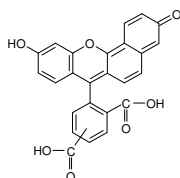


Figure. Intensity ratio versus pH (left column plots) and pressure (right column plots) for 2 µM DND-160 in 50 mM acetate buffers. For the intensity ratio versus pH plots, 1 atm (circle) and 510 atm (triangle) values are shown. The intensity ratio versus pressure plots correspond to samples used in the intensity ratio versus pH plots. Error bars are standard deviations of multiple measurements.

Carboxy-seminaphtho-
fluorescein-1



pH 6.5-9.5

514 / 550

(Lin *et al.*, 2003)
(Kuwana *et al.*, 2003)
(Sanders *et al.*, 1995)

C-SNAFL-1

Molecular Probes
Unit Size: 1 mg

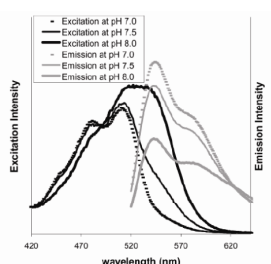


Figure. Excitation (emission at 650 nm) and emission (excitation at 514 nm) spectra of 1 µM C-SNAFL-1 in MOPS buffer.

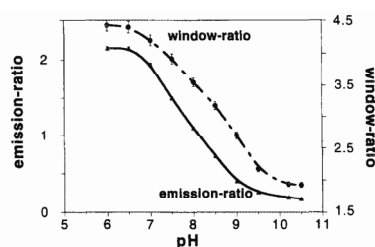
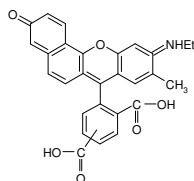


Figure. pH calibration curves of c-SNAFL-1 in buffers, using the emission ratio and the window ratio method. The linear regression performed on the linear part of both curves results in the following equations: $y = 7.27 - 0.77x$ ($R = 0.998$) for the emission ratio and $y = 9.49 - 0.73x$ ($R = 0.997$) for the window ratio.

C-SNARF-6



pH 6.0-9.0

540 / 560

(Lakowicz, 2006)

Molecular Probes
Price: N/A

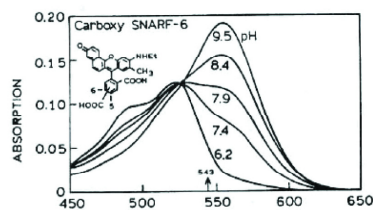
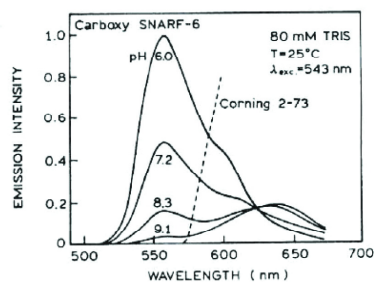
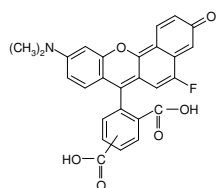


Figure. pH-dependent absorption (left) and emission (right) spectra of C-SNARF-6. The dashed line shows the transmission cutoff of the long-pass filter used for phase and modulation measurements.



C-SNARF-5F



pH 5.0-9.0

530 / 625

(Liu *et al.*, 2001)
(Hille *et al.*, 2008)

Molecular Probes
Unit Size: 1 mg
Price: 189.00 GBP

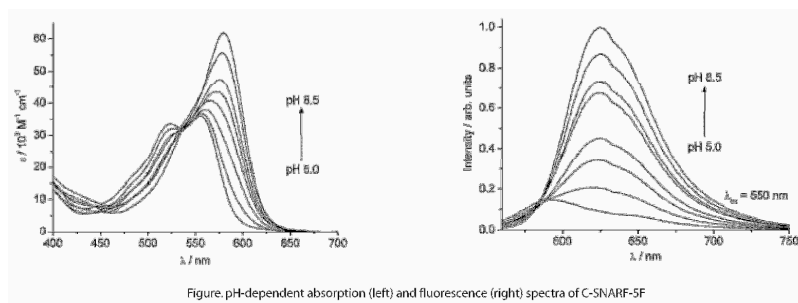
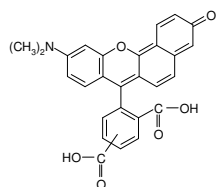


Figure. pH-dependent absorption (left) and fluorescence (right) spectra of C-SNARF-5F

C-SNARF-1



pH 6.0-9.0

535 / 640

(Yassine *et al.*, 1997)
(Vecer *et al.*, 2001)
(Magg *et al.*, 2007)

Molecular Probes
Unit Size: 1 mg
Price: 189.00 GBP

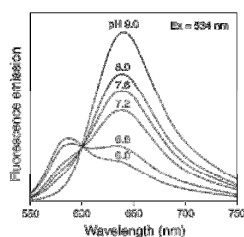


Figure. The pH dependent emission spectra of C-SNARF-1 when it is excited at 534 nm.

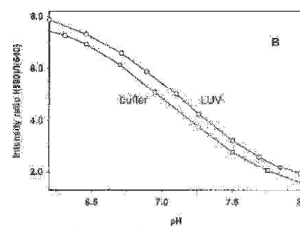
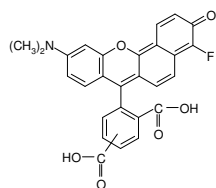


Figure. pH calibration curves of carboxy-SNARF-1 in 10 mM HEPES/150 mM KCl buffer and LUV suspension 70 min after gel filtration.

C-SNARF-4F



pH 5.0-8.0

514 / 660

(Marcotte *et al.*, 2005)
(Liu *et al.*, 2001)

Molecular Probes
Unit Size: 1 mg
Price: 189.00 GBP

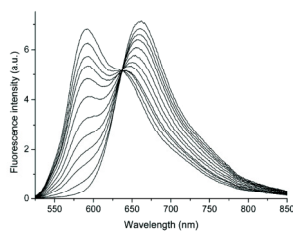


Figure. Fluorescence spectra of C-SNARF-4F (1.3×10^{-6} M) in pH buffered solutions upon excitation at 514 nm. From top to bottom (at 660 nm): pH 8.2, 7.6, 7.2, 7.0, 6.8, 6.6, 6.4, 6.2, 6.0, 5.6, 5.4, and 5.0.

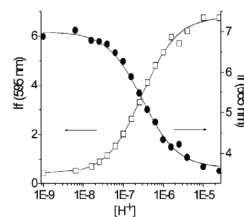
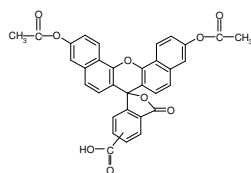


Figure. Emission intensity of C-SNARF-4F versus H^+ concentration at 595 nm (●) and 660 nm (□). The symbols represent experimental data, and the solid lines were calculated by fitting the data.

5(6)-
carboxynaphthofluorescein
CNF



pH 6.5-8.5

633 / 665

(Lakowicz, 2006)
(Song *et al.*, 1997)
(Jorge *et al.*, 2005)

Molecular Probes
Unit Size: 10 mg
Price: 103.00 GBP

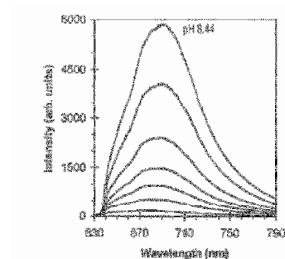
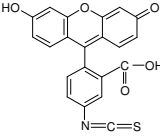


Figure. Emission spectra of the CNF aptode in phosphate buffers using 633 nm excitation wavelength. The pH values from top to bottom at 690 nm are 8.14, 7.95, 7.61, 7.38, 7.15, 6.86, and 6.31.

2.3.2 Temperature sensitive fluorescent dyes

Table 2.2: List of temperature sensitive fluorescent dyes. They are listed by increasing emission wavelengths.

Indicator Name	Chemical Structure	Sensitivity	Excitation / Emission [nm]	References Supplier/Price
Fluorescein isothiocyanate FITC		Temperature	495 / 520	(Liu <i>et al.</i> , 2005) Sigma-Aldrich Unit Size: 250 mg Price: 34.10 GBP

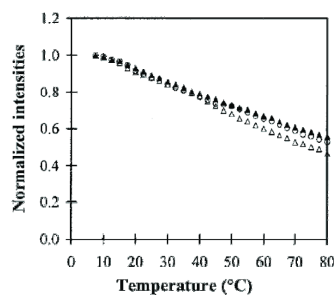
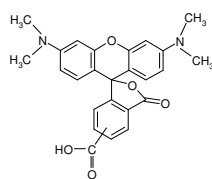


Figure. Effects of salt concentration on fluorophore stabilities with respect to temperature on gel-based microchips. The formamide concentration in the buffer was fixed at 0%. (excitation, 470/40 nm; emission, 525/50 nm) at salt concentrations (10, 100, and 500 mM)

5(6)-
Carboxytetramethylrho
damine

TAMRA



Temperature 540 / 570 (Liu *et al.*, 2005)

Sigma-Aldrich
Unit Size: 100 mg
Price: 91.30 GBP

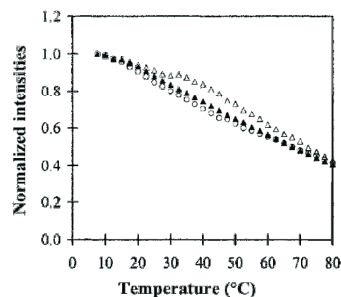
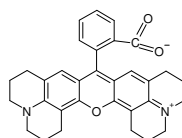


Figure. Effects of salt concentration on fluorophore stabilities with respect to temperature on gel-based microchips. The formamide concentration in the buffer was fixed at 0% (excitation, 470/40 nm; emission, 525/50 nm) at salt concentrations (10, 100, and 500 mM)

Rhodamine 101



Temperature 520 / 580 (Holzwarth *et al.*, 2003)
(Clark *et al.*, 1998)

Sigma-Aldrich
Unit Size: 500 mg
Price: 35.80 GBP

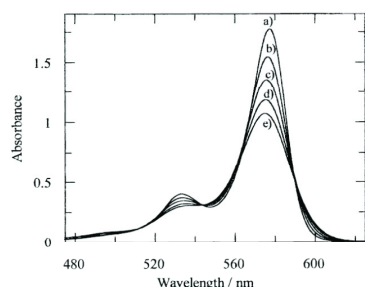


Figure. Temperature dependence of the absorption spectra of 10-4 M rhodamine 101 in acidified ethanol solution: (a) 140 K, (b) 180 K, (c) 220 K, (d) 260 K, and (e) 300 K.

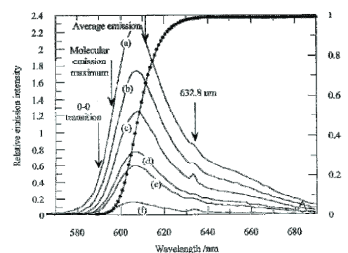
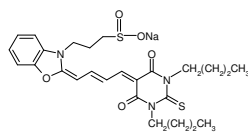


Figure. Dispersed emission spectra of a 10-4 M solution of rhodamine 101 in acidified ethanol in a cylindrical cell at (a) 310 K, (b) 290 K, (c) 270 K, (d) 250 K, (e) 220 K, and (f) 200 K. Also shown is the transmission of the low-energy absorption tail of this sample, the 1 mW He-Ne excitation wavelength, the position of the average wavelength of the measured emission spectrum (610 nm), the position of the average energy of the molecular emission spectrum (595 nm), and the position of the 0-0 band origin (590 nm).

Merocyanine 540

MC540



Temperature 530 / 580 (Langner *et al.*, 1993)
(Sikurova *et al.*, 1997)

Molecular Probes
Unit Size: 25 mg
Price: 63.00 GBP

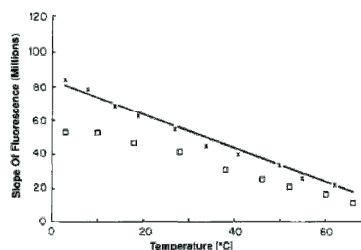
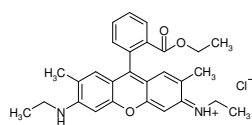


Figure. Fluorescence of MC 540 in the presence of DOPC unilamellar vesicles (□) and ethanol solution (x) as a function of temperature. The solid line represents a least-squares data approximation.

Rhodamine Red



Temperature 570 / 590 (Liu *et al.*, 2005)

Molecular Probes
Unit Size: 1 g
Price: 57.00 GBP

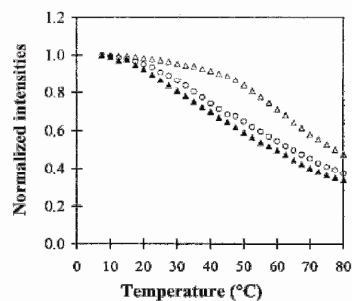
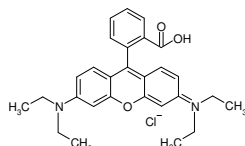


Figure. Effects of salt concentration on fluorophore stabilities with respect to temperature on gel-based microchips. The formamide concentration in the buffer was fixed at 0%. (excitation, 555/50 nm; 610/75 nm) at salt concentrations (10, 100, and 500 mM)

Rhodamine B



Temperature 540 / 625 (Sakakibara *et al.*, 1999)
(Yuen *et al.*, 2009)
(Natrajan *et al.*, 2009)

Molecular Probes
Unit Size: 1 g
Price: 24.10 GBP

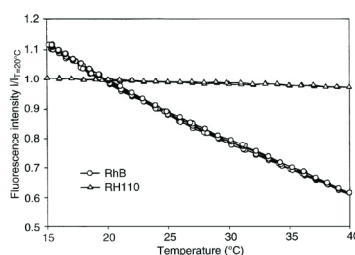
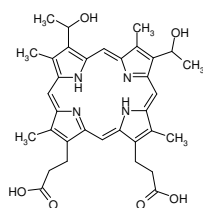


Figure. Variation of the fluorescence intensity against temperature

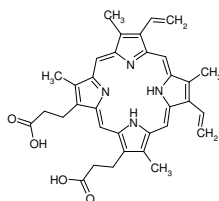
Hematoporphyrin IX



Temperature 520 / 625 (Ricchelli *et al.*, 1995)
(Ricchelli *et al.*, 1998)

Sigma-Aldrich
Price: N/A

Protoporphyrin IX



Temperature 535 / 635 (Ricchelli *et al.*, 1995)
(Ricchelli *et al.*, 1998)

Sigma-Aldrich
Price: N/A

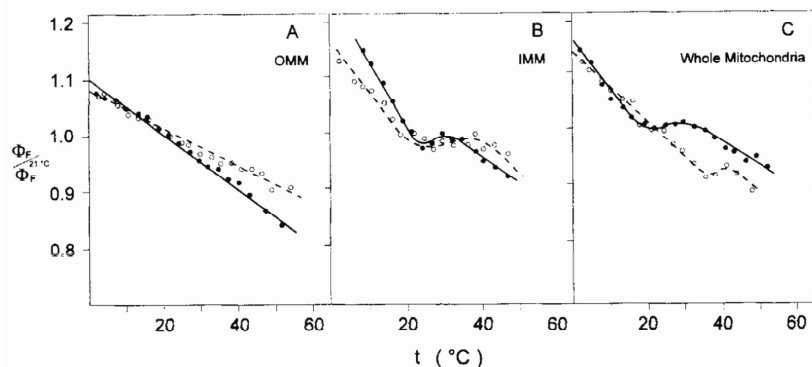


Figure. Temperature dependence of hematoxylin (●) and protoporphyrin (○) fluorescence quantum yield (Φ_F) in OMM (A), IMM (B) and whole mitochondria (C). All fluorescence quantum yields were calculated as a ratio relative to that obtained at 21 °C. Excitation at 400 nm. Hematoxylin and protoporphyrin were dispersed in Pam2Gro/Cho liposomes. Similar curves were obtained when Pam2Gro/Cho/cholesterol or Pam2Gro/Cholcardiolipin were used as dye carriers. Concentration of mitochondrial membranes was 0.5 mg/ml.

2.3.3 Oxygen sensitive fluorescent dyes

Table 2.3: List of oxygen sensitive fluorescent dyes. They are listed by increasing emission wavelength.

Indicator Name	Chemical Structure	Sensitivity	Excitation / Emission [nm]	References Supplier/Price
1-Pyrene butyric acid PBA		O ₂	345 / 375	(Lee <i>et al.</i> , 1987) (Ribou <i>et al.</i> , 2004) (Fujiwara <i>et al.</i> , 2002) Sigma-Aldrich Unit Size: 1g Price: 21.40 GBP

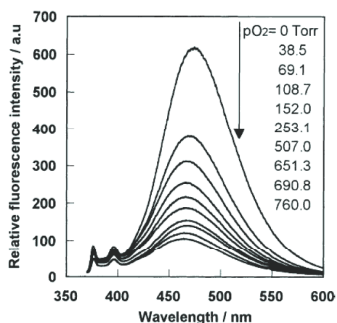


Figure. Fluorescence spectrum change of PBA chemisorption film under various oxygen partial pressures excited at 365 nm.

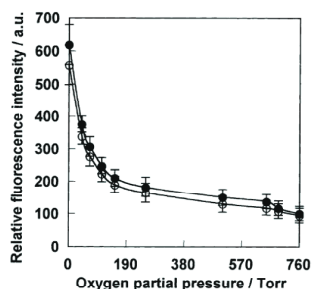
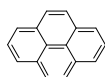


Figure. The relative fluorescence intensity change of PBA chemisorption film under various oxygen partial pressures. Closed and open circles are fluorescence intensity changes of PBA film before and after irradiation with 150W tungsten lamp for 24 h, respectively. Excitation and emission wavelength were 365 and 474 nm, respectively. Each data point represents the mean of at least three separate experiments; bars are the standard error of the mean.

Pyrene



O₂ 340 / 375 (Basu *et al.*, 2004)
(Basu *et al.*, 2005)
(Miller *et al.*, 2007)

Sigma-Aldrich
Unit Size: 1g
Price: 12.10 GBP

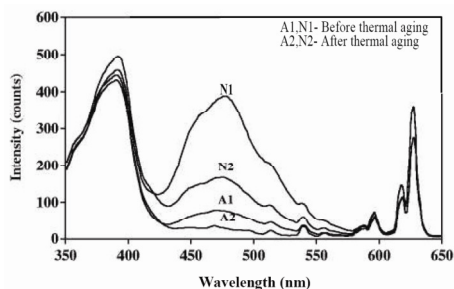


Figure. Fluorescence emission spectra of a pyrene-based coating (1) before and (2) after thermal aging in air (A1, A2) and in the presence of nitrogen (N1, N2).

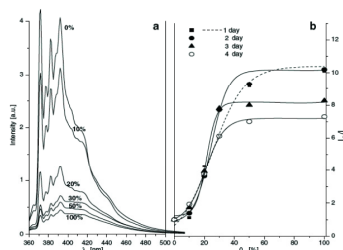
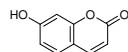


Figure. a Emission spectra of pyrene quenched by oxygen in silane sol on the second day of gelation; b Stern-Volmer plot for pyrene emission in silane sol quenched by oxygen during sol-gel transition; 0, 20, and 100%—gaseous nitrogen, air, and oxygen was transferred through the sol, respectively. A gaseous mixture of nitrogen and oxygen prepared earlier in a cylinder was transferred through the sol—10, 30, and 50% oxygen.

7-hydroxycoumarin



O₂ 346 / 456 (Luo *et al.*, 2009)

Sigma-Aldrich
Unit Size: ampule of 1 g
Price: 30.00 GBP

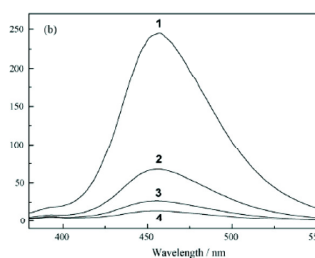
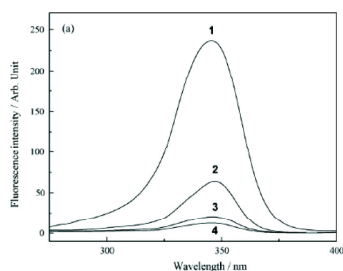
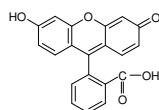


Figure. Excitation (a) and emission (b) spectra of (1) 7-hydroxycoumarin, (2) the system deoxygenated by bubbling with N₂ for 50 min, (3) the basic system with addition of 2.0 mmol L⁻¹ DMSO, and (4) the basic system with addition of 1.0 mol L⁻¹ DPPH. The initial solution pH was 4.0 and the initial concentration of dissolved oxygen was 9.22 mg L⁻¹. The reaction time was 20 min. Excitation wavelength was 346 nm, and emission detection wavelength was 456 nm.

Fluorescein



O₂ 494 / 518 (Arik *et al.*, 2005)

FL

Molecular Probes
Unit Size: 1 g
Price: 67.00 GBP

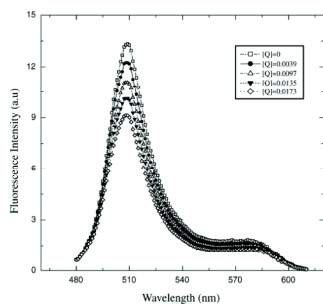


Figure. Corrected fluorescence spectra of fluorescein in alkali aqueous solutions with and without molecular oxygen in solution at 20 °C. [FL] = 1.0 × 10⁻⁶ M in 0.1N NaOH solution.

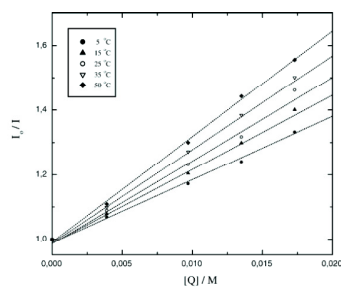
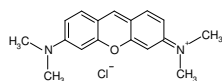


Figure. Stern-Volmer plot for fluorescein with varying molecular oxygen concentration at different temperatures, [FL] = 1.0 × 10⁻⁶ M in 0.1N NaOH solution

Pyronin Y
PyY



O₂ 540 / 570 (Celebi *et al.*, 2007)
(Arik *et al.*, 2003)

Sigma-Aldrich
Unit Size: 5 g
Price: 28.00 GBP

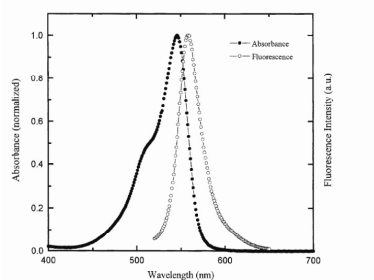


Figure. Normalized absorption and fluorescence spectra of Pyronin Y in deionized water at 20 °C. (Dye concentration is about 1.0 · 10⁻⁷ M.)

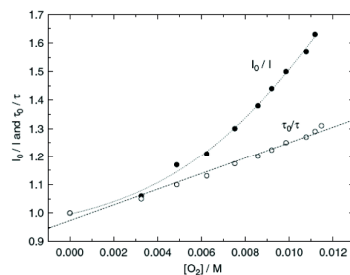
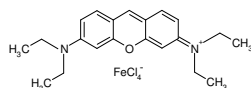


Figure. Stern-Volmer plots for PyY at 25 °C in aqueous solution.

Pyronin B
PyB



O₂ 550 / 580 (Celebi *et al.*, 2007)
(Onganer *et al.*, 1992)
(Arik *et al.*, 2003)

Sigma-Aldrich
Unit Size: 25 g
Price: 108.00 GBP

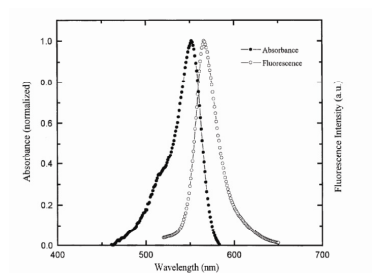


Figure. Normalized absorption and fluorescence spectra of Pyronin B in deionized water at 20 °C. (Dye concentration is about 1.0 · 10⁻⁷ M.)

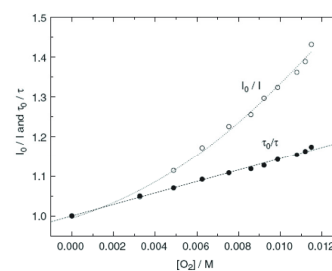
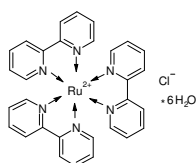


Figure. Stern-Volmer plots for PyB at 25 °C in aqueous solution.

Tris(2,2'-bipyridine)
dichlororuthenium(II)
hexahydrate
RuBpy



O₂ 450 / 620 (Kober *et al.*, 1985)

Sigma-Aldrich
Unit Size: 1 g
Price: 50.00 GBP

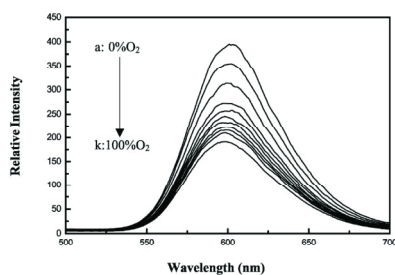


Figure. Emission spectra of the oxygen sensor of [Ru(bpy)₃]Cl₂/sphere at different oxygen concentrations: a=0, b=2.5, c=11, d=16, e=19, f=30, g=36, h=44, i=50, j=70, k=100 vol-%.

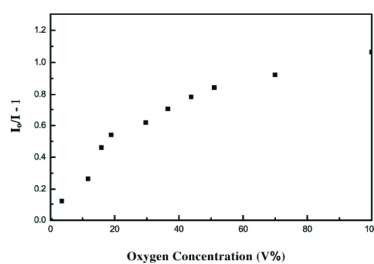
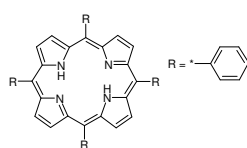


Figure. Stern-Volmer plot for the oxygen sensor of [Ru(bpy)₃]Cl₂/sphere.

5,10,15,20-Tetraphenylporphin, TPP



O₂ 515 / 650 (Potyrailo *et al.*, 1998)

Sigma-Aldrich
Unit Size: 1g
Price: 82.10 GBP

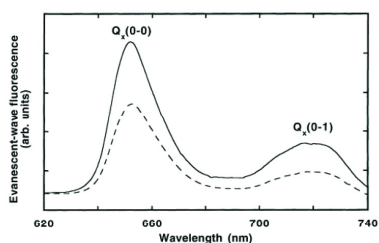


Figure. Evanescent-wave spectra of TPP immobilized into the silicone cladding of a PCS optical fiber. Fluorescence spectra upon exposure to dry nitrogen (solid line) and dry oxygen (dashed line). Excitation wavelength, 515 nm. (Q-bands - fluorescence peaks)

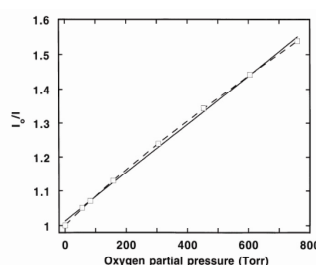
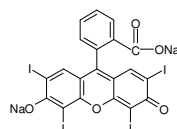


Figure. Stern-Volmer calibration plot for the new oxygen sensor. The 99.9% confidence intervals for nine replicate measurements are smaller than the plotted data points. Fluorescence excitation was provided by a yellow LED at 590 nm. Fluorescence was collected at 650 nm. The solid line is a fit to the Stern-Volmer equation; the dashed line is a fit to the two-site model.

Erythrosin B

EB



O₂ 530 / 690 (Bailey *et al.*, 2002)

Sigma-Aldrich
Unit Size: ampule of 1 g
Price: 30.00 GBP

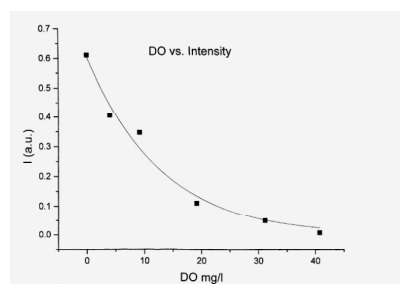


Figure. Variation of fluorescence intensity of erythrosin B in sol-gel at 590 nm with dissolved oxygen concentration.

Platinum(II) coproporphyrin ketone

PtCPK

O₂ 590 / 760 (O'Riordan *et al.*, 2007)

Luxcel Biosciences
Price: N/A

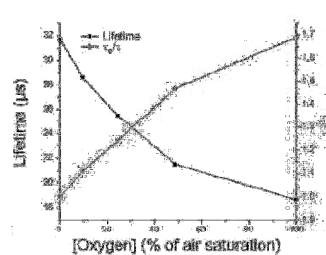
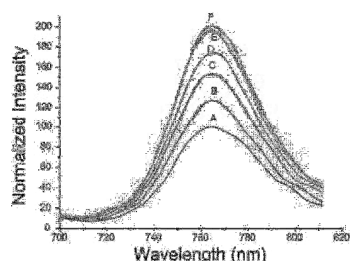
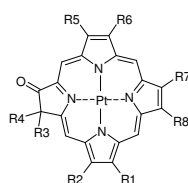


Figure. Emission of 1 M of the PtCPK probe in PBS at different O₂ concentrations: 100% (A), 48.7% (B), 24.4% (C), 9.7% (D), 2.4% (E), and 0% (F) of air saturation (left). Intensity calibration and Stern-Volmer plot for the PtCPK probe (right).

Platinum(II)
octaethylporphyrin
ketone



PtOEPK

O₂ 590 / 760 (Vollmer, 2005)
(Hartmann *et al.*, 1996)
(Papkovsky *et al.*, 1995)

Frontier Scientific
Unit Size: N/A

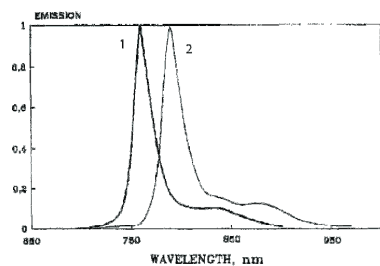


Figure. Corrected emission spectra of PtOEPK (1) and PdOEPK (2) in buffered micellar sulfite solution at 22 °C.

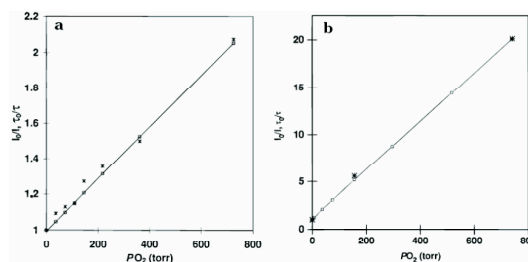


Figure. Stern-Volmer intensity (□) and weighted mean decay time plots (*) for (a) PtOEPK in pure PVC and (b) PtOEPK in PS (at T = 30 °C) versus applied oxygen partial pressure. Solid lines are best fits of a two-component model (eq 3) to the intensity quenching data.

2.3.4 Glucose sensitive fluorescent dyes

Table 2.4: List of glucose fluorescent dyes. They are listed by increasing emission wavelengths.

Indicator Name	Chemical Structure	Sensitivity	Excitation / Emission [nm]	References Supplier/Price
7-amino-4-methyl-coumarin– Concanavalin A AMCA–ConA		Glucose	360 / 450	(Lakowicz <i>et al.</i> , 1993) Molecular Probe Price: N/A
Tetramethylrhodamine isothiocyanate– Mannoside TRITC–Mannoside				

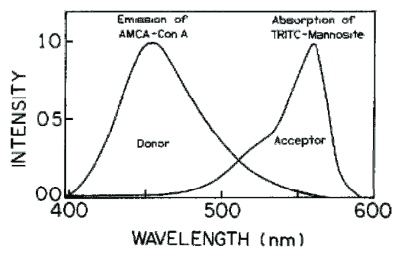


Figure. Emission spectrum of the donor AMCA-Con A and the absorption spectrum of the acceptor TRITC-mannoside.

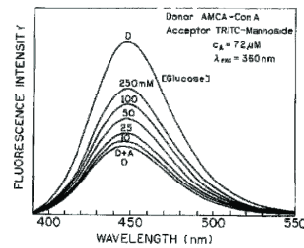
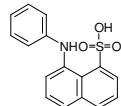


Figure. Bottom displacement of TRITC-mannoside from AMCA-Con A by glucose.

8-anilino-1-naphthalenesulfonic acid



Glucose

425 / 480

(Ibey *et al.*, 2006)
(D'Auria *et al.*, 1999)
(D'Auria *et al.*, 2001)

ANS

Molecular Probes
ANS

APO-Glucose oxidase



Unit Size: 5 g
Price: 17.00 GBP

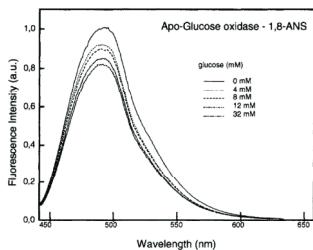


Figure. Emission spectra of 1,8-ANS-Glucose oxidase in the presence of glucose.

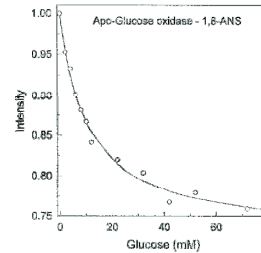
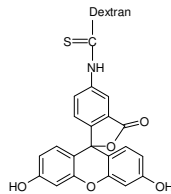


Figure. Glucose-dependent emission intensity of 1,8-ANS bound to apo-glucose oxidase. Excitation at 325 nm, emission at 480 nm.

Fluorescein isothiocyanate-Dextran



Glucose

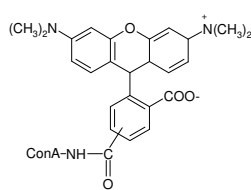
480 / 520

(Ibey *et al.*, 2006)
(McShane *et al.*, 2000)
(Russell *et al.*, 1999)
(Sato *et al.*, 2006)

FITC-Dextran

Sigma-Aldrich
FITC-Dextran
Unit Size: 100 mg
Price: 29.00 GBP
TRITC-Con A
Price: N/A

Tetramethylrhodamine isothiocyanate-Concanavalin A



TRITC-Con A

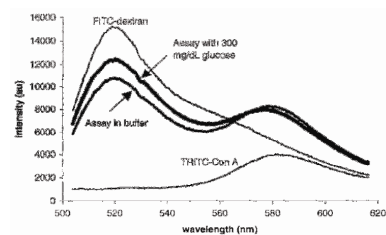


Figure. Plot of the emission spectrum of FITC and TRITC dyes illustrating the formation of Con A dextran complex through a FRET reaction and disruption of the FRET reaction through addition of glucose.

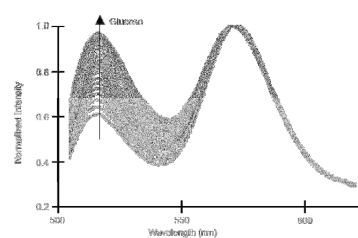


Figure. Normalized fluorescence emission spectra of 250:2.5 TRITC-Con A-FITC dextran mixture for 0-400 mg/dL glucose.

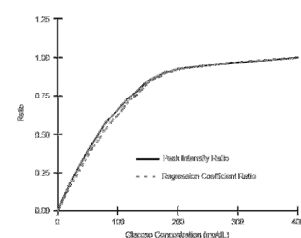
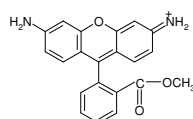


Figure. Sensor response curves showing fluorescence intensity and regression coefficient ratios versus glucose concentration.

Rhodamine 123

Rh123



Glucose

510 / 530

(Borth *et al.*, 1993)
(Pickup *et al.*, 2005)

Molecular Probes
Unit Size: 25 mg
Price: 56.00 GBP

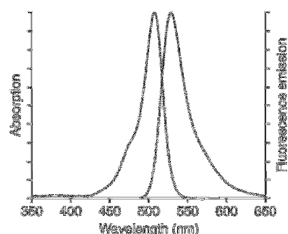


Figure. Absorption and fluorescence emission spectra of rhodamine 123 in methanol.

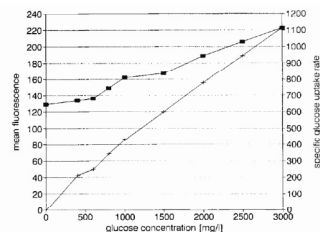


Figure. Culture of 306-C4 cells in media with defined glucose content. ■ Rh123 fluorescence (relative units). Data points shown are the means of triplicate cultures measured 6h after inoculation. The standard deviation was in all cases below 6%. +, specific glucose consumption rates as measured during 24 h (mg/10⁶ viable cells per day). Again data points represent the means of triplicate cultures and had a standard deviation of less than 6%.

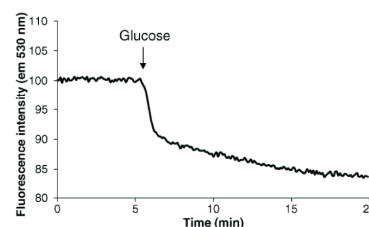
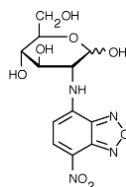


Figure. Glucose-induced quenching of the fluorescence of fibroblasts in culture, stained with the mitochondrial dye rhodamine 123.

2-(N-(7-nitrobenz-2-oxa-1,3-diazol-4-yl)amino)-2-deoxyglucose

2-NBDG



Glucose

465 / 540

(Nitin *et al.*, 2009)
(O'Neil *et al.*, 2005)
(Yamada *et al.*, 2007)

Sigma-Aldrich
Unit Size: 5 g
Price: 105.00 GBP

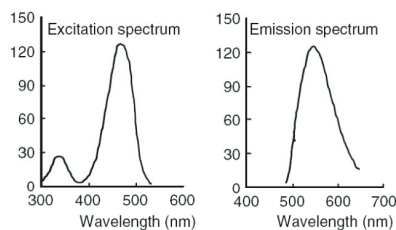


Figure. Fluorescence spectra. Emission spectrum: ex = 475 nm, em = 495-650 nm; excitation spectrum: em = 550 nm, ex = 300-520 nm.

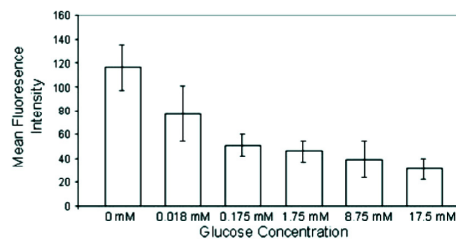
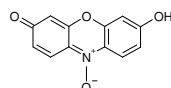


Figure. Average fluorescence intensity of labeled cells with a fixed concentration of 2-NBDG as the media concentration of glucose is varied from 0 to 17.5 mM.

Resazurin



Glucose

568 / 582

(Maeda *et al.*, 2001)

Orgchem
Price: N/A

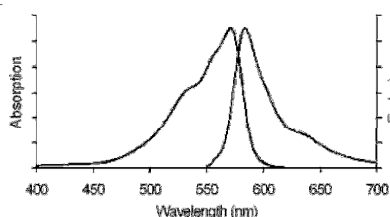


Figure. Absorption and emission spectra of resorufin in pH 8 buffer.

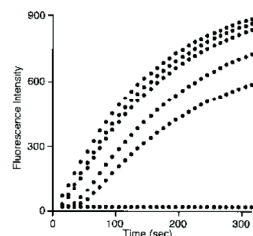
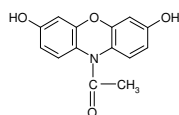


Figure. Effects of concentration of glucose on fluorometric traces obtained during 5 min incubation of a mixture of resazurin (200 nmol/L glucose and 620) (10 mg) in 3.5 ml phosphate buffer at 25 °C. Concentration of glucose (mmol/L): 2.0 (a), 1.0 (b), 0.4 (c), 0.2 (d), 0.1 (e-f). Traces d-f were obtained on different runs under essentially the same conditions (ex = 568 nm, em = 582 nm).

Amplex Red
Glucose/Glucose
Oxidase Assay Kit



Glucose

570 / 585

Molecular Probes
Unit Size: 1 kit
Price: 209.00 GBP

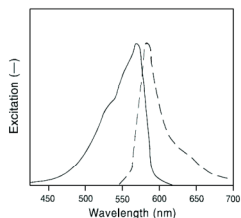


Figure. Normalized fluorescence excitation and emission spectra of resorufin, the product of the Amplex® Red reaction.

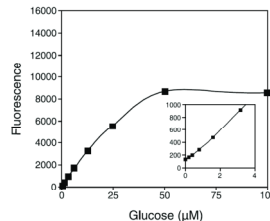
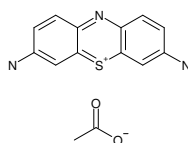


Figure. Detection of glucose using the Amplex Red Glucose/Glucose Oxidase Assay Kit. Reactions containing Amplex Red, HRP, glucose oxidase and glucose in sodium phosphate buffer, pH 7.4. (ex=530 nm, em=590 nm). The inset shows the sensitivity and linearity of the assay at low levels of glucose.

3, 7-diamino-5-
phenothiazinium
acetate



Glucose

590 / 620

(Sharma *et al.*, 1994)
(Salimi *et al.*, 2007)
(Gemeay *et al.*, 2004)

Thionin acetate

Acros Organics
Unit Size: 5 g
Price: 26.40 GBP

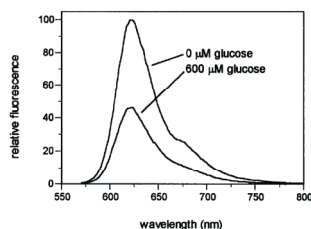


Figure. Effect of 600 µM glucose on the emission spectra of thionin (1 µM) due to SQT, sample excited at a wavelength of 590 nm.

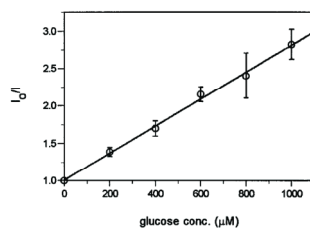


Figure. Substrate induced quenching (SIQ) plot for the SIQ equilibrium of thionin (1 µM) by glucose at an emission wavelength of 620 nm.

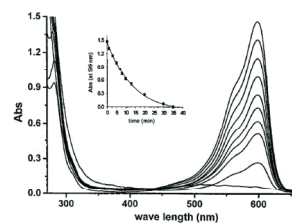
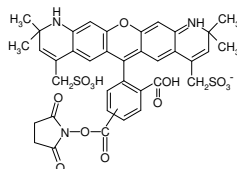


Figure. Time resolved absorption spectra of the reaction of TH of 5×10^{-5} mol dm⁻³ with H2O2 of 0.1 mol dm⁻³ in the presence of 0.01 µg of S(Cu/amm)42+ at 30 °C.

Alexa Fluor 568–
Dextran



Glucose

650 / 668

(Ibey, 2006)
(Ibey *et al.*, 2005)
(Liang *et al.*, 2005)

Alexa Fluor 647
conjugate–
Concanavalin A

Alexa Fluor 568
carboxylic acid,
succinimidyl ester

Alexa Fluor 647 -
proprietary

Molecular Probes
Alexa 647–Con A
Unit Size: 5 mg
Price: 110.00 GBP
Alexa Fluor 568–
Dextran
Unit Size: 5 mg
Price: 229.00 GBP

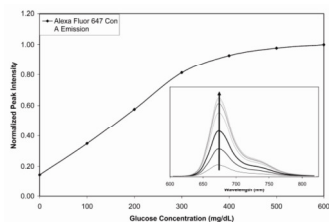


Figure. Normalized peak intensity versus glucose concentration. By removing the AF594 label from the glycoprotein within the assay and titrating glucose into the solution, this figure proves that the devised assay does not require multiple fluorophores and that the AF594 label can serve as an internal reference. The spectra are inset within the figure.

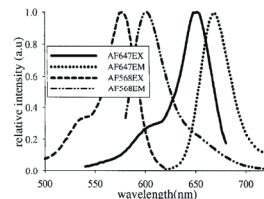


Figure. Normalized excitation (dashed line) and fluorescence (dashed dotted line) spectra of Alexa Fluor (AF) 568-dextran (dextran) and the normalized absorption (solid line) and fluorescence (dotted line) spectra of AF647-concanavalin A (concanavalin A). For clarification and simplification, the donor or acceptor concentrations were denoted as the concentration of dextran or ConA in the entire paper.

2.4 Conclusions

Considering the variety of analytical applications using fluorescence dye indicators in the detection methods it is not possible to determine that one particular dye is generally “better” than others. Instead, a more reasonable approach is to designate which dyes are better suited for particular applications. Therefore, it is necessary to define the desired characteristics of fluorophores that could be used.

The wide spectrum of fluorescent dyes which has been described in literature are commercially available often at relatively low price. They can be classified in relation to characteristic properties of each dye, including various sensitivity, spectral properties, solubility, etc., specific needs of customers (e.g. indicators, energy transfer, drug screening, markers for biological molecules, etc.) and instrument specifications (measurement methods, excitation sources, optical filters or sensitivity). It is particularly valuable when a new assay is developed and it is crucial to choose the most suitable fluorescent labels from all available options.

In this study, appropriate fluorescent dyes were chosen in the first instance due to their high detection sensitivities and dynamic range for given environmental factors, excitation and emission wavelengths in VIS-NIR range of light spectrum, presence of functional chemical groups to enable binding with other molecules, stability to photobleaching as well as excitation coefficient.

It was also important to pay attention to prices of suitable dye-indicators to minimise the cost of measurements. This information was important in further optimisation of the mixture of dyes involving testing of increased number of indicators and aiming to obtain their extensive variety, which could enable analysis of different parameters and analytes within samples.

3. Second objective: optimisation of fluorescent dye mixtures

3.1 Introduction

The specific objective of further investigation was to establish a combination of environmental-sensitive fluorescent dyes suitable to measure changes pH, temperature and dissolved oxygen and glucose concentration. Based on a drawn up list of fluorescent indicators and their characterisation, several probes were chosen for further investigation. The spectroscopic measurements were first performed on single dyes and the obtained excitation and emission spectra were used for hypothetical examination of their simultaneous utilisation. Potential mixtures of pH-sensitive, temperature-sensitive, oxygen-sensitive and hydrogen peroxide-based glucose probes were first illustrated in Matlab, to exclude combinations of dyes, which are not suitable to be used in the same solution. The collection of promising mixtures were later analysed experimentally.

3.2 Selection criteria for a mixture of fluorescent dyes

The favoured dyes were selected according to several important criteria:

- Dyes should have the ability to change their optical properties in response to suitable changes of an environment and it should be possible to monitor at least some contribution from the individual dyes in the total spectrum of their mixture.
- The mixture should contain several fluorescent dyes, preferably more than two.
- They should be responsive in VIS-NIR.
- It is also desired to choose fluorescent dyes with emission maxima at wavelengths separated by at least 20 nm.
- Selected dyes should preferably be soluble in water, possess high quantum yield, low toxicity and low photo-blanching (photo-decomposition).

Additionally, the selected dyes should not be considered as specific in the sense that their response can be triggered by more than one parameter. It is for this reason that

multivariate calibration is further required for quantitative and qualitative analysis of their collective response.

3.3 Experimental section

Following above requirements several suitable fluorescent dyes have been selected and used in further spectrofluorometric analysis.

3.3.1 Chemicals

Fluorescent indicators were obtained from Sigma-Aldrich, except Oregon green 514 purchased from Molecular Probes and Thionin acetate purchased from Acros Organics. Concentrated solutions of dyes were prepared in deionised water and stored in ~ 5 °C and covered with aluminium foil to protect them from light. Various concentrations of water/dyes solutions were used later in optimisation of their mixtures in order to have a balance in measurements of fluorescence intensity.

All measurements were performed in sodium phosphate buffer (PB) consisted of sodium phosphate dibasic (Na_2HPO_4) and sodium phosphate monobasic (NaH_2PO_4) diluted in distilled water. The desired pH of buffer was prepared based on the ratio of monobasic and dibasic sodium phosphate.

3.3.2 Sample preparation

The spectrofluorometric investigation (excitation – emission – intensity spectra) of fluorescent dyes was performed separately for each dyes, as well as together with others. The sample solutions used in measurements were composed of 3 ml 50 mM phosphate buffer (PB) and 10 μl of each water/dye stock solution.

3.3.3 Fluorescence measurements

All measurements were performed using a three-dimensional spectrofluorometer, Jobin Yvon-SPEX, model FL-3D (Instruments SA (Stanmore, Middlesex, UK), (Figure 3.1).



Figure 3.1: The spectrofluorometer capable of acquiring three-dimensional excitation–emission matrix (EEM) fluorescence spectra.

The spectrofluorometer provided three-dimensional, excitation–emission-intensity data of fluorescent compounds. A schematic illustration of a three-dimensional spectrofluorimetry with CCD detection is shown in Figure 3.2.

Light from a broad wavelength excitation source (Xenon lamp) was dispersed in a vertical plane using an excitation polychromator and passed through the sample. Emitted fluorescence was dispersed in a horizontal plane by emission polychromator and collected on a CCD 2D detector array (Setford *et al.*, 2000). For both excitation and

emission, light was dispersed such that its component wavelengths were spatially separated. A shutter arrangement (a high speed emission shutter, 0.01-5 s, located in the emission spectrograph) was used to illuminate the sample for the desired exposure time, after which the photo-generated charge stored within the device was collected and processed (e.g. via CCD read-out operation). The 3D spectrofluorometer was designed to allow imaging of a full excitation and emission matrix (EEM) spectrum from a fluorescent sample over a range of excitation (74 – 691 nm) and emission (228 – 725 nm) wavelengths.

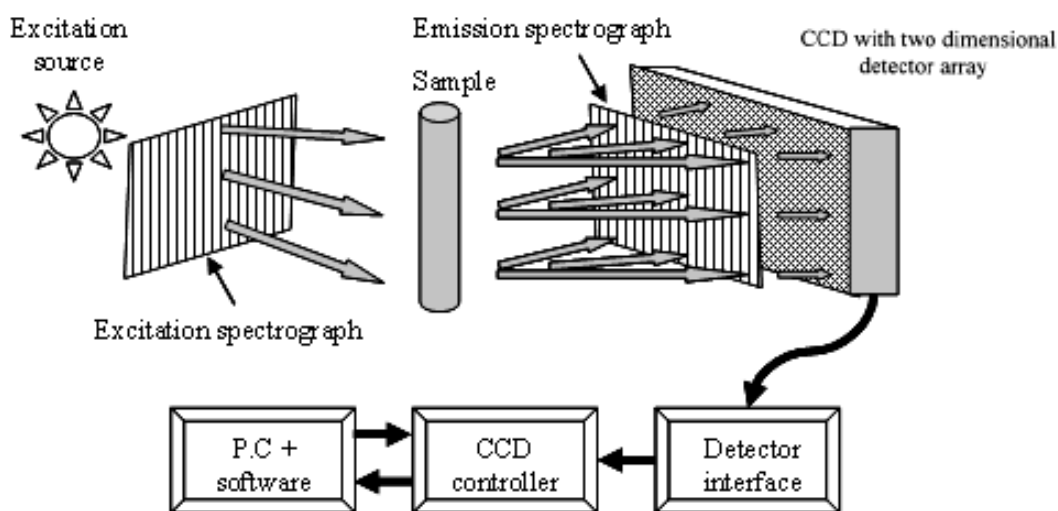


Figure 3.2: Schematic illustration of three-dimensional spectrofluorometry with CCD detection. Adopted from (Cauchi, 2006).

In all experiments, the spectra were recorded over whole range of excitation and emission wavelengths based on the technical specification of the spectrofluorometer. The fluorescence measurements were performed with 0.5 s of time exposure using 4 ml quartz cuvettes with stoppers and a light path of 10 mm.

3.3.4 Three-dimensional data display

The software which was provided for 3D spectrofluorometer (Grams/32 version 4.14, Galactic Inc., 2000) enabled illustration of fluorescence spectra in 3D format, whereby

the x-, y- and z-axes corresponded to the emission, excitation wavelengths and fluorescence intensity. These spectra could also be seen in 2D, whereby the x- and y-axes corresponded to emission and excitation wavelengths, and fluorescence intensity was orientated into the plane of the paper. The contour lines were equated to signal intensity in the same manner as the contour lines on a geographical survey map. Excitation and emission values could also be displayed in pixels.

The problem with the software was that the data could only be exported as an ASCII file in 2D plane (emission wavelengths and fluorescence intensity). The excitation values were not stored. Therefore to enable illustration of 3D pictures, data was exported in original SPC format of spectra and converted into image format using Matlab (version 7.3.0, MathWorks Inc., 2006). The excitation values were calculated based on the first and last values of excitation wavelengths and the known spectral resolution. Creating a Matlab script file suitable to convert data was also part of the work. The pseudo-code of the script is enclosed in Appendix A.1.

3.4 Results and Discussion

3.4.1 Choice of fluorescence dyes

Based on the lists of fluorescent dyes and specific criteria for their mixtures, selected probes for further examination included:

- **pH-sensitive:** Fluorescein (FL), Hydroxypyrene-1,3,6-trisulfonic acid trisodium salt (HPTS), Oregon Green 488 (OG488), Oregon green 514 (OG514);
- **temperature-sensitive:** 5(6)-carboxytetramethylrhodamine (TAMRA), Fluorescein isothiocyanate (FITC), Rhodamine 101 (R101), Rhodamine B (RB);
- **oxygen-sensitive:** Tris(2,2'-bipyridine) dichlororuthenium(II) hexahydrate (RuBpy).

Additionally, hydrogen peroxide-based glucose probe, Thionine Acetate (THA), which is sensitive to hydrogen peroxide (HRP), allows further expansion of possible applications into enzymatic assays, where HRP is a product or substrate of the reaction

(Cardosi, 2000; Gemeay *et al.*, 2004). It has been also reported as carboxylic groups (-COOH) indicator, important in engineering of biocompatible polymer surfaces (Ivanov *et al.*, 1996; Tzoneva *et al.*, 2008).

From an extensive group of readily available fluorescent pH indicators, FL and HPTS were chosen in the first instance because of their well characterised optical properties and frequent use. Criteria for the choice were also their response within visible light spectrum, already proved high sensitivity to pH with wide dynamic range and successful results of their immobilisation. Despite many advantages these indicators are able to sense pH near physiological level yet seem to be unpractical at lower pH. For this reason fluorescence indicator such OG480 and OG514 were selected. Both dyes have shown high sensitivity for low pHs. Further experiment also proved the sensitivity of HPTS to ionic strength (concentration) of PB solution (see Chapter 4.3.2.).

To control the temperature of the sample several dyes were chosen whereat the criteria for the choice of these indicators were: a suitable temperature range of their response (approximately from 20 to 45 °C), excitation and emission wavelengths, photostability, chemical structure and general information, which have been presented in the literature. As mentioned in the introduction of this chapter, most of fluorescent dyes show some response to temperature changes and therefore this is where only dyes responsive to temperature must be chosen.

For the detection of oxygen level RuBpy was chosen considering that its high quality to measure oxygen has already been shown in the literature. Additionally, its responsive for longer wavelength of light, which is promising for combining it with other dyes of the choice.

3.4.2 Excitation/emission spectra of selected fluorescent dyes

Initially, measurements of fluorescence spectra were performed with individual dyes using 3D spectrofluorometer, which allowed fluorescence measurements over multiple excitation/emission wavelengths. These spectra were later used for investigation on the dyes mixtures. Obtained spectra are presented below (Figure 3.3-3.12).

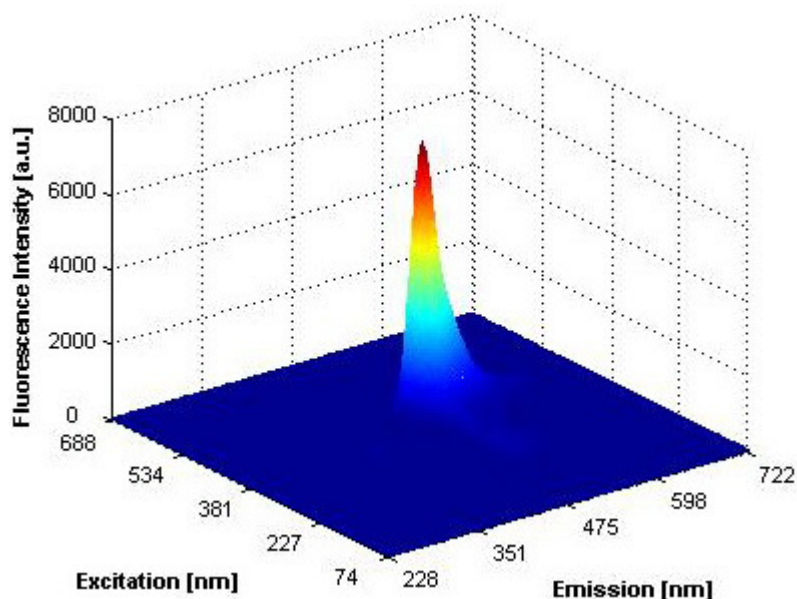


Figure 3.3: Three-dimensional colour mapped surface diagram of FL (0.004 μM) in 50 mM PB buffer (pH 7.4).

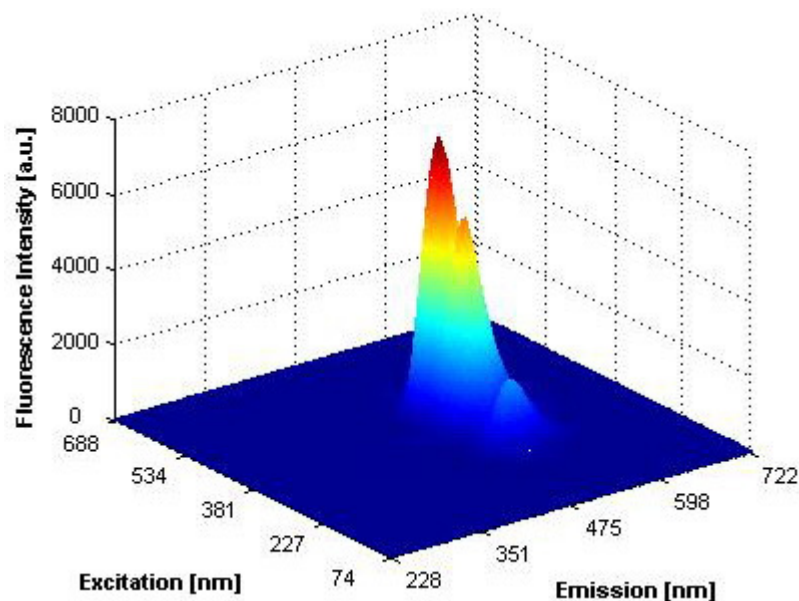


Figure 3.4: Three-dimensional colour mapped surface diagram of HPTS (0.03 μM) in 50 mM PB buffer (pH 7.4).

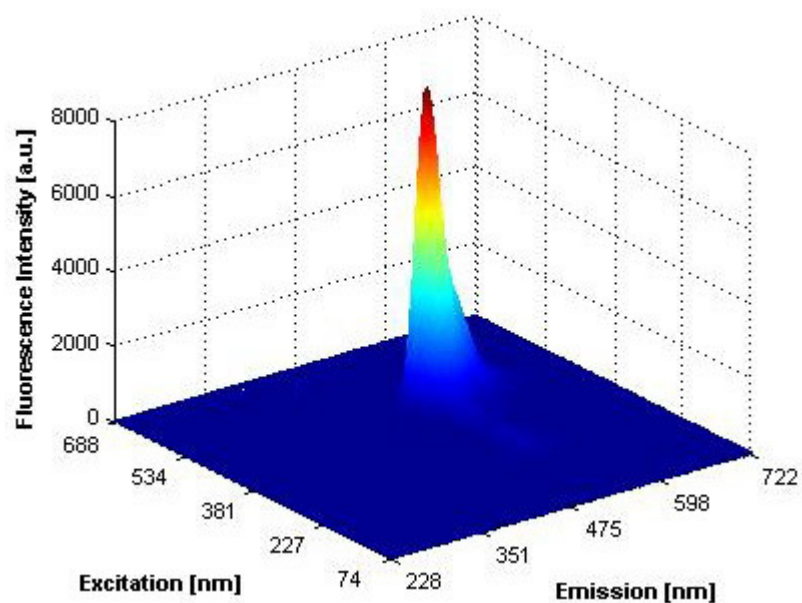


Figure 3.5: Three-dimensional colour mapped surface diagram of OG514 (0.006 μM) in 50 mM PB buffer (pH 7.4).

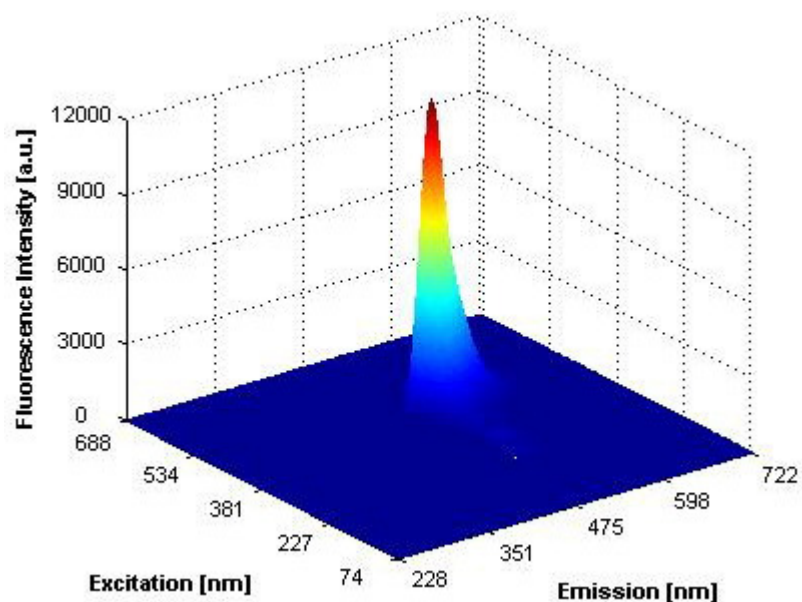


Figure 3.6: Three-dimensional colour mapped surface diagram of OG488 (0.01 μM) in 50 mM PB buffer (pH 7.4).

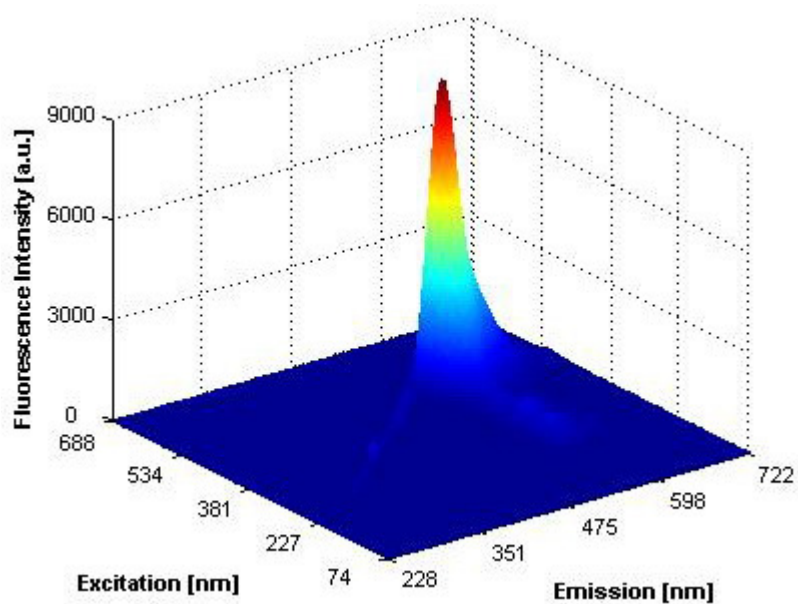


Figure 3.7: Three-dimensional colour mapped surface diagram of TAMRA ($0.02 \mu\text{M}$) in 50 mM PB buffer (pH 7.4).

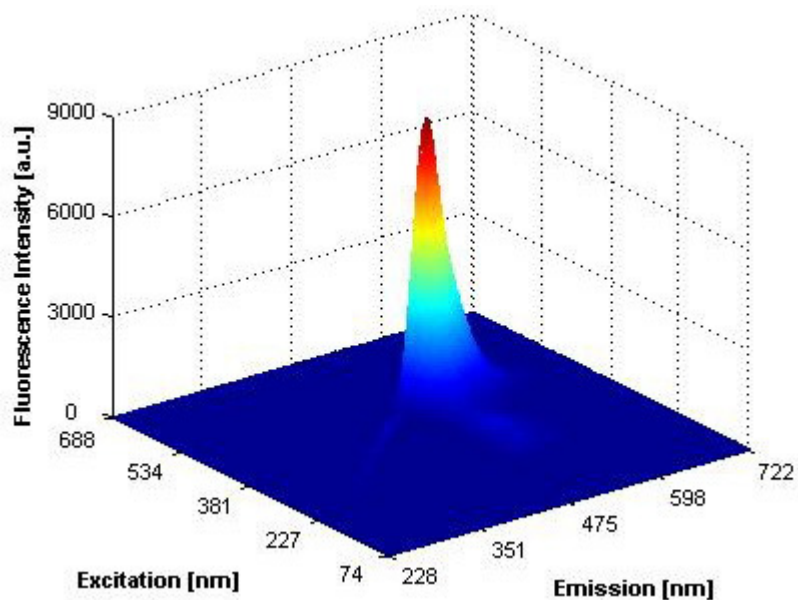


Figure 3.8: Three-dimensional colour mapped surface diagram of FITC ($0.02 \mu\text{M}$) in 50 mM PB buffer (pH 7.4).

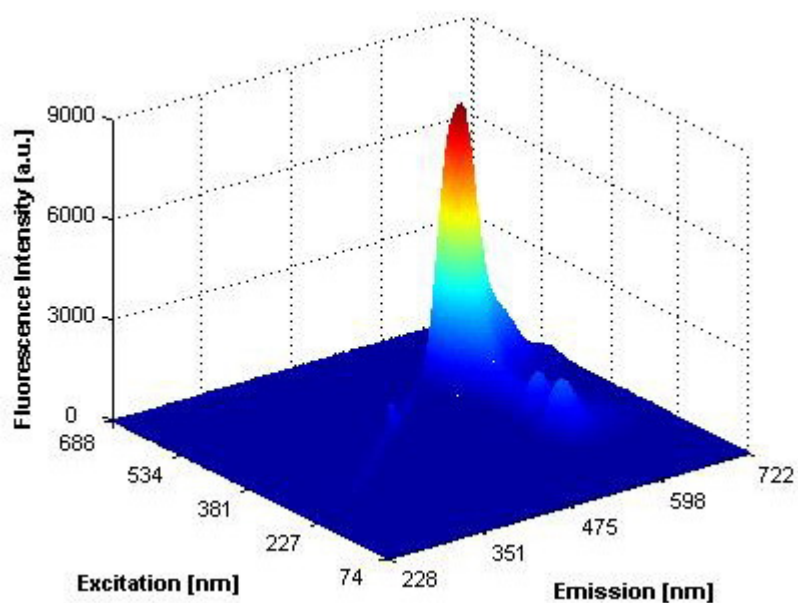


Figure 3.9: Three-dimensional colour mapped surface diagram of R101 (0.02 μM) in 50 mM PB buffer (pH 7.4).

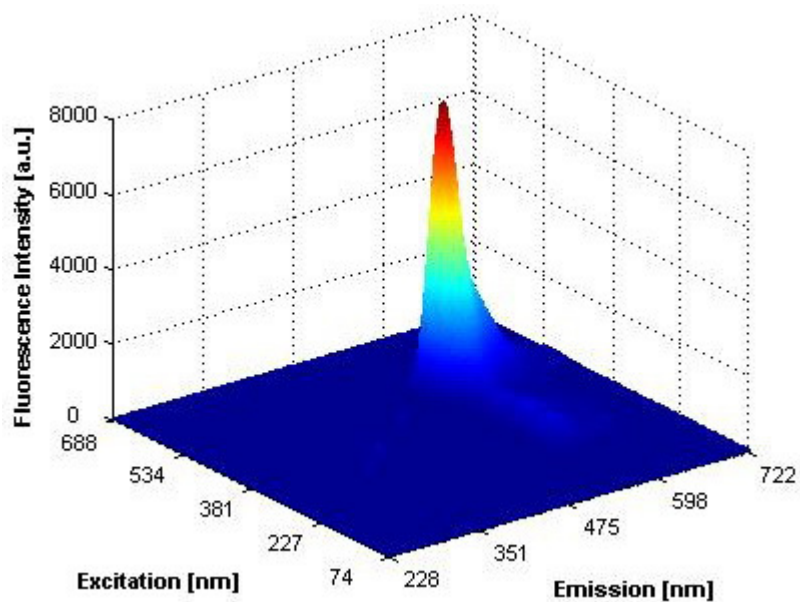


Figure 3.10: Three-dimensional colour mapped surface diagram of RB (0.02 μM) in 50 mM PB buffer (pH 7.4).

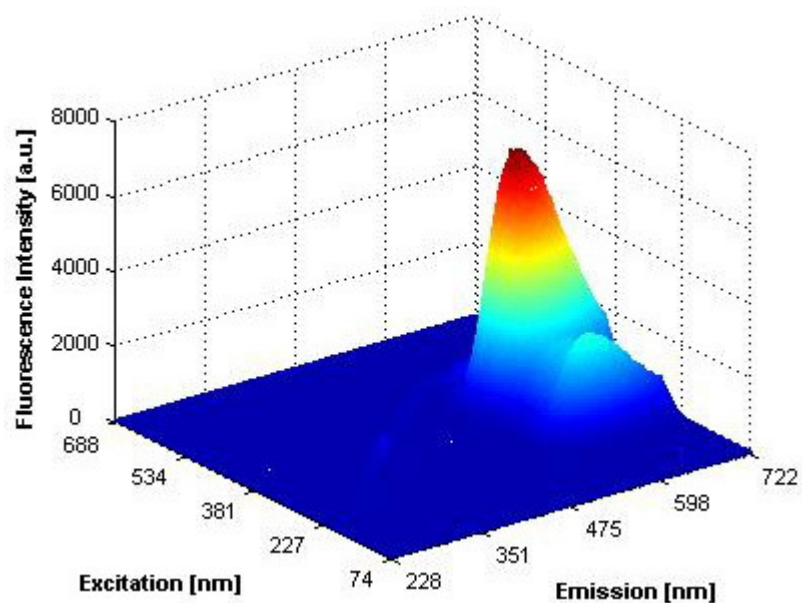


Figure 3.11: Three-dimensional colour mapped surface diagram of RuBpy (2.8 μM) in 50 mM PB buffer (pH 7.4).

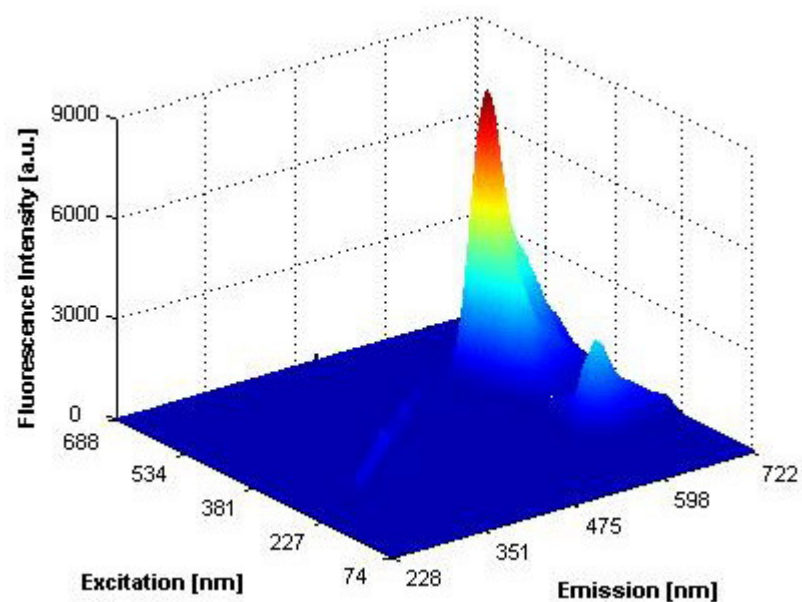


Figure 3.12: Three-dimensional colour mapped surface diagram of THA (2 μM) in 50 mM PB buffer (pH 7.4).

The maxima of excitation and emission for selected fluorescent dyes are listed in Table 3.1. All dyes revealed strong excitation and emission peaks at the wavelengths similar to the data published in the literature (see Chapter 2).

The presented measurements show that distances between emission maxima of some selected probes might be sufficient to make their mixtures feasible, with noticeable separation of their fluorescence intensities. Moreover, these fluorescent dyes are characterised by different sensitivities thus it might be possible to establish mixture with various specifications.

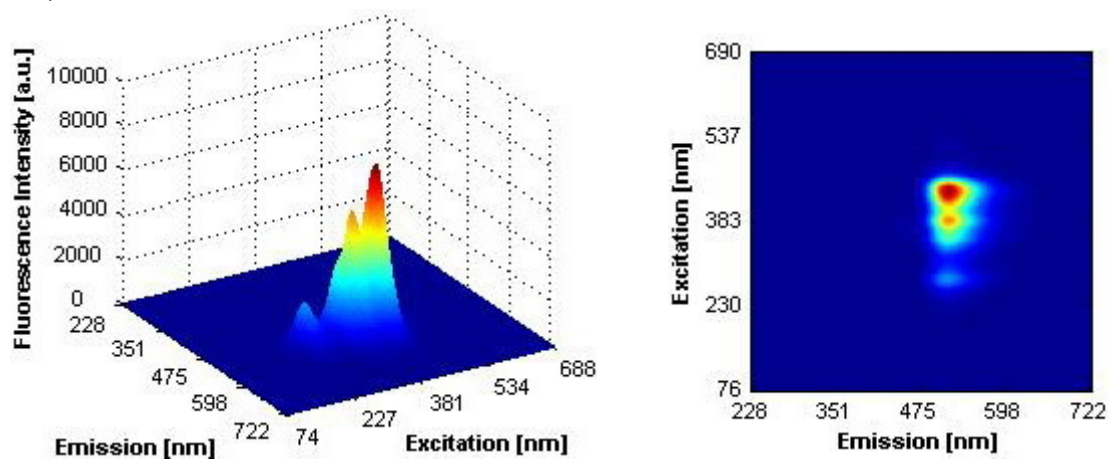
Table 3.1: List of excitation and emission maxima of selected fluorescent dyes.

Dye Name	Excitation [nm]	Emission [nm]
Fluorescein FL	465	516
Hydroxypyrene-1,3,6-trisulfonic acid trisodium salt HPTS	470	527
Oregon green 488 OG488	465	516
Oregon green 514 OG514	480	529
5(6)-carboxytetramethylrhodamine TAMRA	520	575
Fluorescein isothiocyanate FITC	468	521
Rhodamine 101 R101	517	600
Rhodamine B RB	519	579
Tris(2,2'-bipyridine) dichlororuthenium(II) hexahydrate RuBpy	440	623
Thionin acetate THA	520	624

3.4.3 Hypothetical mixtures of environmentally sensitive fluorescent dyes

Potential mixtures of selected dye indicators were illustrated in Matlab by merging their individual excitation/emission/intensity spectra. This hypothetical examination, which is based on a subjective visual inspection, allowed fast analysis of proposed dyes and finding suitable mixtures for further measurements. The favoured combination should contain several dye indicators which are characterised by different sensitivities and have discreet emission maxima separated enough to allow monitoring of the individual dyes contribution in the overall spectrum of their mixture. As a result three possible mixtures composed of five fluorescent dyes were obtained and analysed. The first possible mixture composed of HPTS, FITC, RB, RuBpy and THA is presented in Figure 3.13.1-2. The second, composed of HPTS, OG514, RB, RuBpy and THA, and the third mixture composed of HPTS, FL, RB, RuBpy and THA are presented in Figure 3.14.1-2 and Figure 3.15.1-2 respectively. As shown in figures based on theoretical calculations, three mixtures composed of five fluorescent dyes were possible to obtain, with their intensity peaks quite well separated, specially for mixture two (Figure 3.14.2-E). However to make a final objective decision which of these mixtures should be chosen and used in an optical assay development, this subjective visualisation had to be confirmed by experimental examination.

A)



B)

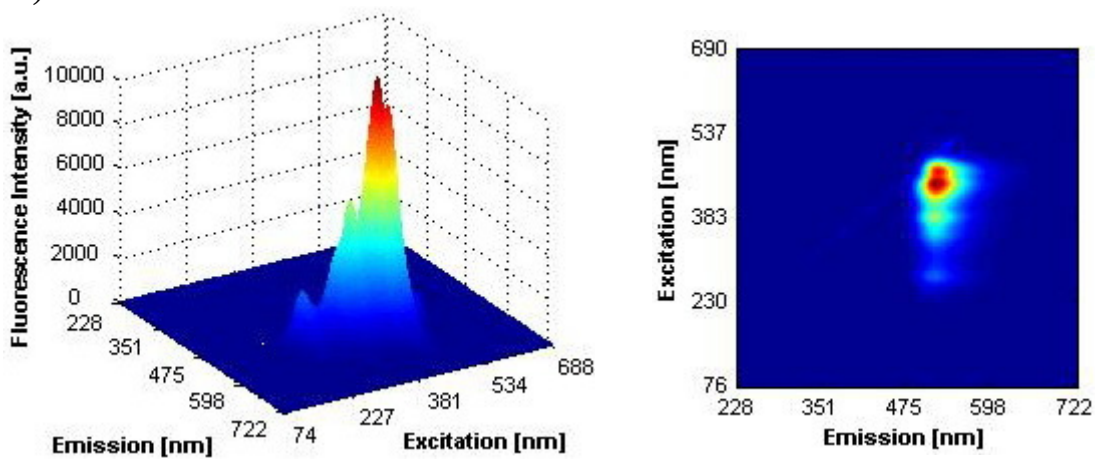
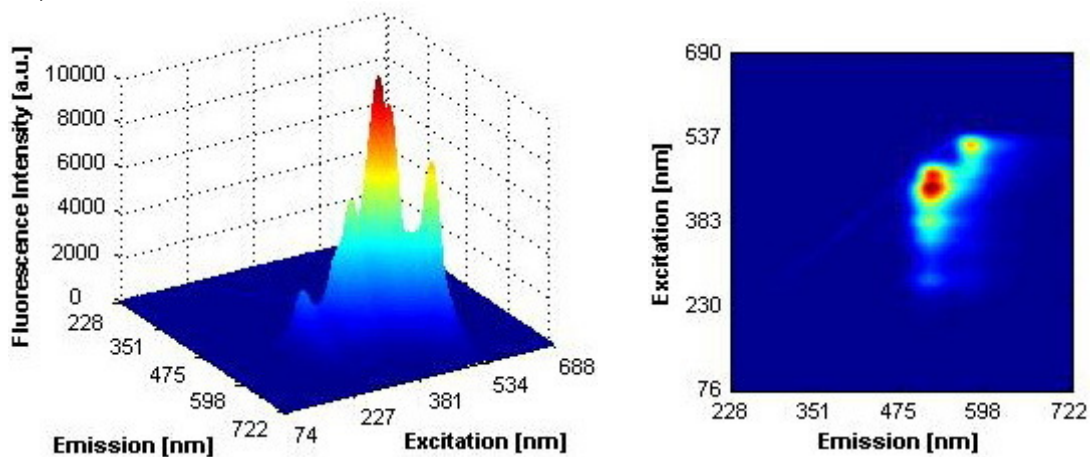
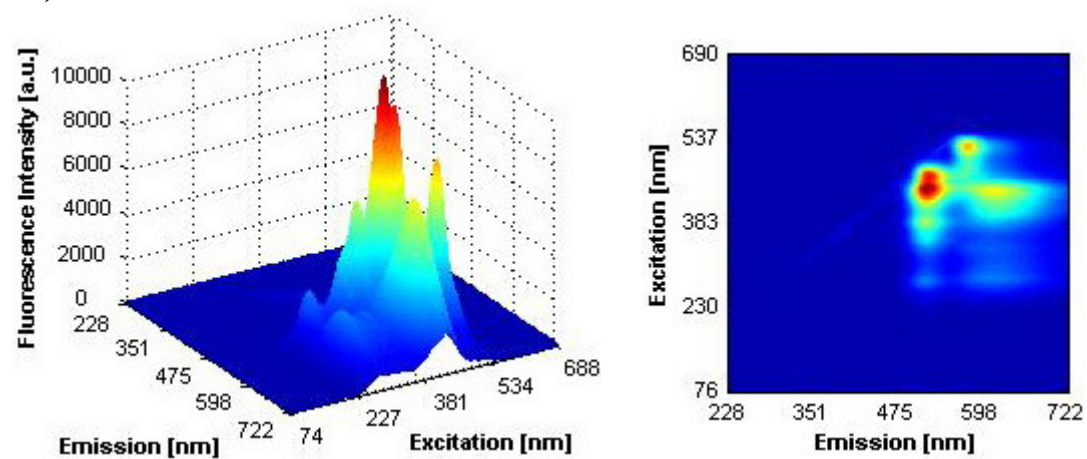


Figure 3.13.1: Three-dimensional colour mapped surface diagrams (right) and colour filled contour diagrams (left): HPTS (A), mixture of HPTS and FITC (B). Measurements of single dyes were performed in 50 mM PB buffer at pH 7.4.

C)



D)



E)

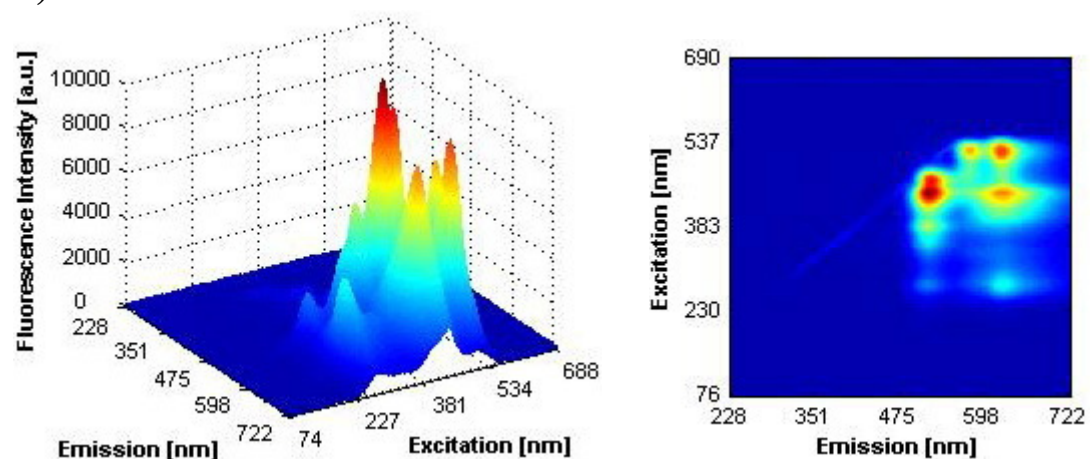


Figure 3.13.2: Three-dimensional colour mapped surface diagrams (right) and colour filled contour diagrams (left): mixture of HPTS, FITC and RB (C), mixture of HPTS, FITC, RB and RuBpy (D), mixture of HPTS, FITC, RB, RuBpy and THA (E). Measurements of single dyes were performed in 50 mM PBS buffer at pH 7.4.

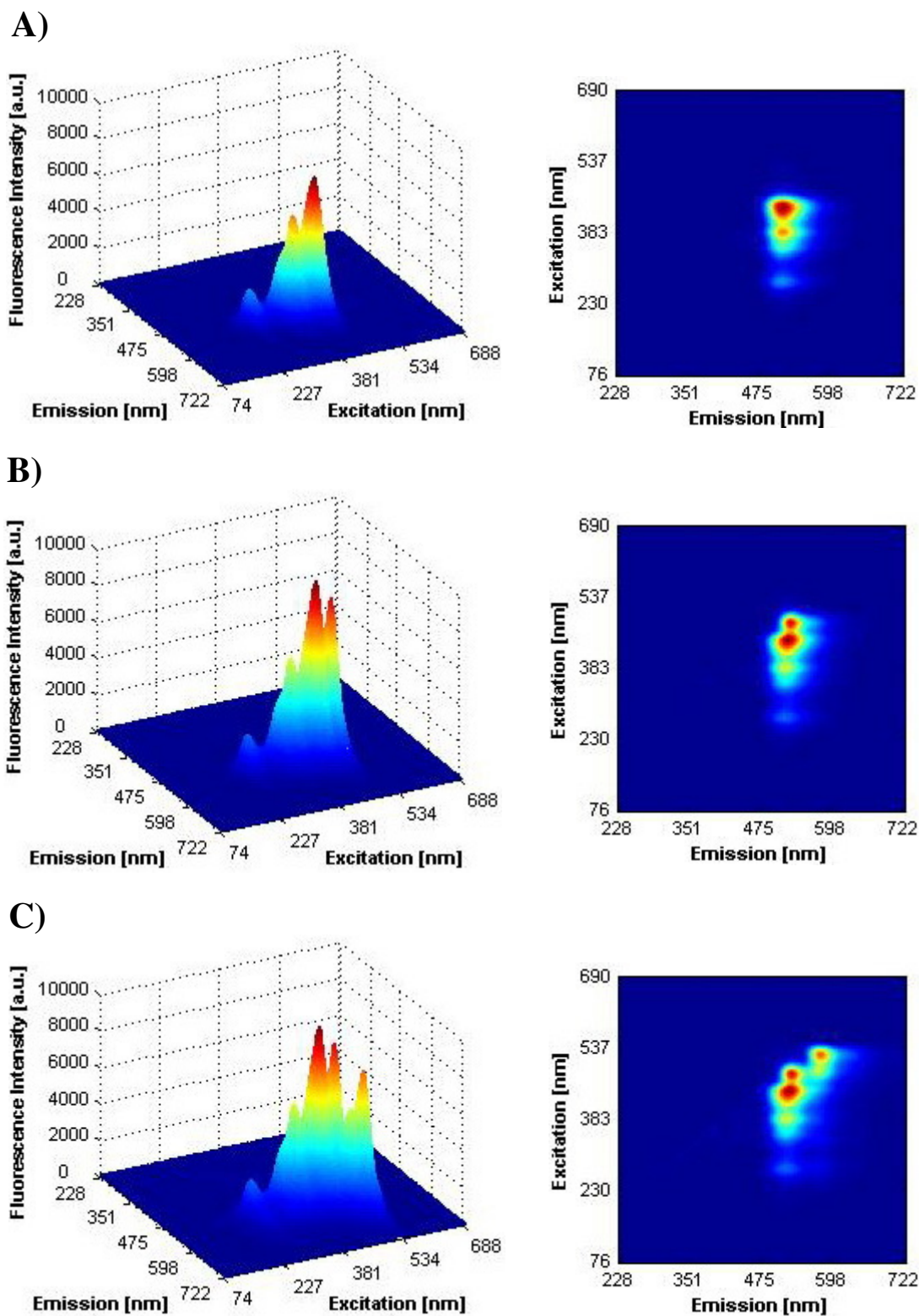
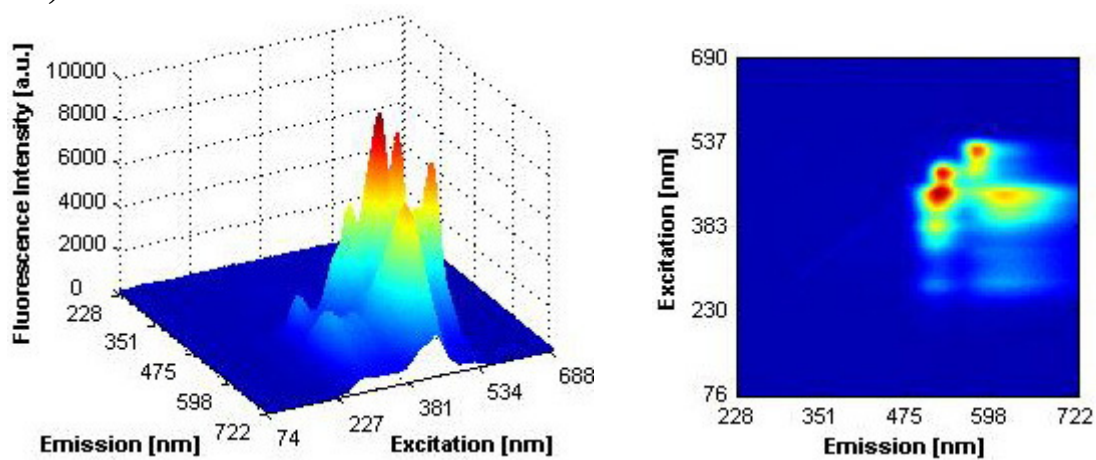


Figure 3.14.1: Three-dimensional colour mapped surface diagrams (right) and colour filled contour diagrams (left): HPTS (A), mixture of HPTS and OG514 (B), mixture of HPTS, OG514 and RB (C). Measurements of single dyes were performed in 50 mM PB buffer at pH 7.4.

D)



E)

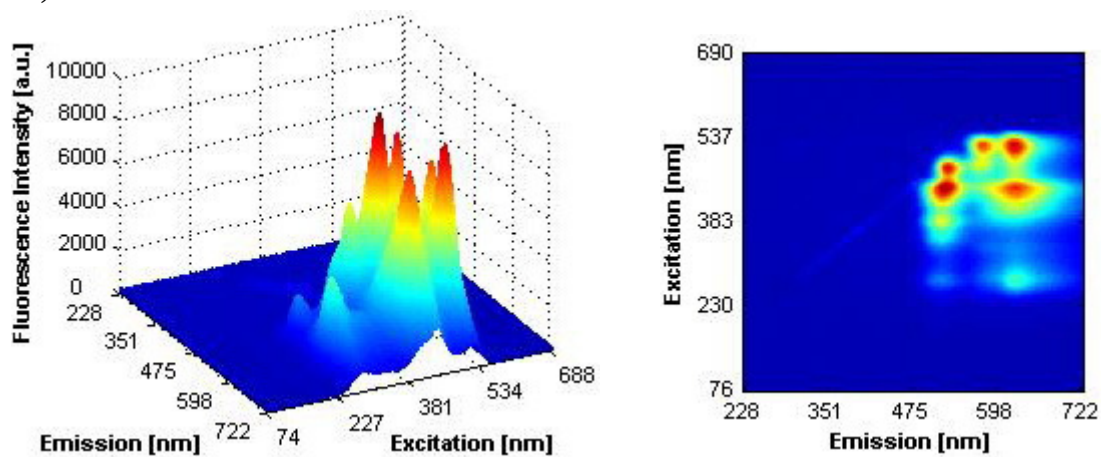
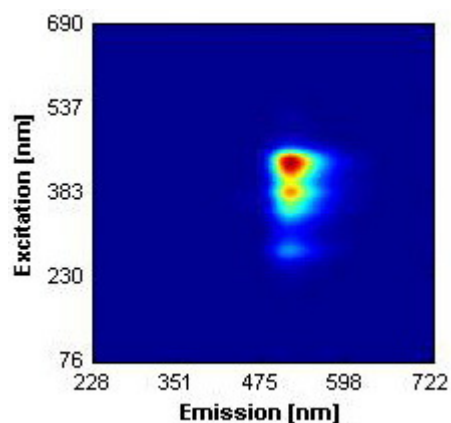
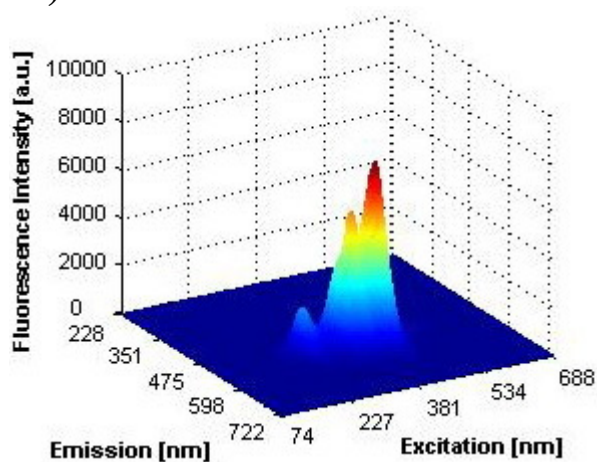
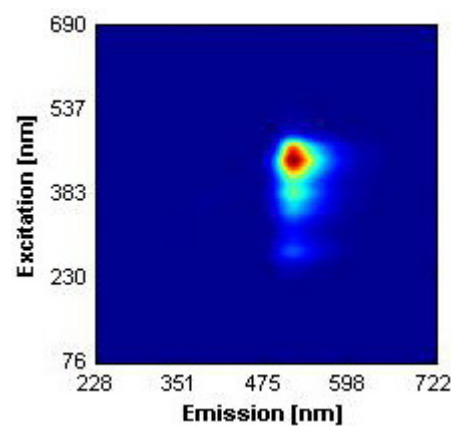
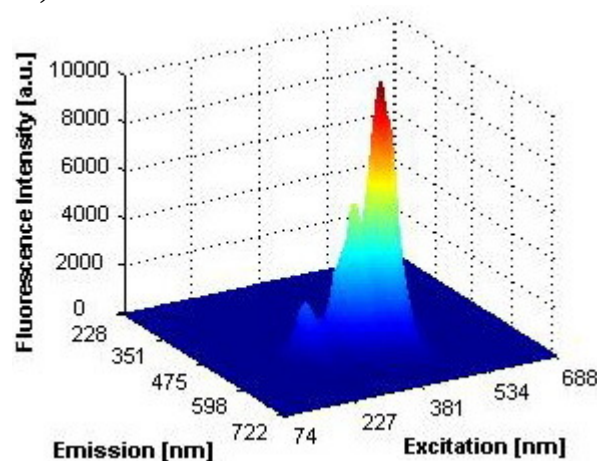


Figure 3.14.2: Three-dimensional colour mapped surface diagrams (right) and colour filled contour diagrams (left): mixture of HPTS, OG514, RB and RuBpy (D), mixture of HPTS, OG514, RB, RuBpy and THA (E). Measurements of single dyes were performed in 50 mM PBS buffer at pH 7.4.

A)



B)



C)

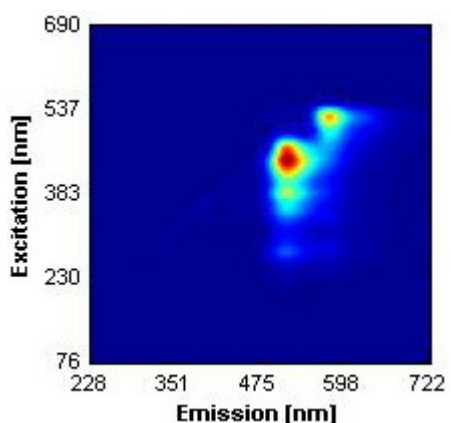
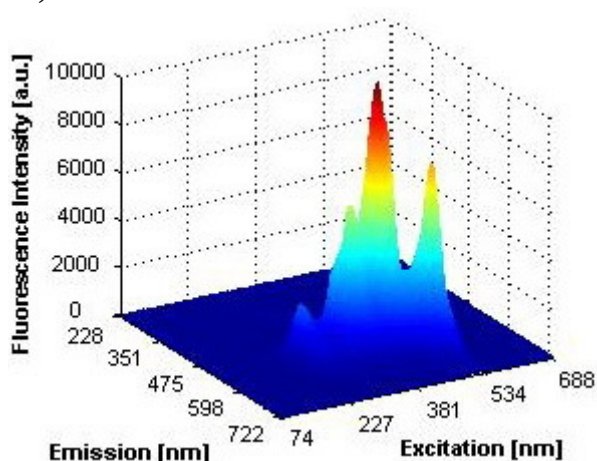
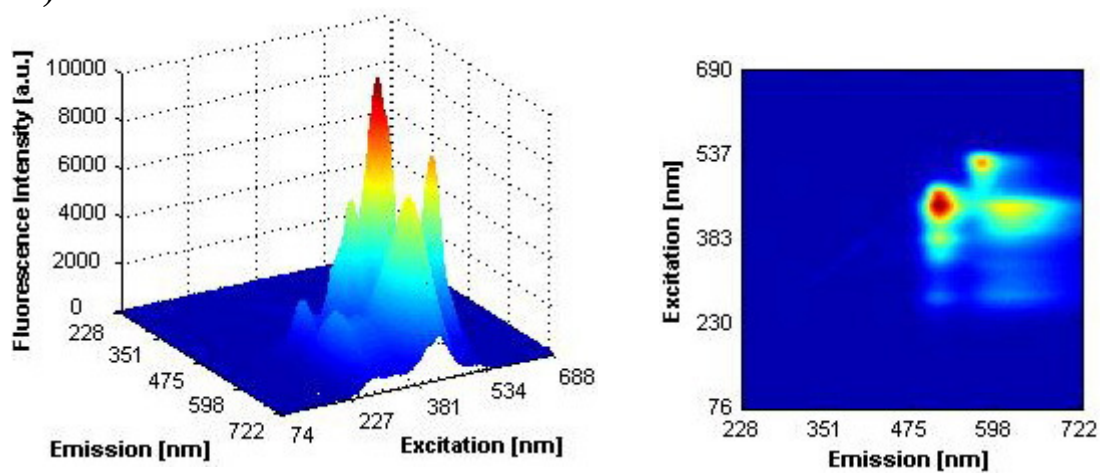


Figure 3.15.1: Three-dimensional colour mapped surface diagrams (right) and colour filled contour diagrams (left): HPTS (A), mixture of HPTS and FL (B), mixture of HPTS, FL and RB (C). Measurements of single dyes were performed in 50 mM PB buffer at pH 7.4.

D)



E)

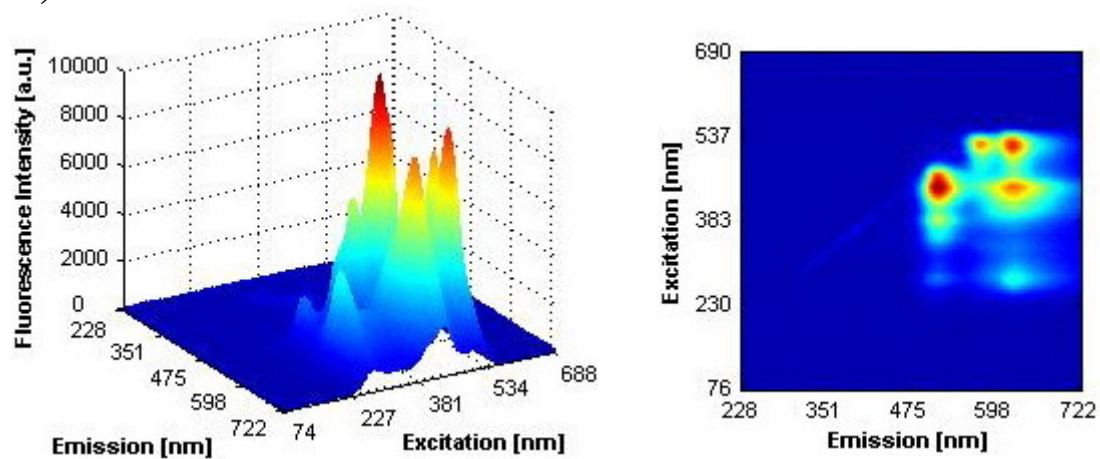


Figure 3.15.2: Three-dimensional colour mapped surface diagrams (right) and colour filled contour diagrams (left): mixture of HPTS, FL, RB and RuBpy (D), mixture of HPTS, FL, RB, RuBpy and THA (E). Measurements of single dyes were performed in 50 mM PBS buffer at pH 7.4.

3.4.4 Experimental examination of fluorescence dye mixtures

Based on the hypothetical examination, three possible mixtures of selected fluorescent dyes were tested using a 3D spectrofluorometer. The result spectra are presented in Figure 3.16, 3.17, 3.18 for the first, second and third mixture respectively. The order and compositions of following mixtures corresponds to the theoretical studies.

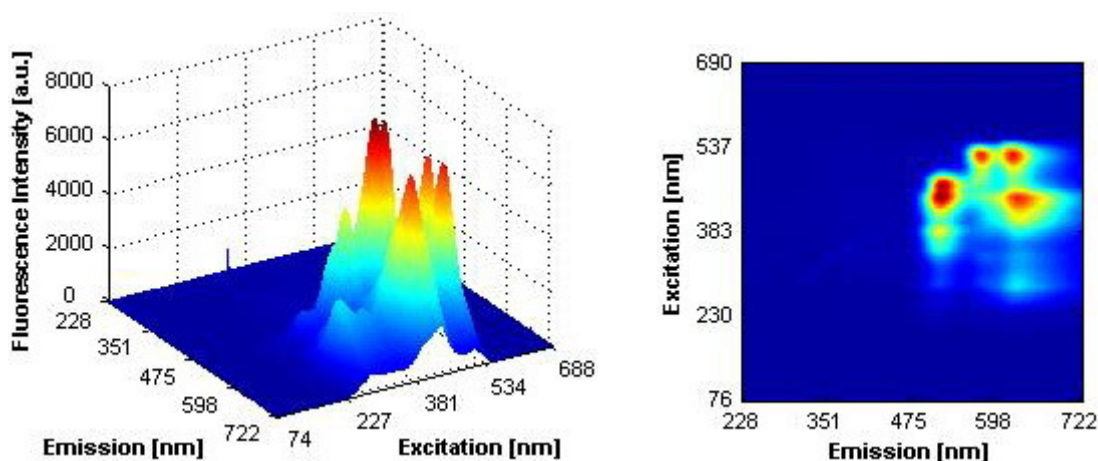


Figure 3.16: Three-dimensional colour mapped surface diagrams (right) and colour filled contour diagrams (left): mixture of HPTS, FITC, RB, RuBpy and THA. Measurements were performed in 50 mM PBS buffer at pH 7.4.

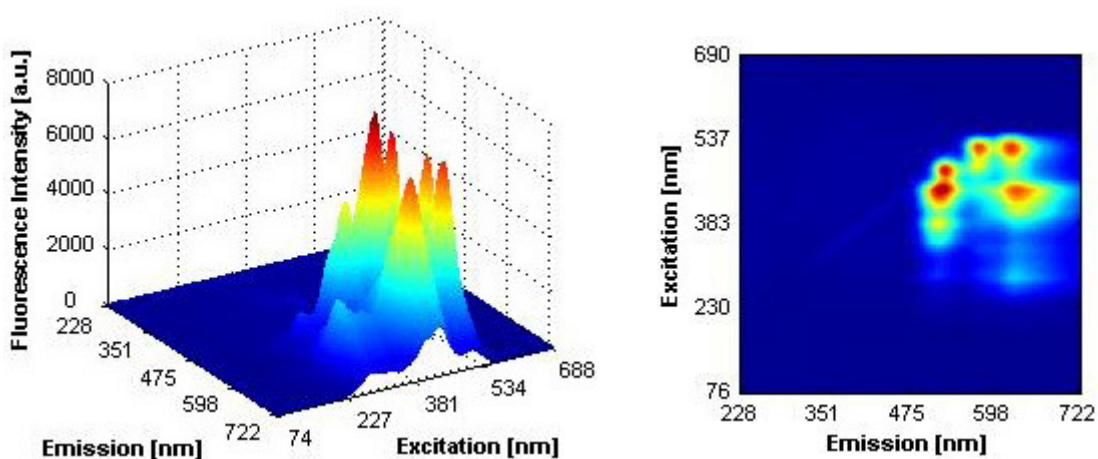


Figure 3.17: Three-dimensional colour mapped surface diagrams (right) and colour filled contour diagrams (left): mixture of HPTS, OG514, RB, RuBpy and THA. Measurements were performed in 50 mM PBS buffer at pH 7.4.

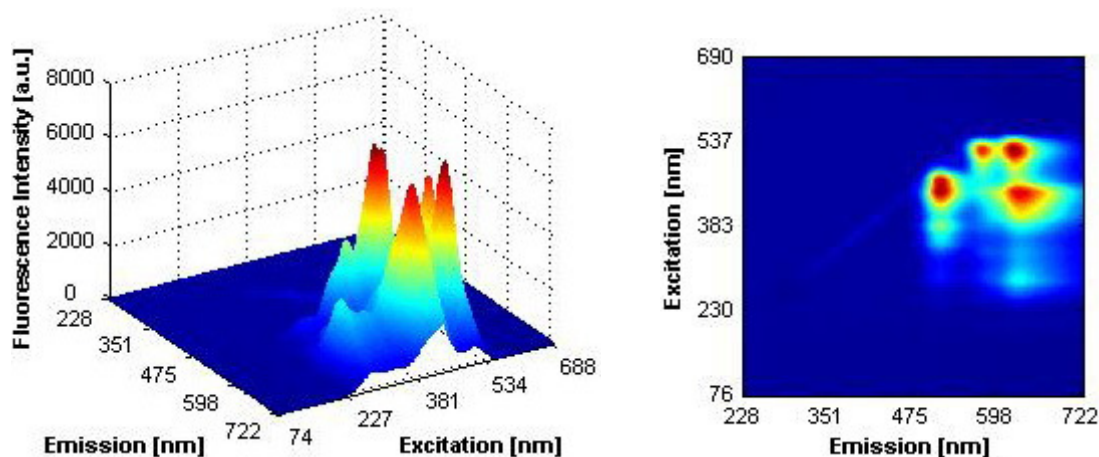


Figure 3.18: Three-dimensional colour mapped surface diagrams (right) and colour filled contour diagrams (left): mixture of HPTS, FL, RB, RuBpy and THA. Measurements were performed in 50 mM PBS buffer at pH 7.4.

Above figures demonstrate close agreement of experimental results using visual display of proposed mixtures. All three combinations of five fluorescent dyes were successfully established, which proves the benefits of subjective visual inspection performed by Matlab. This allows rapid selection of possible combinations of fluorescent dye mixtures.

The most significant separation of the fluorescence maxima of dyes was obtained for the second mixture composed of HPTS, OG514, RB, RuBpy and THA, and therefore this mixture was selected for further experimental investigation. An additional advantage of the choice was that one of the dyes in the mixture (OG514) has been reported as a low pH indicator (Sabnis, 2008). Combined with HPTS, near-neutral and higher pH indicator (Lakowicz, 2006), they should allow measurements in wider range of pH. Two other mixtures are different from the favourable one by FITC (used in a first mixture) and FL (used in the third mixture). They are both sensitive to neutral pH about 7.0 and therefore it was assumed that measurements in lower pH might be not as effective as in the presence of OG514. The mixture also consists of temperature, oxygen and HRP sensitive dye such as RB, RuBpy and THA respectively.

3.5 Conclusions

Literature information and prepared lists of available fluorescent dye-indicators allowed quick selection of several suitable specific dyes with different excitation and emission wavelengths and required sensitivities.

The experimental investigation of selected dyes sensitive to different parameters was performed and proved that some of them can be mixed together with clear separation of their maxima of fluorescence intensities. Therefore, it might be possible to observe changes in fluorescence intensity of individual dyes while the environmental conditions are changing.

Based on excitation-emission spectra of individual probes, the potential mixtures were visualised in Matlab and theoretical predictions proved experimentally. Matlab has been very helpful tool for visual display, thus for an easy illustration and rapid selection of fluorescent dyes, which can be mixed together in the same solution. It is very promising for future, and looking at dye mixtures containing as many suitable dyes as possible to expand the number of parameters or analytes that could be measured.

The 3D spectrofluorometer seems to be the perfect instrument for these measurements because the spectral analysis can be easily made by scanning the sample over a wide range of excitation and emission wavelengths.

4. Third objective: investigation of analytical capability of suitable optical assay

4.1 Introduction

The most suitable mixture composed of five fluorescent dyes (see Table 4.1) was chosen and used in following experiments for quantitative measurements of environmental changes including pH, temperature, ionic strength and dissolved oxygen.

Initially, the optical properties of dyes mixture was analysed depending on changes of single parameter. This involved measurements of different values of pH, temperature and ionic strength of PB. Results of performed experiments have been included in the patent application describing a concept of optical multisensor (Piletsky *et al.*, 2002). Further, simultaneous determination of four parameters (pH, temperature, ionic strength and DO concentration) was performed and the results were recently published (Moczko *et al.*, 2009).

Table 4.1: List of fluorescent dyes selected for the assay.

	Dye Name	Sensitivity	Excitation [nm]	Emission [nm]	Extinction coefficient [$\text{cm}^{-1}\text{M}^{-1}$]	Purity [%]	Supplier CAS Number
1	8 - Hydroxypyrene - 1',3,6 - trisulfonic acid	near-neutral pH ionic strength	470	527	24,000 (water)	≥ 98	Sigma-Aldrich 6358-69-6
3	Rhodamine B	temperature	541	576	88,000 (water)	~ 95	Sigma-Aldrich 81-88-9
2	Oregon green 514 carboxylic acid	low pH	504	528	86,000 (DMF)	94	Molecular Probes N/A
4	Tris (4,7 - diphenyl - 1,10 - phenanthroline) ruthenium dichloride	oxygen	463	637	14600 (water)	99.95	Sigma-Aldrich 50525-27-4
5	Thionin acetate	hydrogen peroxide	541	628	53,000 (water)	> 85	Acros Organics 78338-22-4

4.2 Experimental section

4.2.1 Composition of fluorescent dye mixture

The mixture of selected fluorescent dyes were prepared as a stock solution of following dyes: 0.15 mM 8-Hydroxypyrene-1',3,6-trisulfonic acid, 0.1 mM Rhodamine B, 0.025 mM Oregon green 514, 6 mM Tris (4,7-diphenyl-1,10-phenanthroline) ruthenium dichloride and 2 mM Thionin acetate (see Figure 6.1). Solutions of dyes were prepared in deionised water and stored at ~5 °C, covered with aluminium foil to protect them from light. 200 µl of each water/dye stock solutions were mixed together and used in further experiments. Measurements were carried out using 3 ml of suitable buffer and 50 µl of the mixture.

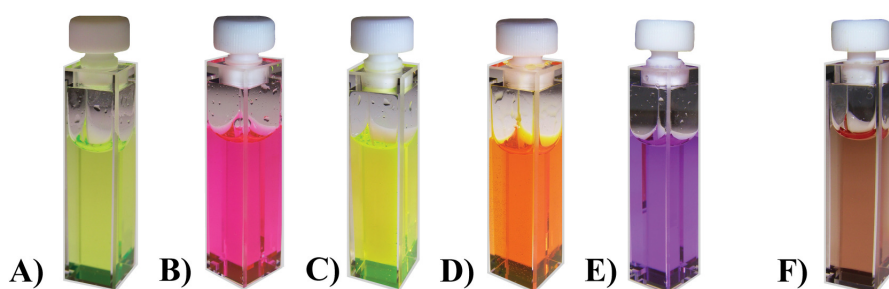


Figure 4.1: Cuvettes containing solutions of five selected fluorescent dyes and their mixture: HPTS (A), RB (B), OG514 (C), RuBpy (D), THA (E) and mixture of five selected dyes (F).

4.2.2 Buffer solutions

A) Measurements of single parameter

Fluorescent measurements were performed in buffers at pH range from 4.0 to 9.0, temperature – from 20 to 40 °C and buffer concentrations - from 5 to 150 mM.

Values of a pH of a buffer was adjusted using acetic acid – sodium acetate ($C_2H_4O_2$ – $NaC_2H_3O_2$) for low values of pH (from 4.0 to 5.0), sodium phosphate dibasic – sodium

phosphate monobasic ($\text{Na}_2\text{HPO}_4 - \text{NaH}_2\text{PO}_4$) for pH from 5.0 to 8.0 and boronic acid –sodium borate ($\text{H}_2\text{B}_4\text{O}_7 - \text{Na}_2\text{B}_4\text{O}_7$) for pH from 8.0 to 9.0.

B) Measurements of four parameters

Simultaneous measurements of four parameters were performed at pH range from 5.0 to 9.0, temperature - from 25 to 40 °C, dissolved oxygen (DO) - from 0 to 21.6 ppm and PB concentration - from 5 to 150 mM.

All measurements were carried out in sodium phosphate buffer (PB) consisted of sodium phosphate dibasic (Na_2HPO_4) and sodium phosphate monobasic (NaH_2PO_4) dissolved in distilled water.

4.2.3 Instrumentation

As in previous experiments, fluorescence intensity measurements were performed using three-dimensional spectrofluorometer with 0.5 s of time exposure.

The pH of a buffer was controlled by using pH meter (Hanna Instruments Ltd., Model 8519, Italy). The ionic strength was varied using different buffer concentrations. The temperature of the cuvette containing dyes solution was adjusted externally using thermostatic water-bath (Grant Instruments Ltd, Model 0331, Cambridge, UK). The concentration of DO was measured using oxygen probe (World Precision Instruments Ltd, OXEL-1, Stevenage, UK) and potentiostat-galvanostat (Uniscan Instrument Ltd, PG580, Buxton, UK). The concentration of oxygen was adjusted by bubbling solutions with air or nitrogen and measured amperometrically. The number of moles of oxygen present in the solution was calculated at different temperatures using the ideal gas law (Sabnis, 2008).

4.2.4 Data evaluation

The spectral characteristics of dyes mixture and changes caused by interactions with its surroundings have been analysed using artificial neural networks. ANNs were implemented in Matlab (version 7.3.0, MathWorks Inc., 2006) using the Neural Network Toolbox (version 5.0.1).

The evaluation of a parameter was based on changes of the height of the fluorescence peaks of all five dyes of the mixture.

A) ANN model for single parameter

The prediction model used for determination of single parameter of the sample was created based on linear neural network classifier (Demuth *et al.*, 2007). The network structure used in this study consisted of linear neuron with five neurons in the input layer corresponding to fluorescent emission of the five fluorescent dyes (taken at wavelengths shown in Table 4.1) and a single neuron in the output layer corresponded to a parameter of interest. The network was designed using the function *newlind* and 33 samples for each parameter being tested. The ability of the model network was tested on a set of previously unseen 11 samples measured at different pH and 5 samples at different temperature.

B) ANN model for four parameters

The prediction model used for simultaneous determination of four parameters was created based on a feedforward network trained using backpropagation of errors (Demuth *et al.*, 2007). The network consisted of an input layer, one hidden layer and an output layer. The same as for simulation of single parameters, the input layer was made up of five neurons corresponding to fluorescent emission of the five fluorescent dyes (taken at wavelengths shown in Table 4.1) and a single neuron in the output layer corresponded to a parameter of interest. A different network was trained with 576 samples for each parameter being tested. The best performance obtained for the hidden layer consisted of 25 neurons and Bayesian regularisation (Demuth *et al.*, 2007) used in

the learning process. To test the ability of the trained network to predict parameters from acquired data, the network was tested with a set of previously unseen 192 samples.

The pseudo-code for Matlab script, which was developed for these calculations, is in Appendix A.2.

4.3 Results and Discussion

4.3.1 Dyes assay characterisation

The spectrum of the fluorescent dye mixture used in the study is shown in Figure 4.2.

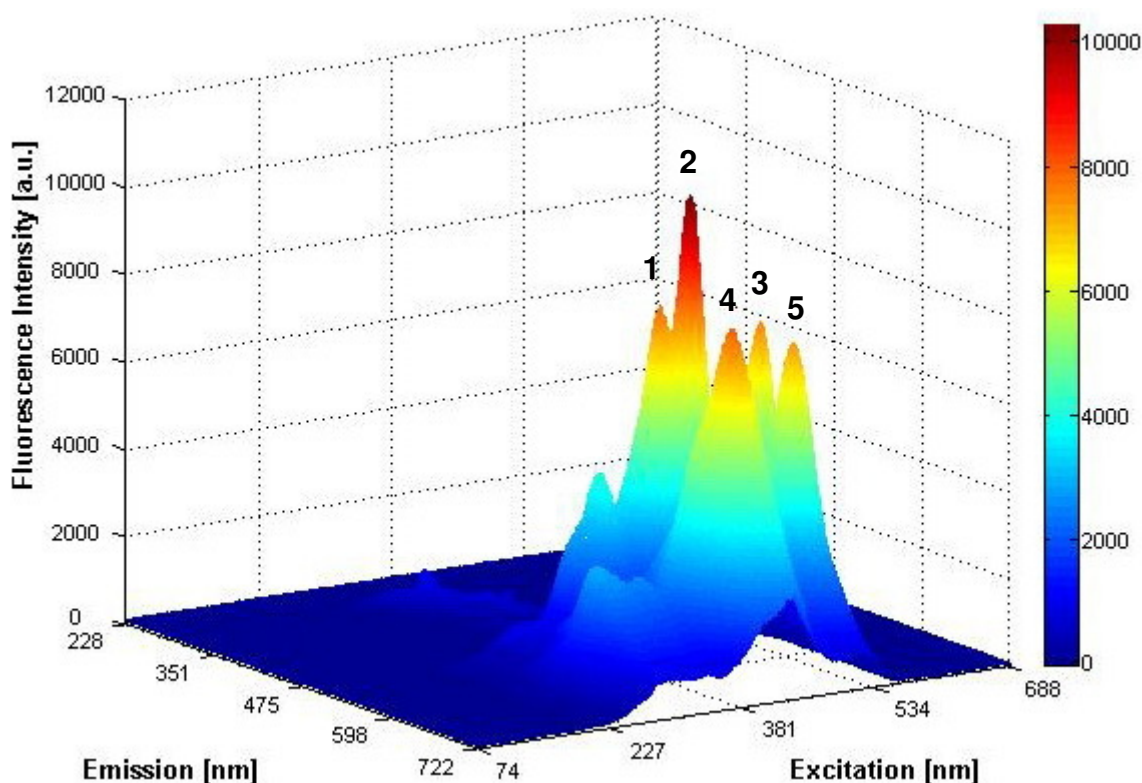


Figure 4.2: Three-dimensional colour mapped surface diagram of 5 fluorescent dyes: Dye 1 is HPTS, Dye 2 is OG514, Dye 3 is RB, Dye 4 is RuBpy, Dye 5 is THA. Measurements were performed in 3 ml of 50 mM PB buffer at pH 7.5.

The concentration of dyes was optimised corresponding to maximum values of their fluorescence intensities to allow clear discreet reading of emission peaks for each fluorescent dye and to provide visualisation of a collective fluorescent patterns of dye mixture. To exclude possible influence on the detected signal response, the concentrations were kept constant in all experiments. Therefore, it was expected that any changes of fluorescence emission of the solution of dyes were caused only by interaction with surrounding medium.

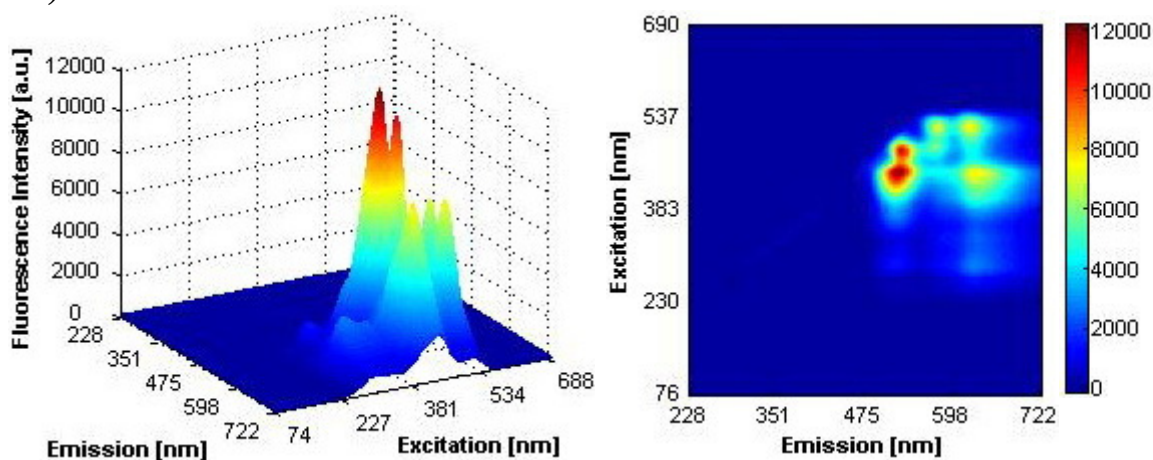
Figure 4.2 shows that fluorescence emission bands of proposed dyes overlap each other but the intensity maxima remain reasonably separated. This gives the possibility to analyse the comprehensive response of the whole mixture, along with each dye's individual impact on the signal.

The dyes mixture in a solution appeared to be stable showing no variation in spectral properties over at least a one month period. Practically, no photobleaching was observed in the process of measurements.

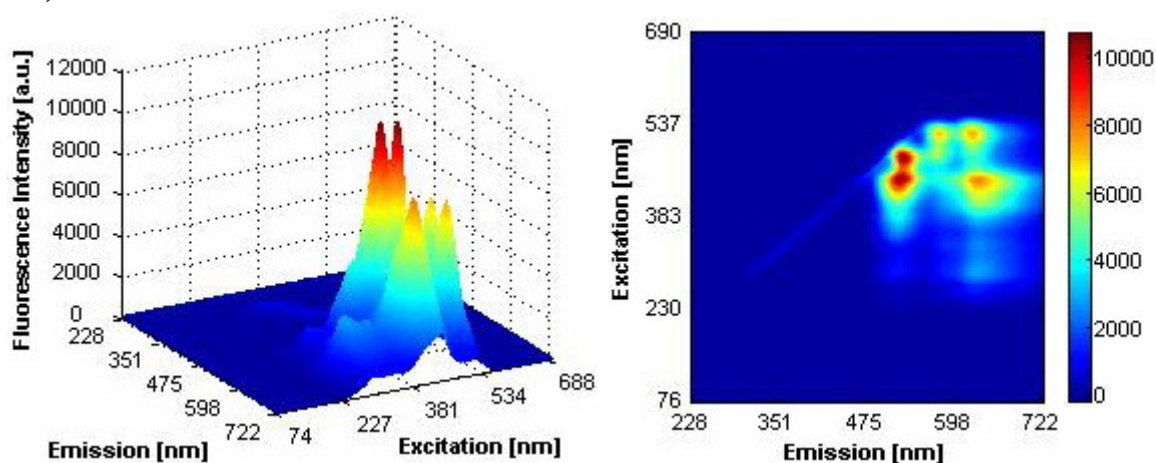
4.3.2 Investigation of analytical capability of the optical assay engendered by changes of single parameter

The initial experiments were performed to establish the influence of single parameter on the spectrum response while other parameters of the dye assay were kept constant. An example of an effect on fluorescence characteristic of the mixture caused by pH changes from 4.0 to 6.0 and from 7.0 to 9.0 is shown in Figure 4.3.1, 4.3.2 respectively. Three-dimensional colour mapped surface diagrams (on the left) and colour filled contour diagrams (on the right) illustrate changes of fluorescence signal of the dyes due to different pH of a buffer. Since the excitation/emission maxima of the intensity of fluorescent dyes are well separated, their individual characteristics due to decreasing pH are easily distinguished.

A)



B)



C)

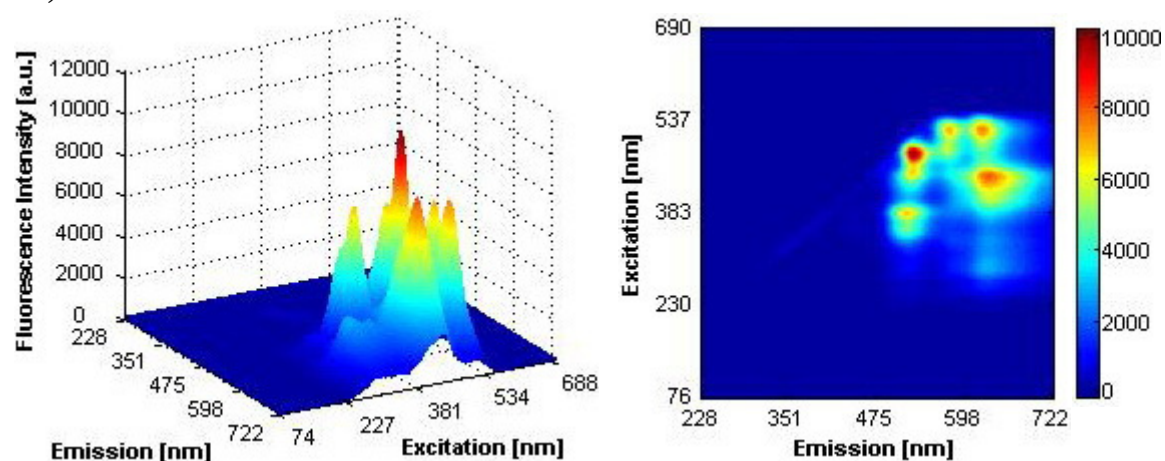


Figure 4.3.1: Three-dimensional colour mapped surface diagrams (left) and colour filled contour diagrams of the fluorescence signal of dyes mixture at pH 9 (A), pH 8 (B) and pH 7 (C) in 50 mM borate buffer (pH 9.0) and phosphate buffer (pH 8.0 and pH 7.0).

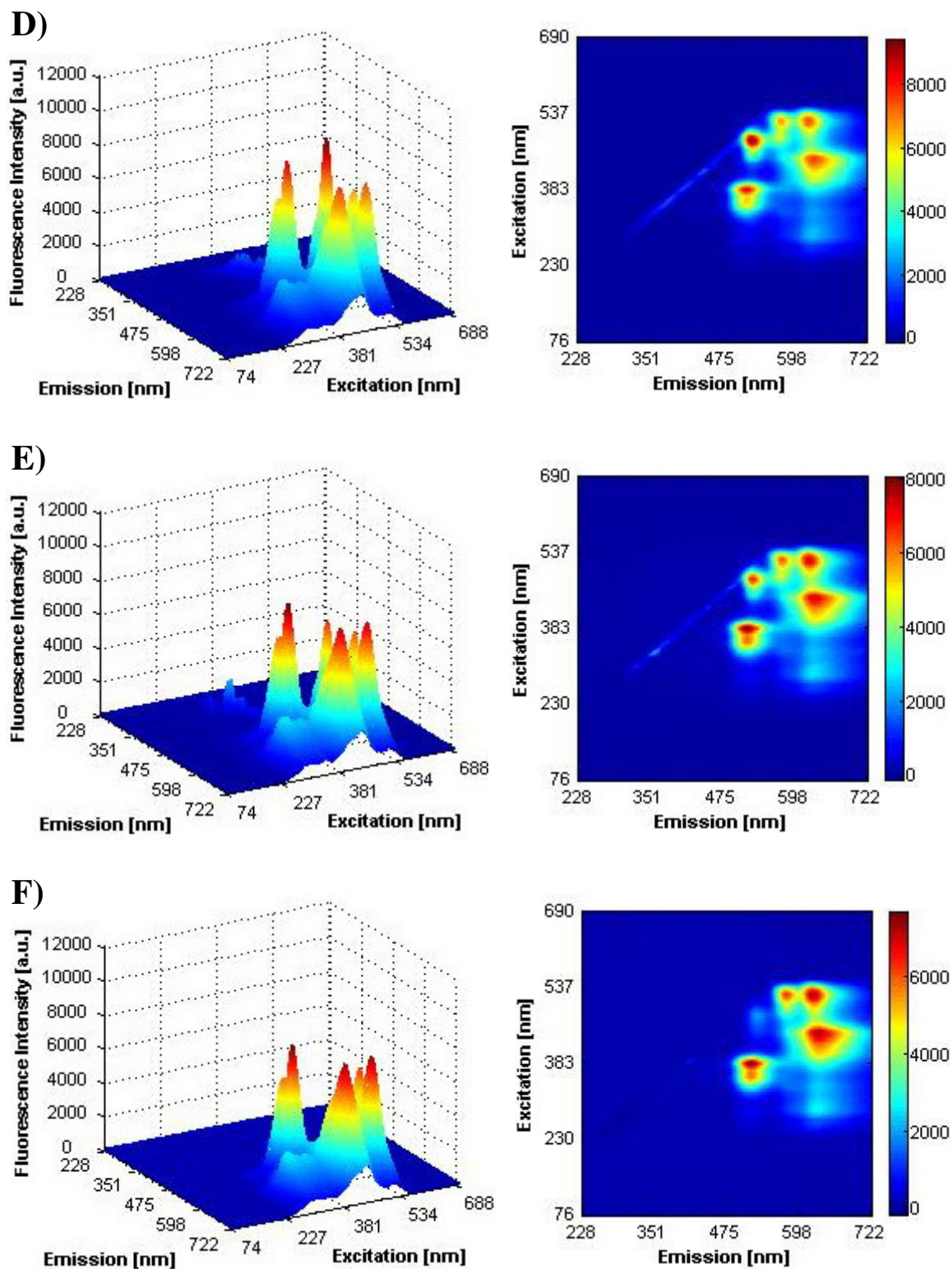


Figure 6.3.2: Three-dimensional colour mapped surface diagrams (left) and colour filled contour diagrams of the fluorescence signal of dyes mixture at pH 6.0 (D), pH 5.0 (E) and pH 4.0 (F) in 50 mM phosphate buffer and acetate buffer.

Fluorescence intensity of dyes changing differently depends on their sensitivity to pH. The most significant changes revealed HPTS which was specified as near-neutral pH indicator and OG514, which is specified as low pH indicator (Lakowicz, 2006; Sabnis, 2008). Colour filled contour diagrams (see right side of the figures) show that while the intensity of fluorescent dyes are changed at different pH, the position of the fluorescence picks of all dyes remained stable.

The pH profile of the maxima of dyes fluorescence intensity is shown in Figure 4.4.

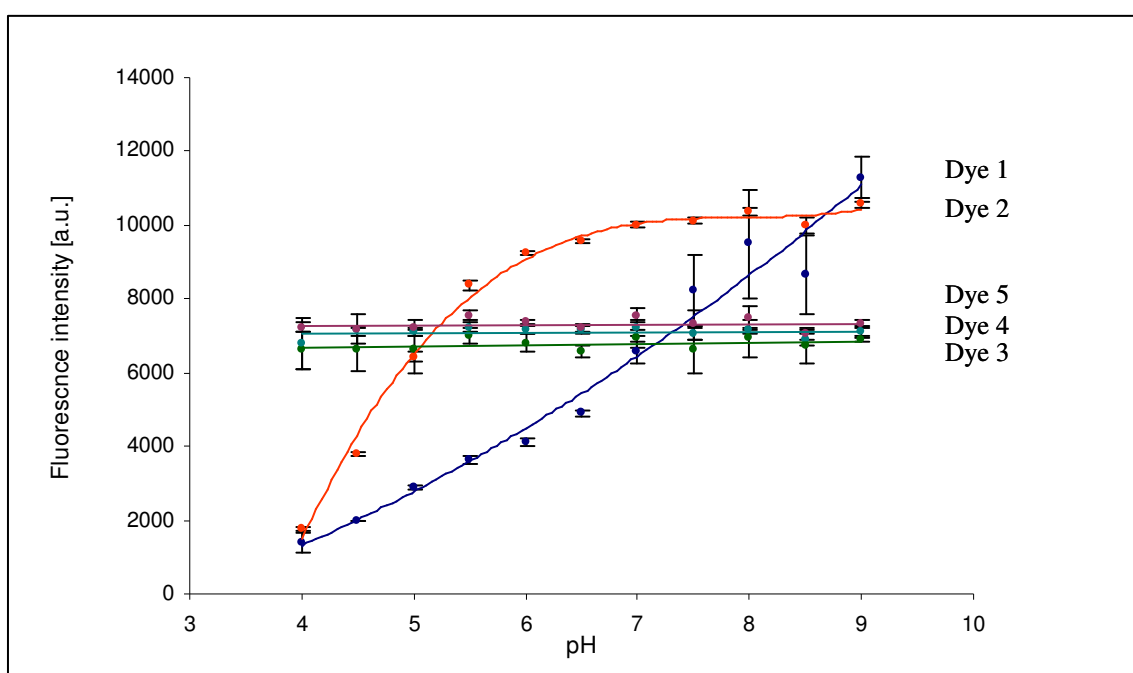


Figure 4.4: Change in fluorescence intensity of dyes mixture as a function of pH. Dye 1 is HPTS, Dye 2 is OG514, Dye 3 is RB, Dye 4 is RuBpy, Dye 5 is THA. Measurements were performed in 50 mM acetate (pH 4.0-5.0), phosphate (pH-5.0-8.0) and borate (pH 9.0) buffers.

Measurements at different pH were recorded in triplicate. Error bars indicate the standard deviation of the results obtained for each data point. As demonstrated in Figure 6.4, the fluorescence intensity of HPTS and OG514 is highly dependent on pH changes. Along with the decreasing of pH the fluorescent intensity of HPTS dropped almost linearly. The lowest signal was recorded at the most acidic (pH 4.0) and the highest at the most basic (pH 9.0) environment. OG514 appeared to be sensitive within the lower

values of pH, in the range of pH 4.0 – 6.0 and then its fluorescence remained almost stable. Emission intensity of other dyes stayed rather constant. The small fluctuations which occurred are possibly due to the changes in concentrations or interferences with other dyes and did not depend on different pH. These results prove that in the solution HPTS and OG514 remained their specific sensitivities described in literature.

Even if HPTS is known as an excellent pH indicator, its sensitivity can be slightly shifted while it is immobilised on different support (Choi, 1997; Zhu *et al.*, 2005) and it is also characterised by very low fluorescence intensity at acidic pH (near background). Therefore another pH sensitive dye, OG514 was chosen as more promising indicator for low pH range.

Further experiments were carried out to establish the sensitivity profile of the dye mixture at different temperatures and ionic strengths of a buffer. Obtained results are presented in Figure 4.5 and Figure 4.6 for the dependence on temperatures and ionic strength respectively.

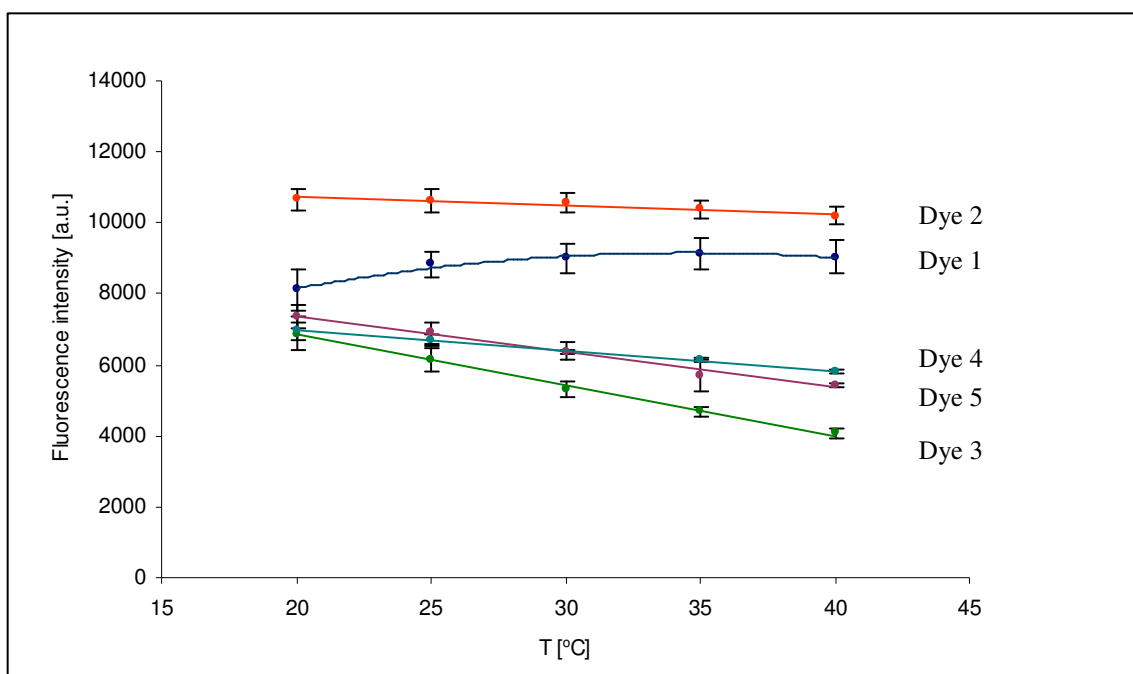


Figure 6.5: Change in fluorescence intensity of dyes mixture as a function of temperature. Dye 1 is HPTS, Dye 2 is OG514, Dye 3 is RB, Dye 4 is RuBpy, Dye 5 is THA. Measurements were performed in 50 mM phosphate buffer at pH 7.5.

It was found that fluorescence intensity of all dyes in the mixture was influenced by temperature (see Figure 6.5). While the temperature increased the intensity of four dyes decreased. The exception was HPTS, where intensity slightly rose up due to temperature increase. The highest changes revealed RB, which has been indicated in literature as temperature sensitive dye (see Section 2.3.2).

Figure 4.6 shows the dependence of the mixture spectral characteristic on ionic strength (buffer concentration).

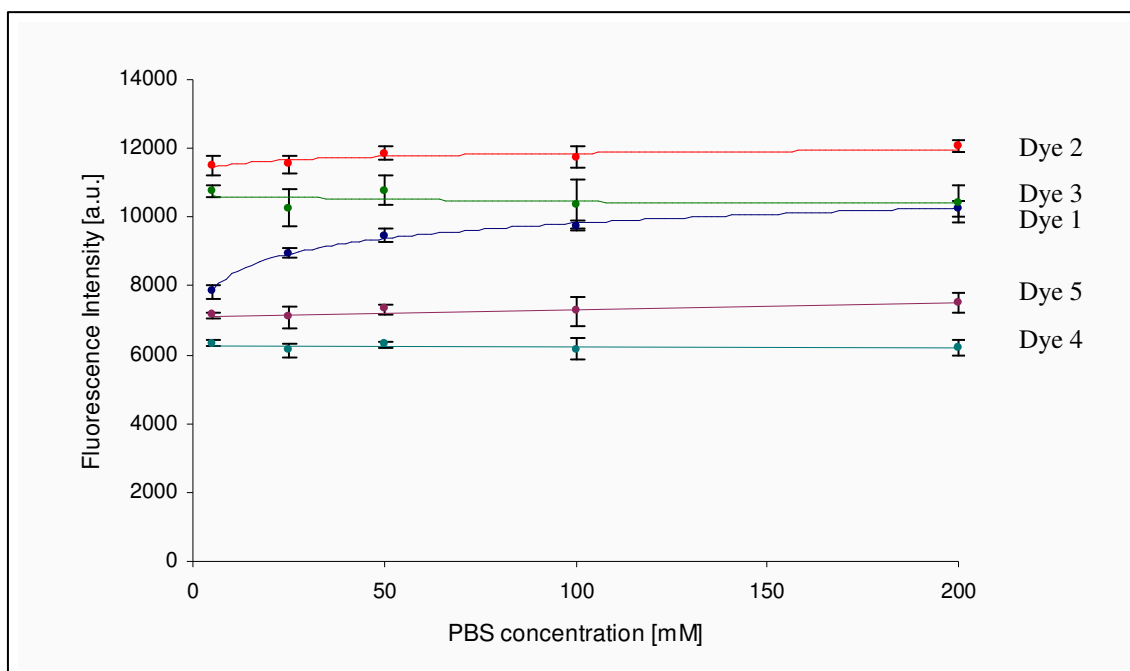


Figure 6.6: Change in fluorescence intensity of dyes mixture as a function of buffer concentration. Dye 1 is HPTS, Dye 2 is OG514, Dye 3 is RB, Dye 4 is RuBpy, Dye 5 is THA. Measurements were performed in 50 mM phosphate buffer at pH 7.5.

There were no substantial changes in the fluorescence intensity of the mixture. Only the intensity of HPTS increased corresponding to the increase in ionic strength and it appeared to be most sensitive in its lower range. Other dyes were not affected by different concentrations of buffer solution.

As a result of measurements of DO concentration, significant changes in fluorescence intensity were observed particularly for RuBpy, with decreasing tendency at higher level of oxygen. Due to limited data points it was difficult to define the curves and therefore this graph is not displayed.

Data evaluation – ANN method

The effect of single parameter on the fluorescence changes of the dye mixture was further analysed based on ANN as a pattern recognition method. It was done to test the analytical capability of the optical assay consisting of the dye mixture and multivariate data analysis engendered by changes of individual factors.

In the prediction of a single parameter, it was sufficient to use the linear neural network classifier whose predictive abilities are equivalent to linear regression models (Samarasinghe, 2007). To design the linear network the function *newlind* was applied, which is used for purposes when input set of data and corresponding targets (values of parameters) are known. To do so, the input set of data consisted of spectral responses of the fluorescent dyes corresponding to known values of output parameters such as pH and temperature. Similar to the analysis of the sensitivity profiles of the mixture, the five wavelength points at the maxima of fluorescence intensity of dyes were chosen for a representation of the profile of original spectra and used as an input data for the ANN. To test if the model network was designed properly its behaviour was simulated with an unseen set of data (the test set). Results of these simulations for different values of pH and temperature are shown in Figure 4.7A-B.

The graphs illustrate very good correlation between real (measured) values (x axis), and the values determined by ANN (y axis). Circles (\circ) indicate the values of data points of the network predictions for test samples and the error bars indicate the errors of the network prediction for each data point. The highest error was obtained for prediction of pH 8.5 and it was 0.3 and 1.6 for temperature at 45 °C.

Therefore, the combination of fluorescence signals of dye assay as a response to changes of single parameters in the environment and simple, linear ANN model was sufficient enough to allow accurate analysis of the parameters.

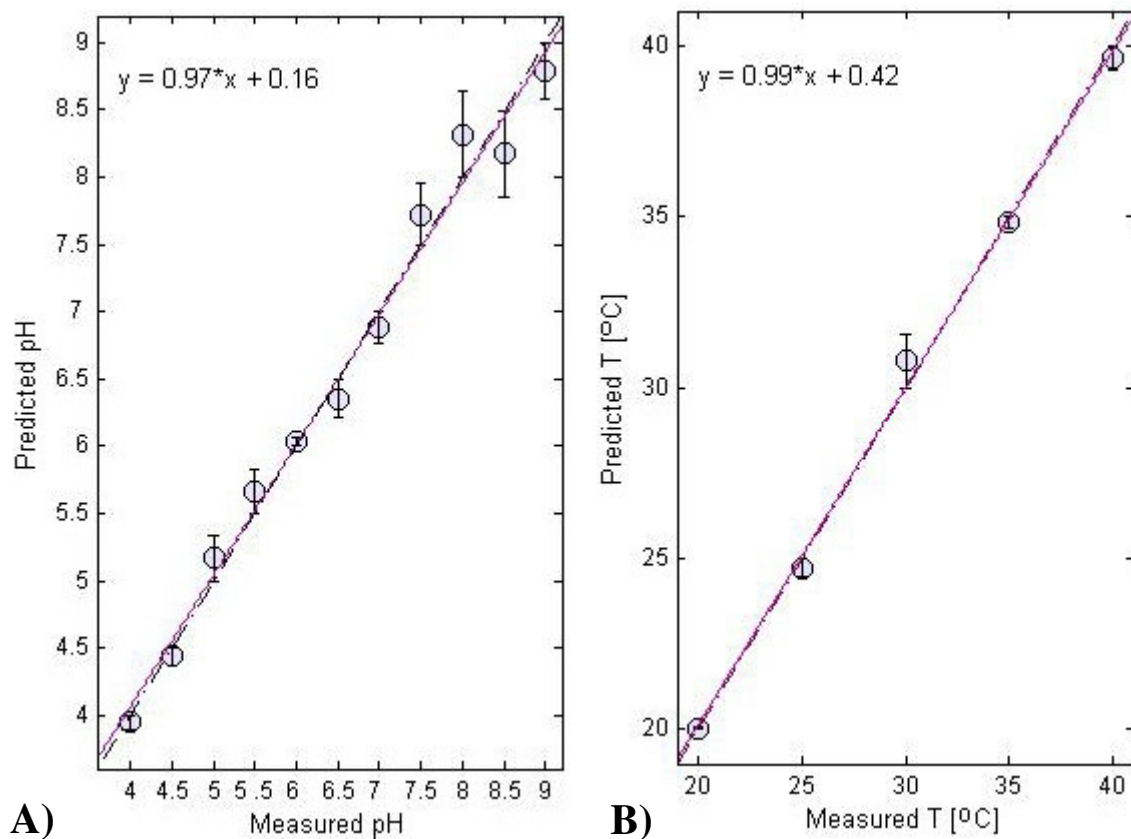


Figure 4.7: Correlation between actual (measured) and determined by ANN values of pH (A), temperature (B). Points marked as circles (○) indicate data points of ANN simulations of unseen samples. Diagonal line (—) indicates best linear fit of data points and the line (-•-) indicates ideal response with zero error. Error bars indicate error of the network prediction.

4.3.3 Investigation of analytical capability of the optical assay engendered by changes of several parameters

As expected, reasonable changes in fluorescent spectrum of dyes mixture were observed in response to change of single parameter. It was also expected that the signal was not just a summation of individual spectral signatures of fluorescent dyes but additionally the product of their interaction and cross-interferences, which complicated the analysis

in the case when several parameters were changing simultaneously. Therefore more advanced network, which would be able to model this non-linear and interference effect between fluorescence of dyes at different conditions, was applied for the data evaluation and the determination of target parameters.

To study the effect of the parameters' variations, the fluorescence emission values were recorded for a number of samples with different values of pH, temperature, DO and PB concentrations.

The key ability of the network has been identified and tested. This includes training the ANN on patterns from samples of known identity and using them to predict the characteristics of new unknown samples with the smallest prediction error. Thus, the optimised network of the best performance was selected and applied for simultaneous determination of four parameters. The input dataset consisted of spectral responses of the fluorescent dyes corresponding to known values of output parameters: pH, temperature, DO and PB concentration. Although it was expected that the use of the whole fluorescent spectra in the training process would give the best contrast of unique responses of the dyes due to changes in a solution, it would also increase amount of processing data and training time of the network. To minimise workload similar as in analysis of single parameter, five wavelength points at the maxima of fluorescence intensity of dyes were chosen for a representation of the profile of original spectra and used as actual input data for the ANN. This decision has been found sufficient for accurate prediction of target parameters.

In order to optimise the ANN, two main steps were carried out. First, the network architecture giving sufficient performance for all four parameters has been optimised by an experiment. The training process was verified using several networks with different number of neurons in hidden layer and applying different learning algorithms. The second stage of the process concerned the improvement of the network performance by optimising and adjusting values of individual training function parameters such as performance goal, momentum or number of training iteration (epochs), in order to reduce the possibility of invalid generalisation of the network with the high performance for one purpose but sacrificing the others.

The efficiency of each ANN model was assessed in terms of root mean square error (RMSE) with units adequate to parameters being measured.

In the optimisation process of ANN, two frequently used algorithms Levenberg-Marquardt algorithm (trainlm) and Bayesian regularization (trainbr) were chosen for testing. While trainlm has been documented as the fastest training algorithm, trainbr provides a better quality of generalisation (Demuth *et al.*, 2007). Their estimates of the actual values of four parameters were compared in Tables 4.2, 4.3, 4.4 and 4.5 for different number of neurons in the hidden layer between 1 and 30 neurons. All other parameters were kept constant and set as shown in the literature (Demuth *et al.*, 2007).

The first parameter used for testing was pH (Table 4.2). As the table shows, for both trading functions the networks performance was very high. However, better results (lower prediction error) have been obtained for trainlm, the values given by trainbr are acceptable because the error is still very low and decreased when the number of neurons in the hidden layer was between 25 and 30 (see NET10 and NET11).

Table 4.2: Effect of the number of neurons in the hidden layer and training algorithm on ANN performance for pH.

Network	Neurons in hidden layer	RMSE1 (trainlm)	RMSE2 (trainbr)
Net1	3	0.1286	0.0045
Net2	5	4.5491e-008	0.0023
Net3	8	8.2235e-005	0.0054
Net4	10	4.0883e-007	0.0041
Net5	13	0.1203	0.0627
Net6	15	9.2789e-005	0.0063
Net7	18	7.4832e-004	0.0108
Net8	20	6.7050e-004	0.0100
Net9	23	0.0019	0.0111
Net10	25	2.2398e-004	3.7477e-004
Net11	28	1.3200e-005	3.5313e-004
Net12	30	9.5878e-004	0.0027

In temperature estimation, trainbr revealed significantly higher performance, which was further enhanced by increasing the number of neurons in the hidden layer (Table 4.3, NET7-NET10).

Table 4.3: Effect of the number of neurons in the hidden layer and training algorithm on ANN performance for temperature.

Network	Neurons in hidden layer	RMSE1 (trainlm) [°C]	RMSE2 (trainbr) [°C]
Net1	3	5.3979	0.8922
Net2	5	2.3940	0.8409
Net3	8	3.1026	0.7137
Net4	10	4.0045	0.7300
Net5	13	2.6404	0.7563
Net6	15	1.4088	0.7912
Net7	18	0.8510	0.6657
Net8	20	1.4679	0.5932
Net9	23	1.3041	0.6310
Net10	25	1.3974	0.6431
Net11	28	0.9731	0.8055
Net12	30	1.5836	0.7114

Similar to the results for temperature, trainbr algorithm showed lower prediction errors for DO (Table 4.4). The performance was additionally enhanced for networks with the neurons in hidden layers of 10, 13, 15 and 18. The highest error showed the network containing 3 neurons in the hidden layer (NET1) but even so it is not higher than the lowest obtained for trainlm (NET7).

The last parameter to test was a buffer concentration. The result of the prediction of this parameter is presented in table 4.5. Despite different algorithms or number of neurons in the hidden layer, networks revealed high estimation error. The highest was obtained when trainlm and low number of neurons was used for training. Better training was achieved for trainbr and slightly improved by increasing the number of neurons in hidden layer. This is getting worse above 25 neurons.

Table 4.4: Effect of the number of neurons in the hidden layer and training algorithm on ANN performance for DO.

Network	Neurons in hidden layer	RMSE1 (trainlm) [ppm]	RMSE2 (trainbr) [ppm]
Net1	3	1.6080	0.4941
Net2	5	1.3999	0.2074
Net3	8	1.5497	0.2153
Net4	10	0.6293	0.0584
Net5	13	1.5694	0.0587
Net6	15	0.5496	0.0759
Net7	18	0.8505	0.4354
Net8	20	1.3703	0.0785
Net9	23	0.5903	0.0769
Net10	25	0.8522	0.0808
Net11	28	1.1819	0.3857
Net12	30	0.6355	0.3123

Table 4.5: Effect of the number of neurons in the hidden layer and training algorithm on ANN performance for buffer concentration.

Network	Neurons in hidden layer	RMSE1 (trainlm) [mM]	RMSE2 (trainbr) [mM]
Net1	3	52.2653	39.6519
Net2	5	52.5966	37.9455
Net3	8	48.2992	31.1647
Net4	10	44.1124	32.4427
Net5	13	34.1128	30.2274
Net6	15	47.1076	26.5737
Net7	18	43.2947	28.1090
Net8	20	32.9877	32.2674
Net9	23	34.4614	30.0214
Net10	25	43.2288	21.0038
Net11	28	39.6913	42.5743
Net12	30	41.3651	45.0022

Since better networks performance for all four parameters was achieved by using trainbr as learning algorithm, it was chosen and applied in the further optimisation of network parameters and testing. Regarding the decision on the number of hidden neurons, it has been shown that when the number of neurons is smaller than 15, the efficiency of the network to adopt the model data and implement them for parameters estimation was very poor. By increasing the number of neurons over 15, improves the network performance; however above 25 neurons is getting worse again. Decisive in the choice of the rough number of neurons was the last parameter to predict, buffer concentration, which reveals the network of best performance when the training function as trainbr and the number of neurons was 25. Following testing and adjusting specific parameters of a network also showed that the architecture of the network containing 25 neurons in the hidden layer provided the best results with a lowest prediction error for all four parameters. It has therefore been selected as an optimal topology of the network and used for further analysis.

The script, which allows optimise the factors of the network was written in such a way that enable a user to choose the target parameter for testing followed by entries of desired values of network factors.

The neural network has been tested for each target parameter separately and for different values of its factors (Samarasinghe, 2007). While the network was trained by varying one of the factors, others were kept constant. The most significant effect on the network performance has been observed for changes of two factors, learning rate, LR, and momentum, MU. The learning rate controls weights and node biases increments at each training step. Setting this parameter to a large value (the maximum of 1.0) allows the network to learn more quickly but it is compensated by lower efficiency in outputs calculations. Therefore, it is usually better to set this factor to a smaller value unless the learning process seems very slow. The momentum factor improves the network stability. It is achieved by adjustment the current weight in respect to the average of the past weight changes. The MU allows the network to pass through the local minima and reach the optimum weights during learning. The momentum rate can increase from 0.0 to 1.0. If its value is set at 0.0, the MU is not considered in training and the network is

more likely to quickly settle into a local minimum which might result in false calculations. Higher values of the factor may however increase the time of the learning process and decrease network stability.

Other parameters to adjust were number of epoch and performance goal. Epochs define the maximum number of training cycles until the performance goal is reached. Their values should be optimised to avoid the overlearning of the network, when too much information is extracted from the individual cases, not relevant for the general case. Therefore the number of epoch and the goal should also be choose carefully, not too high and not too low but sufficient to reach the network optimal performance.

Illustration of the effect of the learning rate and momentum on the ANN performance

The ANN used for training contained five neurons in the input layer, one neuron on the output and 25 hidden neurons. The algorithm applied in the learning process was trainbr. The effect of the MU and LR was analysed using a computer experiment. The network was first trained for different values of the MU while the LR was held constant at 0.9. The RMSE of the performance in each of the cases is shown in Figures 4.8.1, 4.9.1, 4.10.1 and 4.11.1 for pH, temperature, concentrations of DO and PB respectively. Figures 4.8.2, 4.9.2, 4.10.2 and 4.11.2 illustrate further analysis of the effect of varying LR on the network performance. These trials have been made for a constant MU that gave the lowest prediction error for each individual parameter.

First figures, 4.8.1 and 4.8.2, show that both these factors had some impact on the evaluation of pH, but it did not significantly affect the network performance. It was very high in all cases, which is indicated by behaviour of RMSE and even the least efficient network, with the highest error, was sufficient and gave accurate results. The biggest difference between the lowest and the highest error was only 0.002. For the LR of 0.9, a MU of 0.5 gave the best performance and 0.9 gave the worst performance. Finally, the network was trained with MU of 0.5, LR of 0.5. Further, the performance goal was adjusted to 0.01 and number of epoch 100.

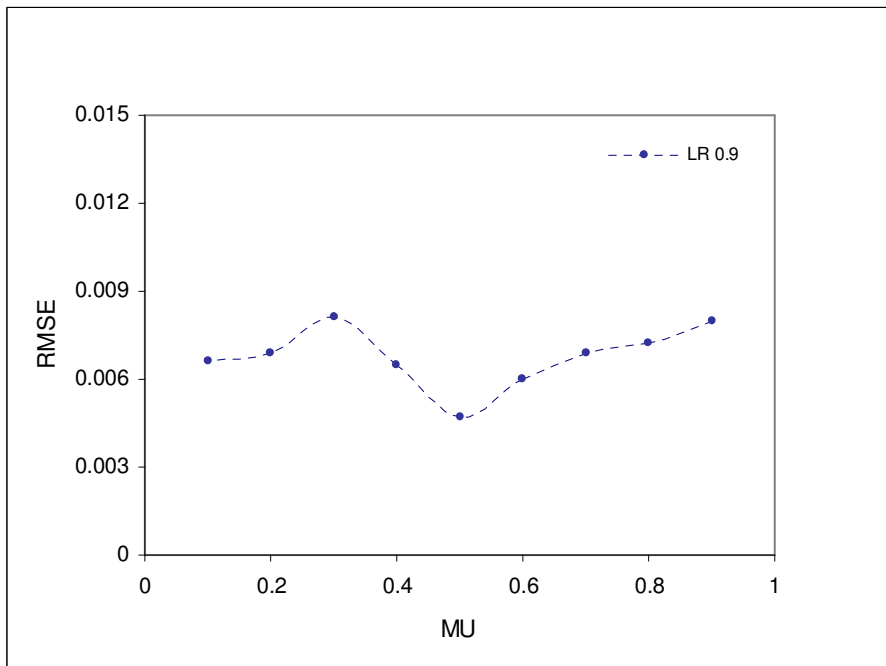


Figure 4.8.1: The effect of momentum on ANN learning in the estimation of pH.

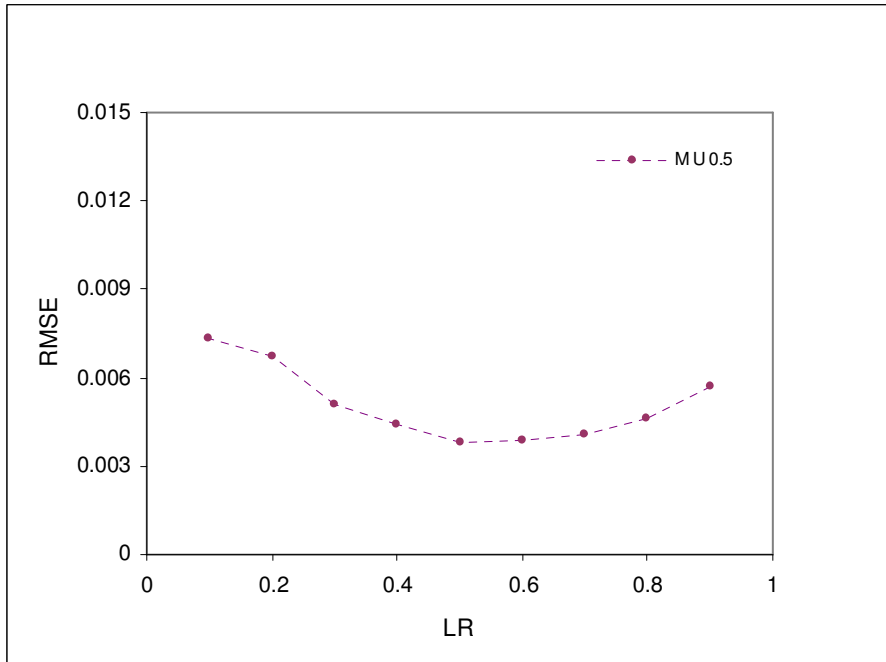


Figure 4.8.2: The effect of learning rate on ANN learning in the estimation of pH.

Figures 4.9.1 and 4.9.2 illustrate the network performance for estimation of different values of temperature. The same as for pH, calculations were made while the momentum or the learning rate of the network was varying between 0.1 and 0.9.

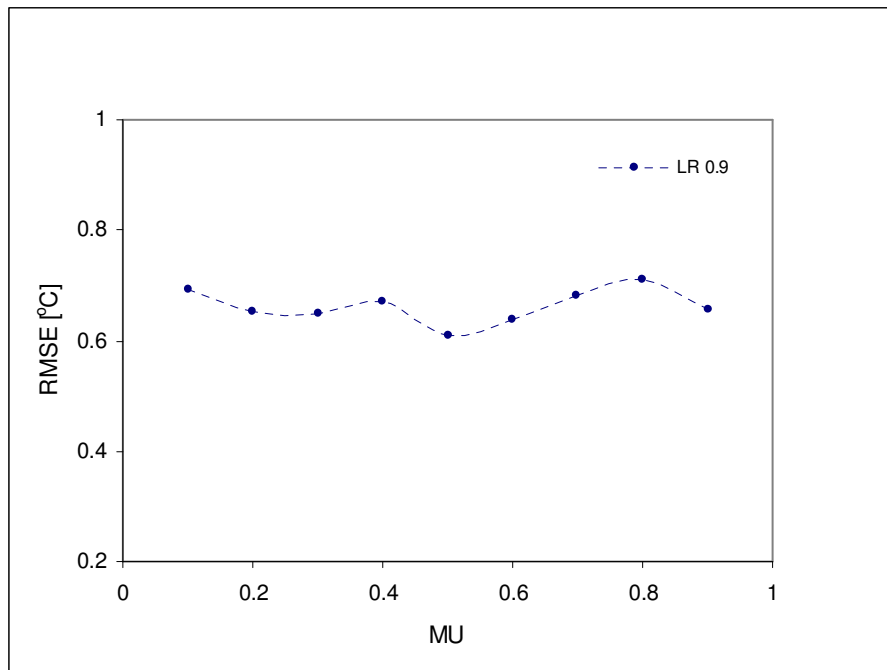


Figure 4.9.1: The effect of momentum on ANN learning in the estimation of temperature.

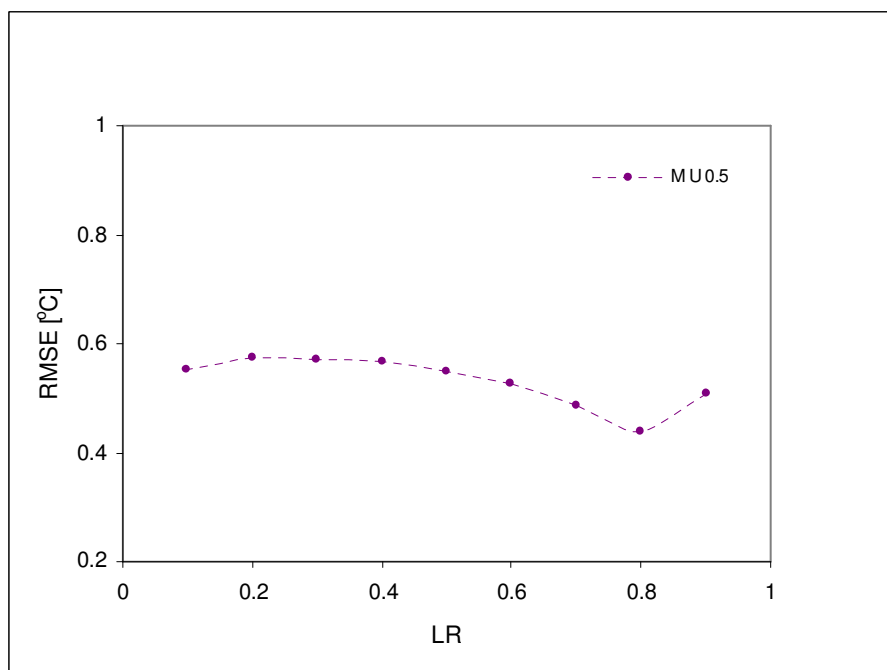


Figure 4.9.2: The effect of momentum on ANN learning in the estimation of temperature.

Figure 4.9.1 shows that the MU did not influence significantly the calculations, the difference between the lowest and the highest RMSE was 0.1 °C. The network performance was slightly improved by changing the LR (see Figure 4.9.1). As a result the error was decreased up to 0.44 °C when the LR was set to 0.8. The training was done for the performance goal of 0.5 and the number of epoch 200.

This procedure was also repeated for estimations of concentration of DO and PB. For these two parameters varying of MU and LR had visible impact on the network performance. As Figure 4.10.1 shows that applying the momentum of 0.5 again gives the highest efficiency of the trained model network. The worst results of DO determination were obtained for high MU above 0.7 and low, below 0.4. Therefore, MU of 0.5 was used for testing the network with different LR (see Figure 4.10.1). This time acceptable error was given in the range of LR between 0.6 and 0.9. The best performance was obtained for MU set to 0.6 and this value was chosen for further application of the model network. Other parameters were set to 0.1 for the performance goal and 200 for epochs. Such an optimisation of the network revealed an improvement of the RMSE from 0.6 up to 0.05 ppm.

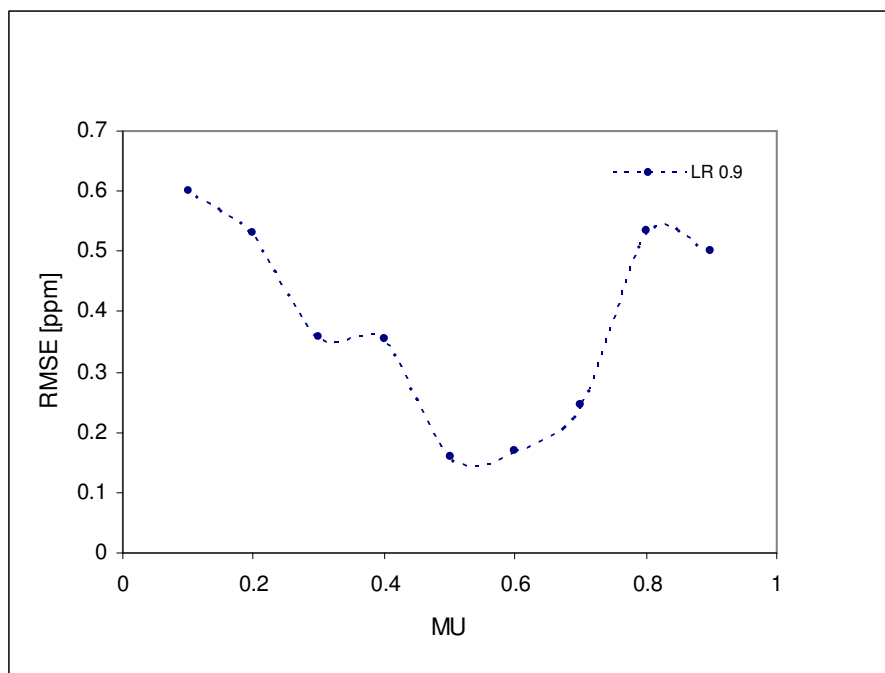


Figure 4.10.1: The effect of momentum on ANN learning in the estimation of DO concentration.

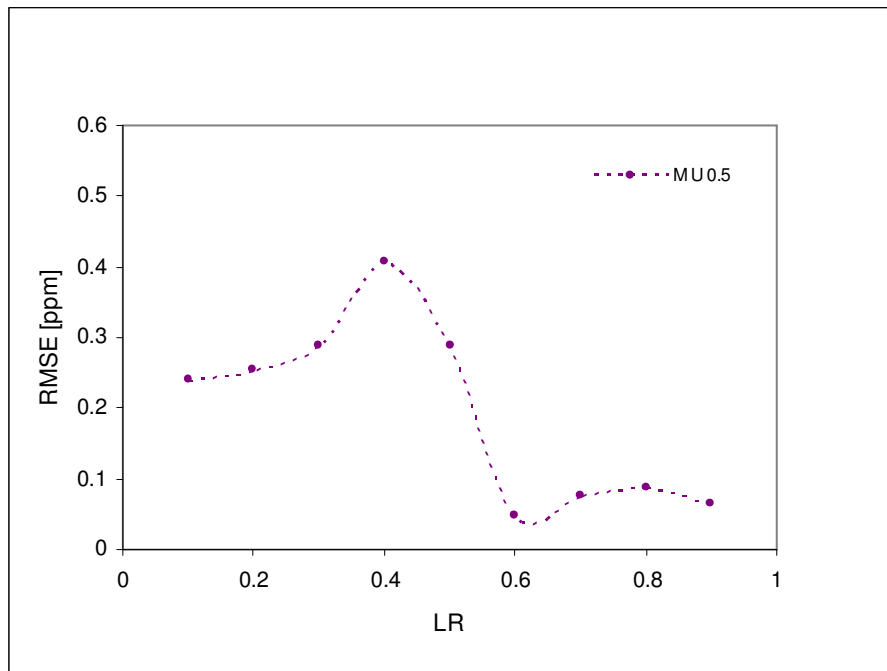


Figure 4.10.2: The effect of momentum on ANN learning in the estimation of DO concentration.

The last parameter to test was PB concentration. In this case both factors play a crucial role for the network performance. Additionally the estimation error was highly improved by increasing the number of epoch of training (see Figure 4.11.1). Changing the number of epoch from 200 to 500 impacted on the changes of RMSE from 23 to 10 mM. Further increase in the number of epoch did not change results significantly. For 1000 epochs the RMSE decreased of only 0.5 mM (see pink dot in the Figure 4.11.1). Because the increase in the number of epoch increase the time of training the model network was set to 500 epoch. The performance was however improved by setting the LR to 0.7 and decreasing the RMSE for next 3 mM (Figure 4.11.1). The performance goal for the network was set to 1.

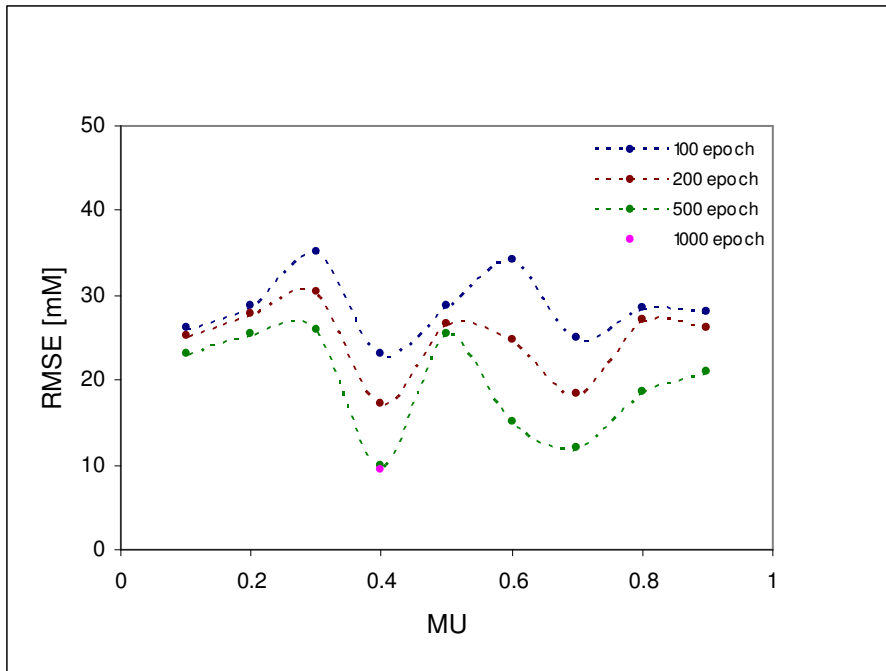


Figure 4.11.1: The effect of momentum on ANN learning in the estimation of PB concentration.

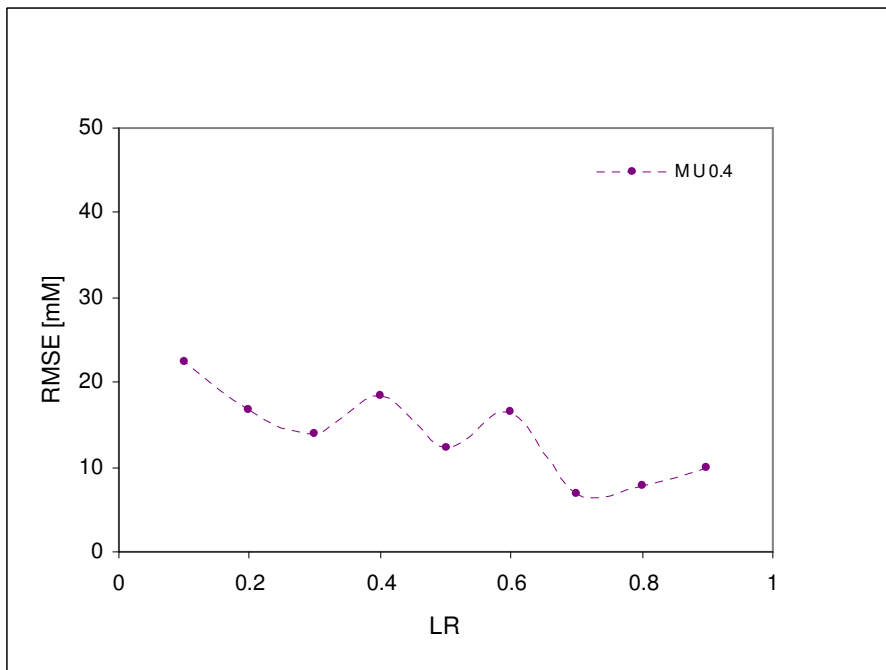


Figure 4.11.2: The effect of momentum on ANN learning in the estimation of PB concentration.

Once the ANN has been optimised it was capable to find the most likely identity of the unknown data pattern and predict output values of parameters of test solutions.

Results of ANN giving the most accurate prediction for different values of target parameters are shown in Figure 4.12 for pH, temperature, DO and PB concentration. The graphs illustrate the correlation between real (measured) values (x axis), and the values determined by ANN (y axis). Circles (\circ) indicate the mean values of data points of the network predictions. The standard deviation was calculated for 48 test samples for pH, temperature and PB concentration and 64 samples for DO for each point.

Analytical performance of the assay is demonstrated with relatively low root means square error (RMSE), which describes the quality of fitting of a regression model. The predictions were obtained with an error of only 0.004 for pH (Figure 4.12-A), 0.437 for temperature (Figure 4.12-B), 0.049 for DO (Figure 4.12-C) and 6.818 for PB concentration (Figure 4.12-D). The slightly higher RMSE obtained for PB concentration is probably because sensitivity of fluorescent dye selected for salt detection is lower than sensitivities of other dyes. The RMSE values seem acceptable especially for measurements at the low PB concentration range.

In these studies the combination of fluorescence signals of dye assay as a response to simultaneous changes of four parameters in the environment together with ANN allowed quick and accurate analysis of all these parameters.

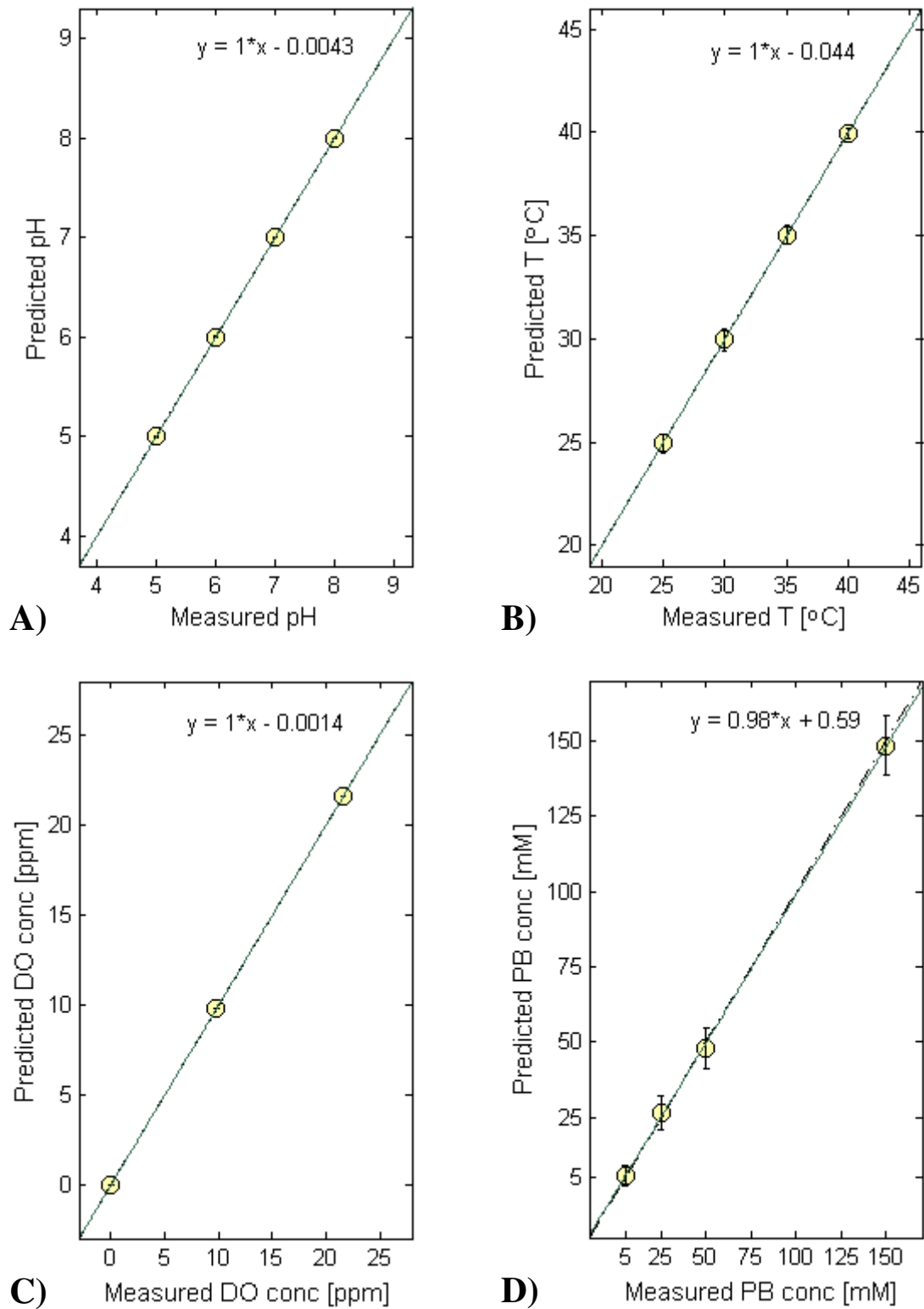


Figure 4.12: Correlation between actual (measured) and determined by ANN values of pH (A), temperature (B), DO concentration (C) and PB concentration (D). Points marked as circles (\odot) indicate mean values of data points of ANN simulations of unseen samples. Diagonal line (—) indicates best linear fit of data points and the line (-•-) indicates ideal response with zero error. Error bars indicate standard deviation.

4.4 Conclusion

The suitable mixture of five fluorescent dyes was designed with separation of their intensity maxima sufficient for discreet reading of the emission intensity changes of individual dyes in response to the changes of the tested environment.

The assay composed of the mixture fluorescent dyes combined with an ANN has been successfully developed for measurements of pH, temperature, dissolved oxygen and ionic strength of a solution. The obtained results have demonstrated high accuracy of the assay in simultaneous identification and calculation of several physicochemical parameters. Analytical performance of the assay was given by relatively low RMSE.

The ANN has shown promising ability in adapting and modelling the non-linear changes in the investigated systems, and providing accurate data analysis for measured solutions and prediction of simultaneously changes of several parameters.

The performance of the network can be improved by optimising the control factors such as momentum, learning rate, number of epoch or performance goal. This can reduce the error in the estimation of target parameters.

The selected fluorescent dyes were stable, soluble in water and had emission in VIS-NIR region making them attractive for analysis of biological samples.

The response time of dyes mixture to all analytes is very short (<1 min, the time for fluorescence scan to be taken) therefore the assay can be suitable for real-time measurements.

5. Fourth objective: testing optical assay with biological samples

5.1 Introduction

Considering the recent surge of attention to optical diagnostics, especially in the field of real-time detection *in vivo*, which is essential for biotechnology and clinical diagnostics, the development of an optical assay aimed not only at precise quantitative analysis of different analytes and physicochemical parameters of samples, but also at their qualitative characterisation. Sufficient diagnostics not always require exact concentration of individual compounds but rather tend to determine general condition of analysed samples. This usually depends on measurements of changes of various parameters and analytes. Therefore it would be more practical if the specificity of a device is related to recognition of response patterns obtained from overall interaction between a sample and all sensing elements. In this case the analytical capability of the system can lie in profiling the chemical or biological processes which occur in the samples and enable their qualitative analysis.

In this chapter the possibility of using the assay for such analysis is investigated. This study has been done to prove the general and diverse analytical ability of the assay. The successful development of the device would be of the great importance for many scientific and industrial sectors, improving the quality, speed of measurements and reducing their costs.

Using pattern recognition the mixture of dyes was tested on its ability to monitor development phases of cell cultures, identification of different strains of cells and diagnosis of several gastrointestinal diseases in human. The mixture of five fluorescent dyes while contacting with samples, generated fluorescence patterns distinctive for different environmental or medical conditions. Using chemometrics these patterns were analysed and the optical signal was further transferred into analytical characteristics of measured solutions.

5.2 Identification of growing phases of cell cultures

The majority of microorganisms have no significant impact on human life, but many certain types of bacteria, fungi, viruses or parasites are very important considering their beneficial or harmful effects.

To control of the growth of microorganisms is necessary for many practical reasons, e.g. in medicine (prevention and treatment of diseases, production of drugs), food industry (improving process of fermentation, food safety, controlling food spoilage) or agriculture science (indicating disinfection and sanitation, water, soil quality and fertility) (Shearer *et al.*, 2009; McMeekin *et al.*, 2010; Corbin *et al.*, 2008; Hornung *et al.*, 2009). This involves the identification of the phases of microbial growth to inhibit the process or recognise and learn favourable environmental conditions, which they need to live and reproduce (Kim *et al.*, 2004; Ingraham *et al.*, 1983).

In this chapter, the feasibility of the proposed approach to control microbial different development phases using the optical assay has been tested in growing *Escherichia coli* cultures.

5.2.1 Experimental part

Sample preparation

The bacterial strain used in the experiment was *Escherichia coli* (JM 83) received from Dr Judith Taylor, Cranfield Health (Cranfield University). Bacteria were recovered from frozen state by growing them in a Miller LB broth (Fluka Biochemica, Cat No. 1.10285), solution of 12.5 g of the medium in 0.5 L of Milli-Q water, overnight at 37 °C and subcultured. A petri dish containing *E. coli* is shown in Figure 5.1. The bacteria colonies were transferred into centrifuge tubes filled with 20 ml of liquid medium and incubated for 60 hours at 37 °C (Stanier *et al.*, 1987). The tubes with bacteria cells were collected at different intervals and centrifuged at 2800 rpm for 20 min. The supernatant was filtrated through a 0.22 µm filters and 3 ml of the filtrate were transferred into

quartz cuvette. 100 μ l of the mixture of fluorescent dyes (concentrations pacified in Chapter 4.2.1) was added to cuvette and the fluorescence of the dyes was measured.



Figure 5.1: *E. coli* growing on the nutrient agar plate.

Instrumentation

Absorption spectra of bacteria suspension at different growing phases were measured with Spectrometer (UVPC 2100, Shimadzu, Japan) at 550 nm. The fluorescence measurements were carried out with 3D spectrofluorometer (see description and specifications in Chapter 3.3.3).

Data evaluation

The obtained fluorescence patterns were analysed using an ANN based on changes of the height of the intensity peaks of fluorescent dyes caused by interactions with its surrounding media. The model network was created based on a feedforward network described in Chapter 4.2.4-B. All network control factors were chosen by default.

The network and trained on data patterns of samples of known identity (45 samples with known time of bacteria growth from 0 to 60 hours) using Bayesian backpropagation of errors. Once the ANN was trained an unseen set of data was used for the model evaluation (18 previously unseen samples). Based on learning experience, the network was capable of identifying unknown fluorescent fingerprints and predicts outputs (identifying test solutions).

5.2.2 Results and discussion

In the analysis of bacteria growth the mixture of dyes was added to supernatants taken from suspensions of growing microorganisms. Samples were collected at different intervals of time. Bacterial growth was monitored by measuring the absorption of the suspensions.

The example of a growth curve obtained for pure culture of *E. coli* (subcultured and left to grow) is presented in Figure 5.2. The curve demonstrated two main phases of bacteria growth (exponential and stationary phase of growth) (Ingraham *et al.*, 1983).

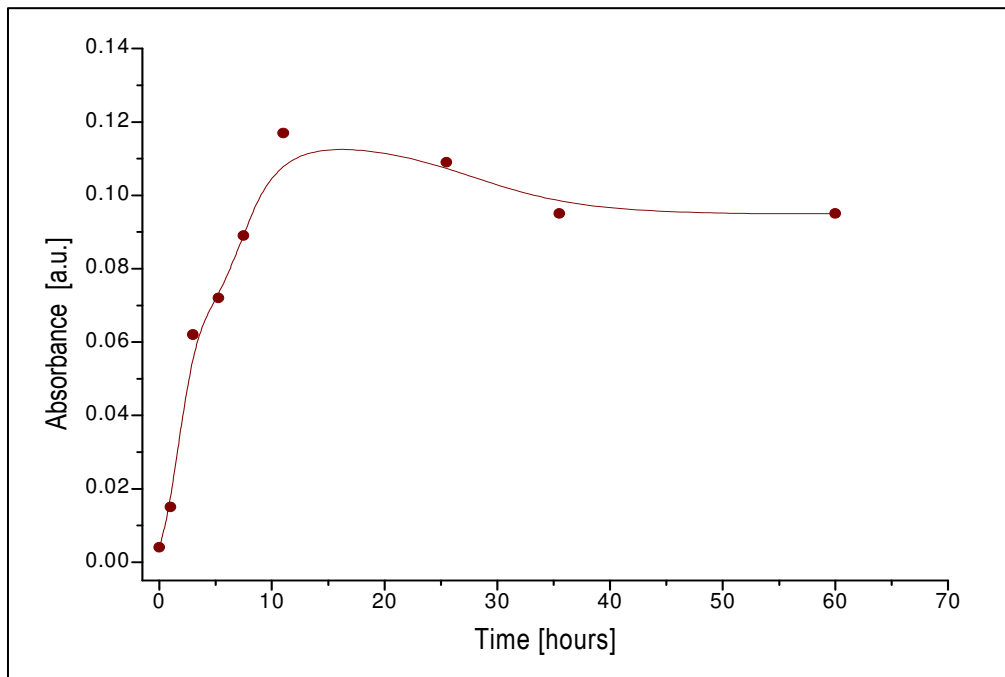


Figure 5.2: Growth curve of *E. coli* culture showing exponential and stationary phase of bacteria growth.

It can be seen that for the first ten hours (after the bacteria culture was transferred to a fresh medium) that there is a rapid increase in the absorption of bacteria suspension. Then, the increase of absorption stopped and it remained more or less constant. This corresponds to the intensive growth of bacteria culture while it is in the fresh medium, rich in nutrients. After they are consumed the culture stops growing and enter the stationary phase, when growth becomes unbalanced.

The curve presented in Figure 5.2 demonstrates control measurements performed along with fluorescence measurements of bacteria culture growth phases using an optical assay (see Figure 5.3). To avoid contamination of bacteria, the pure culture was subcultured to the series of tubes for independent testing (Stanier *et al.*, 1987). In certain time periods the suspension from one of the tubes was used in fluorescence measurements and the rest was left to grow for longer. The fluorescence measurements were performed by adding the mixture of fluorescent dyes to 3 ml of supernatant, which was taken from the tube containing a suspension of growing cells. The experiment was performed in triplicate. The maximum of fluorescence intensity of each dye is plotted as a function of time of bacteria growth.

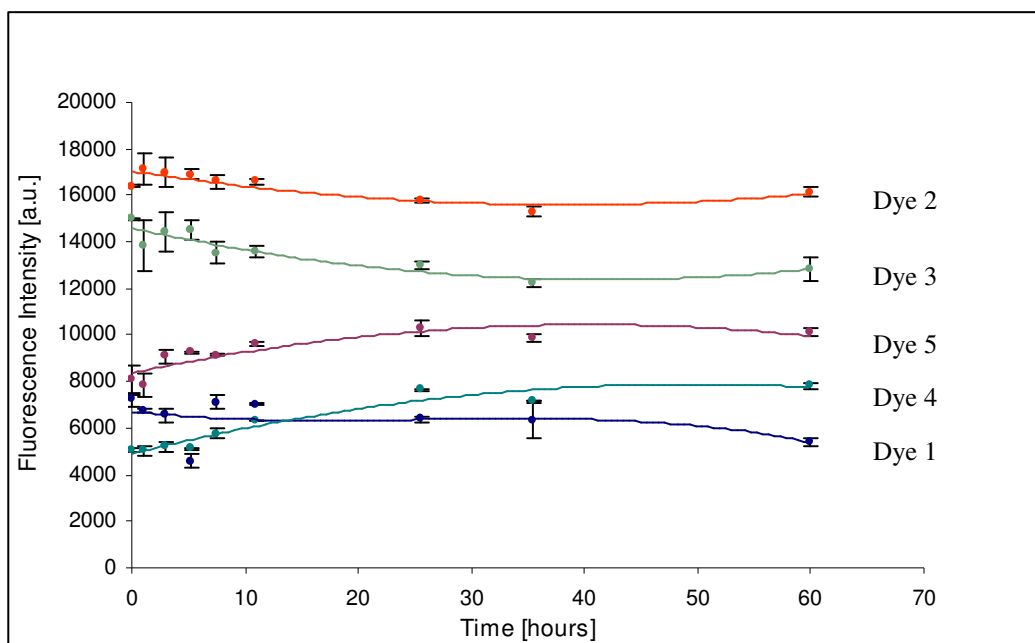


Figure 5.3: Changes in fluorescence intensity of five dyes of the mixture vs. time of bacteria growth. Dye 1 is HPTS, Dye 2 is OG514, Dye 3 is RB, Dye 4 is RuBpy, Dye 5 is THA. Measurements were performed in bacterial supernatant obtained from growing *E.coli*.

As Figure 5.3 shows these results correspond to the absorption measurements presented in Figure 5.2. The most significant changes in the absorption were observed during first 10 hours of the cell growth. Similar results were obtained for measurements of fluorescence intensity of the dyes mixture for different growing phases of bacteria.

Additionally, control measurements were performed using samples consisting of the mixture of fluorescence dyes in solution of only the medium, without growing cells (LB broth). They were kept in the same condition as diagnosed samples. Results for controls are presented in Figure 5.4 and show no changes in fluorescence intensity of dyes, therefore the changes in fluorescence for cell suspensions (see Figure 5.3) were caused by the presence of bacteria.

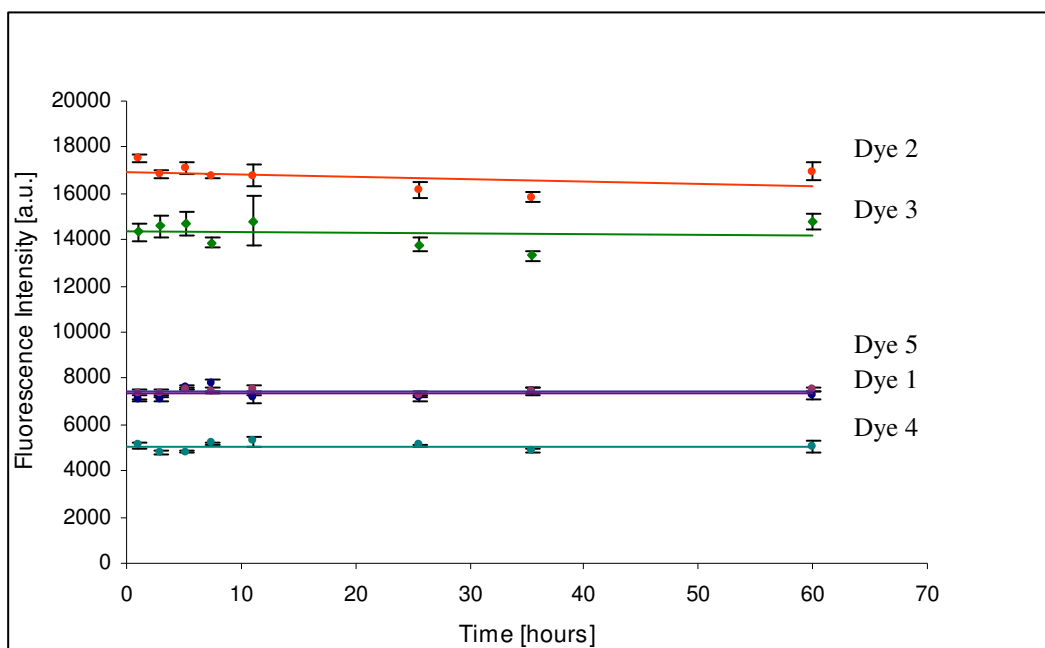


Figure 5.4: Control measurements of fluorescence intensity of the mixture of five dyes in LB broth. Dye 1 is HPTS, Dye 2 is OG514, Dye 3 is RB, Dye 4 is RuBpy, Dye 5 is THA.

The collected fluorescence patterns were analysed using an ANN based on changes of the height of the intensity peaks of fluorescent dyes. The model network, which has been previously optimised for simulations of four different parameters, was applied in the current experiment and revealed high efficiency. Similar to quantitative analysis of samples, the ability of the model network was tested by its training on data patterns of known identity (the known time of bacteria growth) and used this knowledge to determine the time of growth of bacteria in unknown suspensions (previously unseen samples).

Results of ANN predictions are shown in Figure 5.5. The graph illustrates the correlation between real (measured) time of growth of bacteria culture (x axis), and the time predicted by ANN (y axis). Circles (\circ) indicate the mean values of data points of the network prediction and error bars indicate standard deviation. The accurate prediction of time using ANN is demonstrated with the root means square error (RMSE) of 6.41.

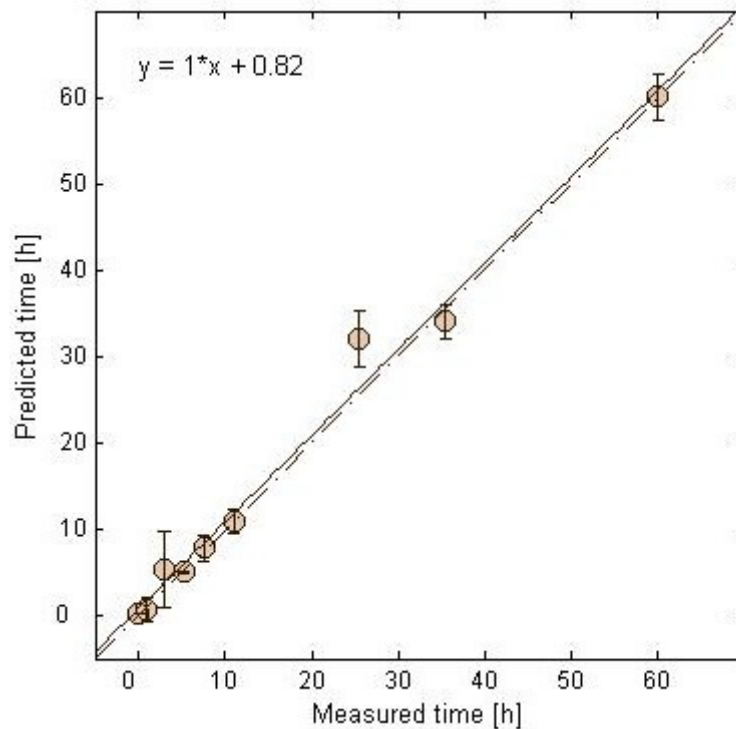


Figure 5.5: Correlation between actual (measured) and determined by ANN time of growth of bacteria culture. Points marked as circles (\circ) indicate mean values of data points of ANN simulations of unseen samples. Diagonal line (—) indicates best linear fit of data points and the line ($- \bullet -$) indicates ideal response with zero error. Error bars indicate standard deviation.

These promising results indicate that it is possible to use the fluorescence signals of a dye assay combined with ANN model in the determination of bacterial presence and their growth phases, which might be helpful for analysis of the quality of medical, food or environmental samples.

Further analysis can be improved by investigation of particular factors which affect bacteria growth, such as pH, oxygen, salt, sugars or nutrients concentration (Spaepen *et*

al., 2009). Usually, these parameters are optimal for one strain but they vary for others and can change frequently the natural environment affecting differently the growth of particular strain of microorganisms. Thus it is important to know the actual effects of these factors on the growth of microbial.

The current results are useful for controlling the growth rate of microorganisms and promising for the future, but for comprehensive control, to inhibit unwanted strain from growing, such as human pathogenic bacteria or to improve the development of the advantageous ones, the impact of certain factors on their growth should be better understood.

5.3 Discrimination between cell strains using mixture of fluorescent dyes

The next objective in the examination of analytical capability of the optical assay was to test the possibility of application of the mixture of fluorescent dyes to differentiate between two microbial species. As mentioned at the beginning of previous chapter, identification of certain kinds of microorganisms is very useful in many fields of science and industry for fast and robust recognition of specific strains, which can be useful for supplying products to improve human lives or harmful, causing diseases (Kopsahelis *et al.*, 2009; Aneesh *et al.*, 2009).

This approach has been carried out using two different strains of yeast.

5.3.1 Experimental part

Sample preparation

Two strains of yeasts used in the experiments were *Debaryomyces Hansenii* CBS. 941 and *pink yeast* - occurring naturally. Both strains were provided by Prof Naresh Magan from Applied Mycology Group, Cranfield Health (Cranfield University). Yeast cultures were grown in solidified agar plates containing the Malt Extract Agar (solution of 12.5 g of the medium in 0.5 L of Milli-Q water) and 100 ppm chloramphenicol at 25 °C and subcultured until pure colonies were obtained (see Figure 5.6, white yeast (left) and

pink yeast (right)). Then they were transferred into six tubes (three tubes for each kind of yeast) containing 20 ml of medium (solution of 1 g of the Yeast Extract Powder medium containing 1 g of glucose in 0.5 L of Milli-Q water) and incubated at 25 °C for 12 hours. The supernatant from two strains of yeast suspensions was taken and filtrated through a 0.22 µm filter and collected in new tubes. 3 ml of liquid were transferred into quartz cuvette and mixed with 100 µl of the mixture of fluorescent dyes was added to cuvette and the fluorescence of the dyes was measured. The concentrations of dyes are reported in Chapter 4.2.1.



Figure 5.6: White yeast (left) and pink yeast (right) growing on nutrient agar plate.

Instrumentation

The fluorescence measurements were carried out with 3D spectrofluorometer (see description and specifications in Chapter 3.3.3).

Data evaluation

The spectral characteristics of dyes mixture and changes caused by interactions with its surroundings were analysed using Principal Component Analysis (PCA). PCA was performed in Matlab (version 7.3.0, MathWorks Inc., 2006) using the PLS Toolbox (version 3.5).

The analysis of two strains of yeasts was based on changes of whole fluorescence spectra of the dye mixture.

5.3.2 Results and discussion

The investigation involved determining whether the two strains of yeast could be distinguished from one another. Measurements of fluorescence intensity of the dye mixture were performed in supernatant of a solution of two strains of yeasts (white and pink) using 3D spectrofluorometer. To exclude the impact of the concentration of cells on measurements, the experiment was carried out in triplicate sets of each type of yeasts. They were subcultured from solidified agar plate into three separate liquid medium and left to grow independently. Figure 5.7 shows the resulting PCA scores plot for these three replicates of each kind of yeast with a good separation of two clusters. The green triangles indicate pink and orange dots white yeasts.

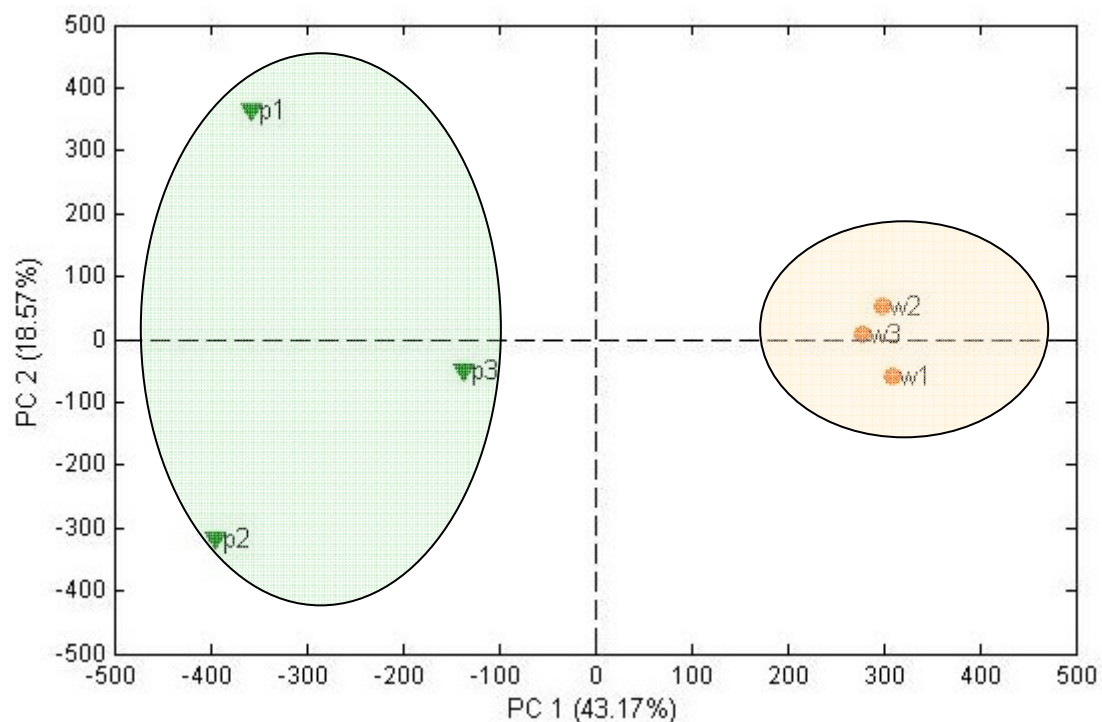


Figure 5.7: PCA score plot showing distinction between two different strains of yeasts.

Two independent variables (PCs) found accounted for 62 % of the variance within data set. This might indicate positively that the distinction between two strains of cell was possible. However, orange dots are clustered tightly together and the triangles are far apart. This suggests that the identification of white yeast could be easier than pink yeast, which did not give well repetitions in their fluorescence patterns. It would be therefore sufficient to control the exact concentration level of the cells in future measurements, to be sure that their effect on the fluorescence signal can be definitely excluded. Later it would also be practical to use more than two types of microorganisms (at least three), to allow more judgemental discussion and to increase the degree of certainty on the result.

5.4 Recognition of various gastrointestinal diseases in human

The final test of the optical assay analytical capability was performed on human urine samples for recognition of several gastrointestinal diseases (Crohn's disease, ulcerative colitis and irritable bowel syndrome). These chronic diseases are currently serious public health problems, which have been forecasted to increase further in most countries around the world (Underhill *et al.*, 2008; Reiff *et al.*, 2010). The identification of the symptoms, early diagnosis and treatment of these diseases is still challenging because the etiology and factors causing these complex disorders are yet not well known. Therefore, their mechanisms are difficult to explain, various types difficult to discriminate and therapeutic targets hard to identify (Wijmenga, 2005; Meuwis *et al.*, 2008). Typically, their diagnosis involves many analytical tests which are often costly and invasive. Therefore it is of a great importance to search for the suitable and sensitive method for controlling gastrointestinal microbiota and early detection of dangerous pathogens (Neish, 2009).

The code of practice (COP) for safely handling of clinical / biological samples is included in Appendix B.1.

5.4.1 Experimental part

Sample collection

The urine samples were taken from volunteers at Addenbrookes Hospital and provided by Dr Claire Turner, Head of the Volatiles Research Group, Cranfield Health, Cranfield University (the copy of the ethics approval is in Appendix B.2). All volunteers were given information, consent forms to read and sign, and a questionnaire, which provide details on their diet, exercise, sleep, medication and general health (a copy of these forms are included in Appendix B.3).

Urine samples were taken from healthy volunteers (CTR) and patients diagnosed with either Crohn's disease (CD), ulcerative colitis (UC), or irritable bowel syndrome (IBS). They were obtained prior to any medical treatment.

The samples were labelled with unique codes and stored in Addenbrookes Hospital at -80°C and then delivered to Cranfield University. At Cranfield the samples were storied at -20 °C until analysed. Before the measurements, each sample was defrosted and transferred into centrifuge tubes and then centrifuged at 2800 rpm for 20 minutes. The supernatant was filtrated through a 0.45 µm glass fibber filters (recommended to use with biological samples such as plasma, urine, serum) (Phenomenex, 2009). 100 µl of the mixture of fluorescent dyes (concentrations pacified in Chapter 4.2.1) was added added into each sample supernatant and measured.

Instrumentation

The fluorescence measurements were carried out with the 3D spectrofluorometer (see description and specifications in Chapter 3.3.3).

Data evaluation

The excitation - emission fluorescence pattern obtained for each samples was first analysed using Principal Component Analysis (PCA). PCA was performed in Matlab (version 7.3.0, MathWorks Inc., 2006) using the PLS Toolbox (version 3.5) and then

ANN probability network was implemented to classify the data (Demuth *et al.*, 2007). The architecture, algorithms and other parameters of this forward feed network were already developed and the modelling was performed in Matlab (version 7.3.0, MathWorks Inc., 2006) using the Neural Network Toolbox (version 5.0.1).

The number of urine (pre-treatment) samples used in analysis included 9 control samples, 11 IBS samples, 6 CD samples and 6 UC samples.

5.4.2 Results and Discussion

The experiments were performed to test whether the dye assay was able to identify different gastrointestinal diseases and healthy control based on the fluorescence patterns obtained from human urine samples so patients could be diagnosed with CD, UC or IBS.

Measurements of fluorescence intensity of the dye mixture were performed in supernatant of urine suspensions using the 3D spectrofluorometer based on changes of whole spectra of the dye mixture. Before measurements samples were centrifuged, filtrated and then, in the analysis the spectra were corrected by the background subtraction. The examination was carried out based on the fluorescence signal from the assay.

Data were first analysed using PCA to attained the most influential emission profiles from the EEM of each sample (Winquist *et al.*, 2000). These were further used as inputs for the ANN probability network to classify the three diseases from the healthy controls by assigning class values to the states: 1 for healthy; 2 for disease. Leave-one-out cross-validation (LOO-CV) permitted each sample to be classified leading to an overall success of classification (Figure 5.8). LOO-CV is commonly used in chemometrics crossvalidation method, where each sample is subsequently excluded from the dataset and others are used for training the network. The idea behind it is to predict the value of a compound from the regression equation obtained for the dataset of all other compounds.

Figure 5.8 shows the results of the combined PCA and ANN results which have been characterised by three features: specificity, which represents the number of true negatives (healthy samples). If the percentage of true negatives was 83% (83 out of 100 healthy samples were classified correctly) then there would be 17% false positives (17 out of 100 healthy samples incorrectly classified, classed as diseased), sensitivity represents the number of true positives (diseased samples). If the percentage of true positives were 92% (92 out of 100 diseased samples correctly classified), then there would be 8% false negatives (8 out of 100 diseased samples incorrectly classified, classed as healthy) and the last is overall success of discrimination.

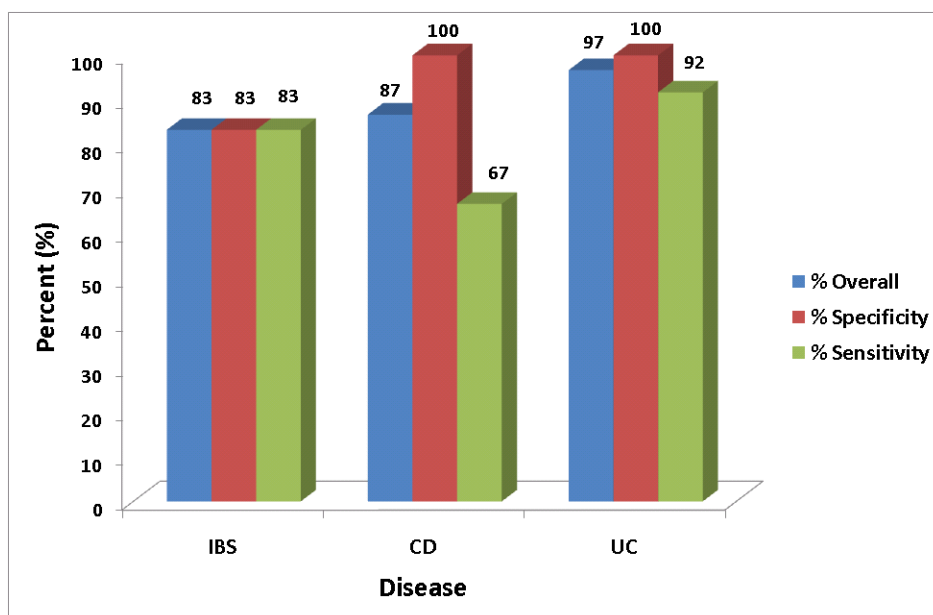


Figure 5.8: Ability of the ANN to discriminate the three diseases from the healthy controls: % Overall means the overall success of discrimination; % Specificity means the success of distinguishing the healthy controls; % Sensitivity means the success of distinguishing the disease.

Figure 5.8 illustrates that each disease can be discriminated from the healthy controls; for CD and UC, it can be seen that the healthy controls were all successfully classified (100%). The overall successes of discrimination (83%, 87%, and 97% for IBS, CD and UC respectively) show that the optical approach combined with chemometrics is highly promising. Identification of a number of true positives gave slightly worse results

especially for CD, 67%, but for IBS and UC (83% and 92% respectively) it remains relatively high.

Summarising, the demonstrated results are very promising, but they still require further investigation such as the discrimination the diseases from one another, and comparing other classification techniques including multi-way techniques.

5.5 Conclusions

Following the approach of optical assay development for quantitative analysis of samples, it has been applied further for qualitative examination of complex biological samples. The specificity of the device based on the interferences between their various components and all fluorescence dyes. The analysis of acquired data was related to recognition of response fluorescence patterns which were unique to particular conditions and considered similar to fingerprints.

Firstly, based on the response data patterns the assay proved to be capable to closely estimate different development phases of growing bacteria cells. However, for a final justification on this ability of the assay to control microbial rate growth, it is important to carry on testing of different microorganisms. If the result stays positive it could be of great importance especially in sectors of research of industry where bacteria are used for supply products beneficial for human life, such as food, pharmaceutical or cosmetic areas, but it is also essential for inhibition of dangerous pathogens or monitoring the bacteria, which are used for decomposition of waste materials.

Another experiment which was carried out involved the discrimination between strains of yeasts (white and pink species). Although the discrimination was successful, it has been limited only to two types of yeasts and therefore it would be reasonable to expend the experiment to at least three different kinds of microorganisms, which would give better view on the different types of variation in the patterns and would be closer to the natural environment thus provide more reliable results.

In the final experiment the optical assay was used for diagnosis of clinical samples (human urine) for recognition of three gastrointestinal diseases and healthy controls. It has been shown that by using this assay it was possible to discriminate between healthy patients and those with different diseases and also differentiate Crohn's disease, ulcerative colitis and irritable bowel syndrome. However, the technique does not give information on the composition of samples, however the promising results indicate possibility of using the assay for accurate, noninvasive, not expensive and quick diagnosis of human gastrointestinal microbiota.

6. Overall discussion and conclusions

The leading objective of this thesis was to develop a novel, optical diagnostic assay with an operating principle similar to electronic nose and tongue sensors and to suggest its potential applications. This study was based on a mixture of fluorescence dyes pattern analysis for quantitative and qualitative characterisation of complex samples.

The proposed optical assay was composed of a mixture of five environment-sensitive fluorescent dyes combined with chemometric techniques for the processing of distinctive spectra of the dye mixture in response to changes in environment.

6.1 Dyes selection

The appropriate fluorescence dyes were selected based on the published information on their physical and chemical properties, especially high sensitivities, good stability, suitable spectral characteristics, commercial availability and low price. They are well known dye-indicators for pH, temperature or DO concentration and characterised by low photobleaching and high excitation coefficient, which are of a great importance in giving reliable results and improving the assay stability and efficiency.

It was also advantageous that in the selection of dyes the cross-sensitivity was not an issue, which has been an significant problem in the research on optical sensors before. The selective dyes had to be sensitive to target analyte without cross-interferences with others. This approach is however almost impossible to realise in real samples and outside control, laboratory conditions. In this approach various compounds of samples are detected by all elements of the assay, all dyes in the mixture, and combine with chemometrics to process this data, easy to understand by users.

Experimental studies on the dye mixture were in a close correlation with data from the literature. The assay has revealed high sensitivity within a wide dynamic range for the given parameters and similar excitation and emission wavelengths, advantageous shifted

of about 20 nm to longer values in excitation for rhodamine B (from 519 to 541 nm), oregon green 514 (from 480 to 504 nm), tris (4,7 - diphenyl - 1,10 - phenanthroline) ruthenium dichloride (from 440 to 463 nm) and thionin acetate (from 520 to 541 nm). Values in the emission wavelengths changed only for thionin acetate (from 623 to 638 nm) and 8 - hydroxypyrene - 1',3,6 - trisulfonic acid did not change its fluorescence spectrum. Therefore, the mixture of dyes did not have a significant impact on the dyes spectral characteristics however it affected their stability. When dyes have been stored as separate solutions and mixed together before measurements, the same stock solutions could be used for months but when their mixture was stored, dyes were permanently losing their ability to fluoresce after one day. This was however tested only when the stock solutions of dyes were prepared in water. Therefore, their stability might be improved through the preparation of high concentrated mixture of dyes in organic solvent and then dissolved the mixture in water before measurements, or dry the mixture, and then when necessary, dissolve the powder.

This approach gives also the possibility of modification of mixture of dyes by choosing dyes with different properties, depending on the various requirements (eg. sensitivity, excitation and emission wavelengths or decay time).

6.2 Quantitative and qualitative analysis

Since different dyes with varying sensitivities were included in the mixture, the assay has been proposed for multiply measurements of several parameters such as pH, temperature and dissolved oxygen concentration in a single sample. Such ability can be crucial for quantitative analysis, especially when these parameters or analytes changing simultaneously. In addition, a mixture of dyes may reveal an enhanced sensitivity to other parameters than those defined, like it happened with salt concentration of a buffer solution. It increases, the assay's ability to determine more than four parameters at the same place and time and thus enabled chemical or physicochemical sensors to be compensated for the effect of pH, temperature, oxygen or salt level when compared with monosensors.

This feature would be useful especially for qualitative study of clinical, food or environmental samples wherein changes are usually triggered by more than one factor and when these factors interfere with each other. Thus, the combination of several different dyes with known sensitivities could allow specific assay to be made more unspecific if necessary. Using the assay enables also smaller samples volume to be analysed for more information being provided. It is especially important when the volume of the sample is limited (eg. clinical samples).

In the first approach, the mixture of dyes was combined with ANN for determination and quantification of four parameters, such as pH temperature, DO and ionic strength of PB buffer. Measurements were carried out in two stages. Initially, only one parameter of the solution was changing while others were kept constant and later all four parameters have been changed and the analysis of the simultaneous determination of four parameters was tested.

ANN has showed great ability to adapt and model non-linear changes of fluorescence patterns and accurate determination of given parameters for all measured solutions. Presented experiments have shown that the structure of model network depended on the complexity of the analysed problem. While single parameter of the sample was changing and others were constant, the prediction model network was based on simple linear neural network classifier, revealed sufficient enough to allow quick and accurate predictions. In a more complicated approach, when several parameters had to be simultaneously determined, the network performance was enhanced by using a more advanced model. This included modification of a structure by increasing the number of neurons in the hidden layer and optimisation of control factors and algorithm used in the network learning process.

The ANN was also used for qualitative analysis of biological samples and determination of growth rate of microbial as well as identification and classification of clinical samples from patients with different gastrointestinal conditions. Obtained results were promising and have shown that the optical assay combined with ANN can also be used as a helpful tool to control development phases of cell cultures and diagnosis of clinical

samples. It suggests wide and diverse applications including biological, clinical and environmental analysis.

Beside ANN, PCA have been applied in the processing of the acquired fluorescence patterns of the dyes mixture for discrimination between two strains of yeasts. PCA has shown the ability for profiling the data and by extracting the “dominant patterns” in the dataset, it allowed the observation of the relationships between the samples, suggesting some differences or similarities among them.

The main limitation of PCA is that this method is not optimised for data classification and does not account for class separation. The results of the PCA recognition do not guarantee that assign directions of maximum variance in the data will contain sufficient features for discrimination of new samples. Thus, the information is not fully reliable and therefore further classification of samples should be made using a different and more advanced method. This was demonstrated in the last experiment, when patients with different gastrointestinal conditions had to be identified and PCA was used for data pre-treatment. It was performed to reduce the number of variables prior to ANN modelling.

These initial experiments and promising results demonstrated the potential of using the optical assay and chemometrics as a new marker for rapid screening of specific diseases and other complex disorders or contaminants and diverse changes in biological or environmental samples. This work has shown that the type of cell cultures, their age, as well as the microbial species and cell lines, all influence fluorescence pattern of the mixture of dyes. However, the assay should be further tested, especially for the ability of qualitative analysis at low concentrations, which is of the great importance for prevention, early diagnosis or immediate treatment implementation.

6.3 Suggestions and future work

The presented work provides the basis and practical framework for the future development of the optical assay. Although, a number of open issues related to its implementation must be solved in order to complete the statement of the assay performance, feasibility and benefits of its applications, it was expected that this research will provide guidance and encouragement for the future research on similar optical systems.

Further investigation should involve additional tests of the assay on other biological, clinical and environmental samples, e.g. waste water, food, soil, or human blood samples. It is advisable to try to discriminate between fluorescence patterns of more than two microbial species and analyse their responses to different environmental conditions, which could improve the qualitative control of food or environmental samples by establishing the correlation between specific factors and samples quality, and provide an easy and efficient screening method. It would also be interesting to try to identify and quantify the parameters or compounds responsible for such changes in the fluorescence patterns. This would help to understand the physiology of the processes and enable their regulation. Additionally, it could be helpful for development of a sensor for detection and monitoring of specific compounds or parameters within biological or environmental samples and define the assay detection limit. However it has been done in buffer solution, never for biological media.

To claim the potential of using the optical assay also for medical applications it is important to make more tests on clinical samples. Additionally, it is decisive to optimise the data analysis and automate the system. Although much work is still required before the system is ready for clinical studies, initial experiments have been done towards attaining this goal.

Another issue in question is the assay stability. Further studies should include the integration of fluorescent dyes with polymers in order to increase the assay thermal and chemical stability and also to reduce possible toxicity of dyes for *in vivo* applications.

The major plan for the future includes using the optical assay as a smart ‘vanishing tattoo’ (similar to temporary child’s tattoos), which could be painlessly impregnated into the human skin and applied for the real-time multi detection and monitoring of physiological parameters and chemical analytes in the human body (this idea was already mentioned in Chapter 2.2). Such a smart tattoo can possibly be applied in routine clinical diagnostics, general therapeutic management, skin care, cosmetic products testing or monitoring transcutaneous drug delivery.

Skin diagnostics may include measurements of physiological parameter and metabolites concentrated within human skin. It is an area of increasing interest especially for the pharmaceutical and cosmetic industries. Skin monitoring is also important for understanding and improving drug efficiency.

The basic parameters, which can be monitored within the human skin, are: pH (pH 4.0-6.0), redox sensitivity, temperature (32-35 °C), humidity, and the level of oxygenation (5.3 kPa (40 mmHg), the average partial pressure of oxygen (pO_2) in a tissue). The main metabolites that can be detected, and their levels, include: glucose, saccharides, oxygen, creatinine, lactic acid and urea.

The *pH* of human skin is acidic and varies from pH 4.0-6.0 (Buraczewska *et al.*, 2005). The pH is an important parameter and with, for example; the skin thickness, *moisture* and *temperature*, can play a crucial role for the skin permeability, its barrier function and its recovery (Lee *et al.*, 2006; Martinez-Pla *et al.*, 2003). This can have an impact in the pharmaceutical industry, (solubility and partitioning of drugs in the skin layers), and for skin care. With age skin’s pH becomes more neutral and thus more susceptible to bacterial growth and infections, as the reduced acidity of the skin can kill fewer bacteria. However, it is important to maintain the right microflora of the skin, and therefore, the normal pH and the moisture for each skin type.

Another physiological parameter that is important to control in human skin is the *redox status*. The skin is constantly exposed to chemical oxidants, air pollutants and ultraviolet (UV) solar light, which is the major generator for reactive oxygen species (ROS) that induct oxidative stress (Briganti *et al.*, 2003; Ziosi *et al.*, 2006). The skin

antioxidant network protects cells against oxidative injury, but when the oxidative stress overwhelms the skin antioxidant capacity, degenerative processes begin to occur. This can lead to many diseases (including skin cancer).

Other compounds used for detection and monitoring in the skin are *saccharides* or *glucose*. Knowing the glucose level is especially important for diabetics. They suffer from a chronic disease, diabetes, which affects the ability of the body to produce or respond to insulin, the hormone that allows glucose to enter the body's cells and to be stored or used for energy. Most diabetics require insulin injections, and most of the time they have to carefully monitor and manage their blood glucose levels themselves. Because glucose levels can fluctuate widely throughout the day for optimal control they have to do the blood test several times a day (usually from finger pricks). Therefore, novel, rapid and minimal-invasive method for measurements of glucose level could have a significant impact on new developments in medicine.

Also, the quantitative visualisation of *oxygen flux* or *molecular oxygen* distribution in the skin is very important for medical diagnosis. The oxygen content in the skin can indicate its viability. Monitoring the level of *creatinine*, *lactic acid*, ***urea*** and other metabolites concentrated in human skin is also possible and important to control.

The essential task in the approach would be the integration of fluorescent dye mixture with polymers, not only to improve its stability but also to facilitate the controlled delivery of the dyes into the skin. Additionally, it should reduce toxicity of dyes and risk of possible reaction in patients. Therefore, the choice of suitable polymers used for dyes conjugation would be extremely important. Next, the toxicity of dyes-polymer conjugates must be analysed in *in vitro* tests.

The long term plan also includes the development and optimisation of geometry of the vanishing tattoo pattern, delivery protocol for skin impregnation and industrial prototypes for the signal processing.

The optical properties of human skin are described in Appendix C1.

7. References

- Abegunde, D. O., Mathers, C. D., Adam, T., Ortegón, M. and Strong, K. (2007). Chronic diseases 1 - The burden and costs of chronic diseases in low-income and middle-income countries. *Lancet*, 370(9603), 1929-1938.
- Agostiano, A., Mavelli, F., Milano, F., Giotta, L., Trotta, M., Nagy, L. and Maroti, P. (2004). pH-sensitive fluorescent dye as probe for proton uptake in photosynthetic reaction centers. *Bioelectrochemistry*, 63(1-2), 125-128.
- Ahmad, A. L. and Hairul, N. A. H. (2009). Protein-membrane interactions in forced-flow electrophoresis of protein solutions: effect of initial pH and initial ionic strength. *Separation and Purification Technology*, 66(2), 273-278.
- Ahmed, M. U., Hossain, M. M. and Tamiya, E. (2008). Electrochemical biosensors for medical and food applications. *Electroanalysis*, 20(6), 616-626.
- Alegret, S. (2006). Chemical sensors as integrated analytical systems. *Revista Mexicana De Fisica*, 52(2), 99-103.
- Amao, Y. (2003). Probes and polymers for optical sensing of oxygen. *Microchimica Acta*, 143(1), 1-12.
- Aneesh, T. P., Hisham, M., Sekhar, M. S., Madhu, M. and Deepa, T. V. (2009). International market scenario of traditional Indian herbal drugs - India declining... *International Journal of Green Pharmacy*, 3(3), 184-190.
- Arik, M., Celebi, N. and Onganer, Y. (2005). Fluorescence quenching of fluorescein with molecular oxygen in solution. *Journal of Photochemistry and Photobiology a-Chemistry*, 170(2), 105-111.
- Arik, M. and Onganer, Y. (2003). Molecular excitons of pyronin B and pyronin Y in colloidal silica suspension. *Chemical Physics Letters*, 375(1-2), 126-133.
- Asaria, P., Chisholm, D., Mathers, C., Ezzati, M. and Beaglehole, R. (2007). Chronic diseases 3 - chronic disease prevention: health effects and financial costs of strategies to reduce salt intake and control tobacco use. *Lancet*, 370(9604), 2044-2053.
- Aschi, M., D'Archivio, A. A., Fontana, A. and Formiglio, A. (2008). Physicochemical properties of fluorescent probes: experimental and computational determination of the overlapping pK(a) values of carboxyfluorescein. *Journal of Organic Chemistry*, 73(9), 3411-3417.
- Bachinger, T. and Mandenius, C. F. (2000). Searching for process information in the aroma of cell cultures. *Trends in Biotechnology*, 18(12), 494-500.

- Badugu, R., Kostov, Y., Rao, G. and Tolosa, L. (2008). Development and application of an excitation ratiometric optical pH sensor for bioprocess monitoring. *Biotechnology Progress*, 24(6), 1393-1401.
- Bai, H. and Shi, G. Q. (2007). Gas sensors based on conducting polymers. *Sensors*, 7(3), 267-307.
- Bailey, R. T., Cruickshank, F. R., Deans, G., Gillanders, R. N. and Tedford, M. C. Characterization of a fluorescent sol-gel encapsulated erythrosin B dissolved oxygen sensor. In: *5th Workshop on Biosensors and Biological Techniques in Environmental Analysis*, Ithaca, New York, May 31-Jun 04, 2002.
- Bake, K. D. and Walt, D. R. (2008). Multiplexed spectroscopic detections. *Annual Review of Analytical Chemistry*, 1, 515-547.
- Baker, G. A., Watkins, A. N., Pandey, S. and Bright, F. V. (1999). Static and time-resolved fluorescence of fluorescein-labeled dextran dissolved in aqueous solution or sequestered within a sol-gel-derived hydrogel. *Analyst*, 124(3), 373-379.
- Baldini, F., Giannetti, A. and Mencaglia, A. A. (2007). Optical sensor for interstitial pH measurements. *Journal of Biomedical Optics*, 12(2), 7.
- Baldini, S., Chester, A. N., Homola, J. and Martellucci, S., Eds. (2006). Optical chemical sensors. Mathematics, Physics and Chemistry. Springer, Firenze.
- Baleizao, C., Nagl, S., Schaferling, M., Berberan-Santos, M. N. and Wolfbeis, O. S. (2008). Dual fluorescence sensor for trace oxygen and temperature with unmatched range and sensitivity. *Analytical Chemistry*, 80(16), 6449-6457.
- Bally, M., Halter, M., Voros, J. and Grandin, H. M. (2006). Optical microarray biosensing techniques. *Surface and Interface Analysis*, 38(11), 1442-1458.
- Basabe-Desmonts, L., Benito-Lopez, F., Gardeniers, H., Duwel, R., van den Berg, A., Reinhoudt, D. N. and Crego-Calama, M. (2008). Fluorescent sensor array in a microfluidic chip. *Analytical and Bioanalytical Chemistry*, 390(1), 307-315.
- Basabe-Desmonts, L., Reinhoudt, D. N. and Crego-Calama, M. (2007). Design of fluorescent materials for chemical sensing. *Chemical Society Reviews*, 36(6), 993-1017.
- Basu, B. J. and Rajam, K. S. (2004). Comparison of the oxygen sensor performance of some pyrene derivatives in silicone polymer matrix. *Sensors and Actuators B-Chemical*, 99(2-3), 459-467.
- Basu, B. J., Thirumurugan, A., Dinesh, A. R., Anandan, C. and Rajam, K. S. (2005). Optical oxygen sensor coating based on the fluorescence quenching of a new pyrene derivative. *Sensors and Actuators B-Chemical*, 104(1), 15-22.
- Bawa, P., Pillay, V., Choonara, Y. E. and du Toit, L. C. (2009). Stimuli-responsive polymers and their applications in drug delivery. *Biomedical Materials*, 4(2), 022001.

- Beaglehole, R. and Bonita, R. (2008). Global public health: a scorecard. *Lancet*, 372(9654), 1988-1996.
- Beaglehole, R., Ebrahim, S., Reddy, S., Voute, J., Leeder, S. and Chronic Dis Action, G. (2007). Chronic Diseases 5 - prevention of chronic diseases: a call to action. *Lancet*, 370(9605), 2152-2157.
- Begu, S., Mordon, S., Desmettre, T. and Devoisselle, J. M. (2005). Fluorescence imaging method for in vivo pH monitoring during liposomes uptake in rat liver using a pH-sensitive fluorescent dye. *Journal of Biomedical Optics*, 10(2), 6.
- Bhattarai, N., Ramay, H. R., Gunn, J., Matsen, F. A. and Zhang, M. Q. (2005). PEG-grafted chitosan as an injectable thermosensitive hydrogel for sustained protein release. *Journal of Controlled Release*, 103(3), 609-624.
- Boens, N., Qin, W. W., Basaric, N., Orte, A., Talavera, E. M. and Alvarez-Pez, J. M. (2006). Photophysics of the fluorescent pH indicator BCECF. *Journal of Physical Chemistry A*, 110(30), 9334-9343.
- Borisov, S. M. and Klimant, I. (2009). Luminescent nanobeads for optical sensing and imaging of dissolved oxygen. *Microchimica Acta*, 164(1-2), 7-15.
- Borisov, S. M., Krause, C., Arain, S. and Wolfbeis, O. S. (2006). Composite material for simultaneous and contactless luminescent sensing and imaging of oxygen and carbon dioxide. *Advanced Materials*, 18(12), 1511-1516.
- Borth, N., Kral, G. and Katinger, H. (1993). Rhodamine 123 fluorescence of immortal hybridoma cell lines as a function of glucose concentration. *Cytometry*, 14(1), 70-73.
- Brereton, R. G. (2007). Applied chemometrics for scientists. John Wiley & Sons Ltd, Chichester.
- Brettar, I. and Hofle, M. G. (2008). Molecular assessment of bacterial pathogens - a contribution to drinking water safety. *Current Opinion in Biotechnology*, 19(3), 274-280.
- Bronzino, J. D. (2000). Biomedical engineering handbook. 2nd ed. CRC Press, Boca Raton.
- Cai, Y., Shinar, R., Zhou, Z. and Shinar, J. (2008). Multianalyte sensor array based on an organic light emitting diode platform. *Sensors and Actuators B-Chemical*, 134(2), 727-735.
- Cammann, K., Lemke, U., Rohen, A., Sander, J., Wilken, H. and Winter, B. (1991). Chemical sensors and biosensors - principles and applications. *Angewandte Chemie-International Edition in English*, 30(5), 516-539.
- Cardosi, M. F. (2000). Encyclopedia of analytical chemistry: applications, theory and instrumentation. John Wiley & Sons Ltd, Chichester.

- Careri, M., Elviri, L. and Mangia, A. (2009). Element - tagged immunoassay with inductively coupled plasma mass spectrometry for multianalyte detection. *Analytical and Bioanalytical Chemistry*, 393(1), 57-61.
- Casalinuovo, I. A., Di Pierro, D., Coletta, M. and Di Francesco, P. (2006). Application of electronic noses for disease diagnosis and food spoilage detection. *Sensors*, 6(11), 1428-1439.
- Castillo, J., Gaspar, S., Leth, S., Niculescu, M., Mortari, A., Bontidean, I., Soukharev, V., Dorneanu, S. A., Ryabov, A. D. and Csoregi, E. (2004). Biosensors for life quality - design, development and applications. *Sensors and Actuators B-Chemical*, 102(2), 179-194.
- Cauchi, M. (2006). 2-Dimensional and 3-Dimensional fluorescence spectroscopy. Environmental diagnostics MSc. Silsoe, Cranfield University.
- Celebi, N., Arik, M. and Onganer, Y. (2007). Analysis of fluorescence quenching of pyronin B and pyronin Y by molecular oxygen in aqueous solution. *Journal of Luminescence*, 126(1), 103-108.
- Chang, C. C., Saad, B., Surif, M., Ahmad, M. N. and Shakaff, A. Y. M. (2008). Disposable e-tongue for the assessment of water quality in fish tanks. *Sensors*, 8(6), 3665-3677.
- Chang, J. B. and Subramanian, V. (2008). Electronic noses sniff success. *Ieee Spectrum*, 45(3), 50-56.
- Choi, M. F. (1997). Spectroscopic behaviour of 8-hydroxy-1,3,6-pyrenetrisulphonate immobilized in ethyl cellulose. *Journal of Photochemistry and Photobiology a-Chemistry*, 104(1-3), 207-212.
- Chow, E., Herrmann, J., Barton, C. S., Raguse, B. and Wieczorek, L. (2009). Inkjet-printed gold nanoparticle chemiresistors: influence of film morphology and ionic strength on the detection of organics dissolved in aqueous solution. *Analytica Chimica Acta*, 632(1), 135-142.
- Ciosek, P., Grabowska, I., Brzozka, Z. and Wroblewski, W. (2008). Analysis of dialysate fluids with the use of a potentiometric electronic tongue. *Microchimica Acta*, 163(1-2), 139-145.
- Ciosek, P. and Wroblewski, W. (2007). Performance of selective and partially selective sensors in the recognition of beverages. *Talanta*, 71(2), 738-746.
- Ciosek, P. and Wroblewski, W. (2007). Sensor arrays for liquid sensing - electronic tongue systems. *Analyst*, 132(10), 963-978.
- Citterio, D. and Suzuki, K. (2008). Smart taste sensors. *Analytical Chemistry*, 80(11), 3965-3972.

Clark, J. L., Miller, P. F. and Rumbles, G. (1998). Red edge photophysics of ethanolic rhodamine 101 and the observation of laser cooling in the condensed phase. *Journal of Physical Chemistry A*, 102(24), 4428-4437.

Codinachs, L. M. I., Baldi, A., Merlos, A., Abramova, N., Ipatov, A., Jimenez-Jorquera, C. and Bratov, A. (2008). Integrated multisensor for FIA-based electronic tongue applications. *Ieee Sensors Journal*, 8(5-6), 608-615.

Cohen-Kashi, M., Deutsch, M., Tirosh, R., Rachmani, H. and Weinreb, A. (1997). Carboxyfluorescein as a fluorescent probe for cytoplasmic effects of lymphocyte stimulation. *Spectrochimica Acta Part a-Molecular and Biomolecular Spectroscopy*, 53(10), 1655-1661.

Collings, A. F. and Caruso, F. (1997). Biosensors: recent advances. *Reports on Progress in Physics*, 60(11), 1397-1445.

Collison, M. E., Aebli, G. V., Petty, J. and Meyerhoff, M. E. (1989). Potentiometric combination ion/carbon dioxide sensors for in vitro and in vivo blood measurements. *Analytical Chemistry*, 61(21), 2365-2372.

Corbin, B. D., Seeley, E. H., Raab, A., Feldmann, J., Miller, M. R., Torres, V. J., Anderson, K. L., Dattilo, B. M., Dunman, P. M., Gerads, R., Caprioli, R. M., Nacken, W., Chazin, W. J. and Skaar, E. P. (2008). Metal chelation and inhibition of bacterial growth in tissue abscesses. *Science*, 319(5865), 962-965.

Cortez, D. V. and Roberto, I. C. (2006). Effect of phosphate buffer concentration on the batch xylitol production by *Candida guilliermondii*. *Letters in Applied Microbiology*, 42(4), 321-325.

Coskun, T., Chu, S. and Montrose, M. H. (2001). Intragastric pH regulates conversion from net acid to net alkaline secretion by the rat stomach. *American Journal of Physiology-Gastrointestinal and Liver Physiology*, 281(4), G870-G877.

D'Amico, A., Di Natale, C., Paolesse, R., Macagnano, A., Martinelli, E., Pennazza, G., Santonico, A., Bernabei, M., Roscioni, C., Galluccio, G., Bono, R., Agro, E. F. and Rullo, S. (2008). Olfactory systems for medical applications. *Sensors and Actuators B-Chemical*, 130(1), 458-465.

D'Auria, S., Herman, P., Rossi, M. and Lakowicz, J. R. (1999). The fluorescence emission of the apo-glucose oxidase from *Aspergillus niger* as probe to estimate glucose concentrations. *Biochemical and Biophysical Research Communications*, 263(2), 550-553.

D'Auria, S. and Lakowicz, J. R. (2001). Enzyme fluorescence as a sensing tool: new perspectives in biotechnology. *Current Opinion in Biotechnology*, 12(1), 99-104.

Daar, A. S., Singer, P. A., Persad, D. L., Pramming, S. K., Matthews, D. R., Beaglehole, R., Bernstein, A., Borysiewicz, L. K., Colagiuri, S., Ganguly, N., Glass, R. I., Finegood, D. T., Koplan, J., Nabel, E. G., Sarna, G., Sarrafzadegan, N., Smith, R., Yach, D. and

- Bell, J. (2007). Grand challenges in chronic non-communicable diseases. *Nature*, 450(7169), 494-496.
- Danaei, G., Ding, E. L., Mozaffarian, D., Taylor, B., Rehm, J., Murray, C. J. L. and Ezzati, M. (2009). The preventable causes of death in the United States: comparative risk assessment of dietary, lifestyle, and metabolic risk factors. *Plos Medicine*, 6(4), 23.
- de Leon, C. P., Campbell, S. A., Smith, J. R. and Walsh, F. C. (2008). Conducting polymer coatings in electrochemical technology - part 2 - application areas. *Transactions of the Institute of Metal Finishing*, 86(1), 34-40.
- del Valle, M. (2008). Electrochemical micro(bio)sensor arrays. *Microchimica Acta*, 163(1-2), 1-2.
- Delmotte, C. and Delmas, A. (1999). Synthesis and fluorescence properties of Oregon green 514 labeled peptides. *Bioorganic & Medicinal Chemistry Letters*, 9(20), 2989-2994.
- Demchenko, A. P. (2005). Optimization of fluorescence response in the design of molecular biosensors. *Analytical Biochemistry*, 343(1), 1-22.
- Demuth, H., Beale, M. and Hagan, M. (2007). NN Toolbox 5: users guide. The MathWorks Inc, Natick.
- DePedro, H. M. and Urayama, P. (2009). Using LysoSensor yellow/blue DND-160 to sense acidic pH under high hydrostatic pressures. *Analytical Biochemistry*, 384(2), 359-361.
- Diamond, D. (1998). Principles of chemical and biological sensors. John Wiley & Sons Inc, New York.
- Dickinson, T. A., White, J., Kauer, J. S. and Walt, D. R. (1996). A chemical-detecting system based on a cross-reactive optical sensor array. *Nature*, 382(6593), 697-700.
- Distante, C., Indiveri, G. and Reina, G. (2009). An application of mobile robotics for olfactory monitoring of hazardous industrial sites. *Industrial Robot-an International Journal*, 36(1), 51-59.
- DTI (2006). Photonics: a UK strategy for success. UK, Department of Trade and Industry.
- Duckett, S. J. (2009). Are we ready for the next big thing? *Medical Journal of Australia*, 190(12), 687-688.
- Esbensen, K., Kirsanov, D., Legin, A., Rudnitskaya, A., Mortensen, J., Pedersen, J., Vogensen, L., Makarychev-Mikhailov, S. and Vlasov, Y. (2004). Fermentation monitoring using multisensor systems: feasibility study of the electronic tongue. *Analytical and Bioanalytical Chemistry*, 378(2), 391-395.

Esbensen, K. H., Guyot, D., Westad, F. and Houmøller, L. P. (2002). Multivariate data analysis: in practice. An introduction to multivariate data analysis and experimental design. 5th ed. Camo Process AS, Oslo.

Ferguson, J. A., Healey, B. G., Bronk, K. S., Barnard, S. M. and Walt, D. R. (1997). Simultaneous monitoring of pH, CO₂ and O₂ using an optical imaging fiber. *Analytica Chimica Acta*, 340(1-3), 123-131.

Fernandes, D. L. A. and Gomes, M. (2008). Development of an electronic nose to identify and quantify volatile hazardous compounds. *Talanta*, 77(1), 77-83.

Fernandes, D. L. A., Oliveira, J. and Gomes, M. (2008). Detecting spoiled fruit in the house of the future. *Analytica Chimica Acta*, 617(1-2), 171-176.

Fisher, K. A., Huddersman, K. D. and Taylor, M. J. (2003). Comparison of micro- and mesoporous inorganic materials in the uptake and release of the drug model fluorescein and its analogues. *Chemistry-a European Journal*, 9(23), 5873-5878.

Fraden, J. (2003). Handbook of modern sensors: physics, designs, and applications. 3rd ed. Springer, New York.

Frost, M. C. and Meyerhoff, M. E. (2002). Implantable chemical sensors for real-time clinical monitoring: progress and challenges. *Current Opinion in Chemical Biology*, 6(5), 633-641.

Fujiwara, Y., Okura, I., Miyashita, T. and Amao, Y. (2002). Optical oxygen sensor based on fluorescence change of pyrene-1-butyric acid chemisorption film on an anodic oxidation aluminium plate. *Analytica Chimica Acta*, 471(1), 25-32.

Funfak, A., Cao, J. L., Wolfbeis, O., Martin, K. and Kohler, J. (2009). Monitoring cell cultivation in microfluidic segments by optical pH sensing with a micro flow-through fluorometer using dye-doped polymer particles. *Microchimica Acta*, 164(3-4), 279-286.

Ganter, M. and Zollinger, A. (2003). Continuous intravascular blood gas monitoring: development, current techniques, and clinical use of a commercial device. *British Journal of Anaesthesia*, 91(3), 397-407.

Garcia-Gonzalez, D. L. and Aparicio, R. (2002). Sensors: from biosensors to the electronic nose. *Grasas Y Aceites*, 53(1), 96-114.

Ge, F. Y. and Chen, L. G. (2008). pH fluorescent probes: chlorinated fluoresceins. *Journal of Fluorescence*, 18(3-4), 741-747.

Gemeay, A. H., Mansour, L. A., El-Sharkawy, R. G. and Zaki, A. B. (2004). Kinetics of the oxidative degradation of thionine dye by hydrogen peroxide catalyzed by supported transition metal ions complexes. *Journal of Chemical Technology and Biotechnology*, 79(1), 85-96.

Genuis, S. J. (2008). Medical practice and community health care in the 21st century: a time of change. *Public Health*, 122(7), 671-680.

Gopel, W. (1998). Chemical imaging: concepts and visions for electronic and bioelectronic noses. *Sensors and Actuators B-Chemical*, 52(1-2), 125-142.

Gründler, P. (2007). Chemical sensors: an introduction for scientists and engineers Springer, Berlin.

Gutes, A., Cespedes, F. and del Valle, M. (2007). Electronic tongues in flow analysis. *Analytica Chimica Acta*, 600(1-2), 90-96.

Gutierrez, M., Alegret, S., Caceres, R., Casadesus, J., Marfa, O. and Del Valle, M. (2008). Nutrient solution monitoring in greenhouse cultivation employing a potentiometric electronic tongue. *Journal of Agricultural and Food Chemistry*, 56(6), 1810-1817.

Gutierrez, M., Alegret, S. and del Valle, M. (2008). Bioelectronic tongue for the simultaneous determination of urea, creatinine and alkaline ions in clinical samples. *Biosensors & Bioelectronics*, 23(6), 795-802.

Gutierrez, M., Gutierrez, J. M., Alegret, S., Leija, L., Hernandez, P. R., Favari, L., Munoz, R. and Del Valle, M. (2008). Remote environmental monitoring employing a potentiometric electronic tongue. *International Journal of Environmental Analytical Chemistry*, 88(2), 103-117.

Gutierrez, M., Moo, V. M., Alegret, S., Leija, L., Hernandez, P. R., Munoz, R. and del Valle, M. (2008). Electronic tongue for the determination of alkaline ions using a screen-printed potentiometric sensor array. *Microchimica Acta*, 163(1-2), 81-88.

Haddad, R., Lapid, H., Harel, D. and Sobel, N. (2008). Measuring smells. *Current Opinion in Neurobiology*, 18(4), 438-444.

Hanson, K. M., Behne, M. J., Barry, N. P., Mauro, T. M., Gratton, E. and Clegg, R. M. (2002). Two-photon fluorescence lifetime imaging of the skin stratum corneum pH gradient. *Biophysical Journal*, 83(3), 1682-1690.

Hartmann, P. and Trettnak, W. (1996). Effects of polymer matrices on calibration functions of luminescent oxygen sensors based on porphyrin ketone complexes. *Analytical Chemistry*, 68(15), 2615-2620.

Hassing, H. C., Twickler, T. B., Kastelein, J. J. P., Cramer, M. J. M. and Cassee, F. R. (2009). Air pollution as noxious environmental factor in the development of cardiovascular disease. *Netherlands Journal of Medicine*, 67(4), 116-121.

Haugland, R. P. (1996). The handbook - a guide to fluorescent probes and labeling technologies. 6th ed. Molecular Probes, Eugene.

Hille, C., Berg, M., Bressel, L., Munzke, D., Primus, P., Lohmannsroben, H. G. and Dosche, C. (2008). Time-domain fluorescence lifetime imaging for intracellular pH sensing in living tissues. *Analytical and Bioanalytical Chemistry*, 391(5), 1871-1879.

Holzwarth, J. F., Couderc, S., Beeby, A., Parker, A. W. and Clark, I. P. Laser temperature jump experiments with micrometre space resolution using rhodamine 101 anti-Stokes fluorescence from nanoseconds to milliseconds. In: *225th ACS National Meeting*, New Orleans, LA, 2003.

Hornung, M., Biener, R. and Schmauder, H. P. (2009). Dynamic modelling of bacterial cellulose formation. *Engineering in Life Sciences*, 9(4), 342-347.

Huang, Y. Q., Kangas, L. J. and Rasco, B. A. (2007). Applications of artificial neural networks (ANNs) in food science. *Critical Reviews in Food Science and Nutrition*, 47(2), 113-126.

Hulanicki, A., Glab, S. and Ingman, F. (1991). Chemical sensors: definitions and classification. *Pure and Applied Chemistry*, 63(9), 1247-1250.

Hulth, S., Aller, R. C., Engstrom, P. and Selander, E. (2002). A pH plate fluorosensor (optode) for early diagenetic studies of marine sediments. *Limnology and Oceanography*, 47(1), 212-220.

Ibey, B. L. (2006). Enhancement of a fluorescent sensor for monitoring glucose concentration in diabetic patients. *PhD thesis*, Biomedical Engineering, Texas A&M University, Galveston, TX.

Ibey, B. L., Beier, H. T., Rounds, R. M., Cote, G. L., Yadavalli, V. K. and Pishko, M. V. (2005). Competitive binding assay for glucose based on glycodendrimer-fluorophore conjugates. *Analytical Chemistry*, 77(21), 7039-7046.

Ingraham, J. L., Maaloe, O. and Neidhardt, F. C. (1983). Growth of cells and cultures. In: *Growth of the bacterial cell*. Sinauer Associates Inc, Sunderland.

Ivanov, V. B., Behnisch, J., Hollander, A., Mehdorn, F. and Zimmermann, H. (1996). Determination of functional groups on polymer surfaces using fluorescence labeling. *Surface and Interface Analysis*, 24(4), 257-262.

James, D., Scott, S. M., Ali, Z. and O'Hare, W. T. (2005). Chemical sensors for electronic nose systems. *Microchimica Acta*, 149(1-2), 1-17.

Janata, J., Josowicz, M. and Devaney, D. M. (1994). Chemical sensors. *Analytical Chemistry*, 66(12), R207-R228.

Janzen, M. C., Ponder, J. B., Bailey, D. P., Ingison, C. K. and Suslick, K. S. (2006). Colorimetric sensor arrays for volatile organic compounds. *Analytical Chemistry*, 78(11), 3591-3600.

Jiang, J. J., Gao, L., Zhong, W., Meng, S., Yong, B., Song, Y. L., Wang, X. D. and Bai, C. X. (2008). Development of fiber optic fluorescence oxygen sensor in both in vitro and in vivo systems. *Respiratory Physiology & Neurobiology*, 161(2), 160-166.

Jokerst, N., Royal, M., Palit, S., Luan, L., Dhar, S. and Tyler, T. (2009). Chip scale integrated microresonator sensing systems. *Journal of Biophotonics*, 2(4), 212-226.

Jorge, P. A. S., Caldas, P., Da Silva, J., Rosa, C. C., Oliva, A. G., Santos, J. L. and Farahi, F. (2005). Luminescence-based optical fiber chemical sensors. *Fiber and Integrated Optics*, 24(3-4), 201-225.

Ju, X. J., Xie, R., Yang, L. and Chu, L. Y. (2009). Biodegradable 'intelligent' materials in response to physical stimuli for biomedical applications. *Expert Opinion on Therapeutic Patents*, 19(4), 493-507.

Kemnitzer, N. U., Zilles, A., Arden-Jacob, J., Drexhage, K. H., Michael Gross, M. and Hamers, M. (2002). Fluorescent dyes - detection methods of the future. *Bioforum International*, 5, 242-243.

Kim, J., Cho, M., Oh, B., Choi, S. and Yoon, J. (2004). Control of bacterial growth in water using synthesized inorganic disinfectant. *Chemosphere*, 55(5), 775-780

Kober, E. M., Marshall, J. L., Dressick, W. J., Sullivan, B. P., Caspar, J. V. and Meyer, T. J. (1985). Synthetic control of excited states. Nonchromophoric ligand variations in polypyridyl complexes of osmium(II). *Inorganic Chemistry*, 24(18), 2755-2763.

Kocincova, A. S., Borisov, S. M., Krause, C. and Wolfbeis, O. S. (2007). Fiber-optic microsensors for simultaneous sensing of oxygen and pH, and of oxygen and temperature. *Analytical Chemistry*, 79(22), 8486-8493.

Kocincova, A. S., Nagl, S., Arain, S., Krause, C., Borisov, S. M., Arnold, M. and Wolfbeis, O. S. (2008). Multiplex bacterial growth monitoring in 24-well microplates using a dual optical sensor for dissolved oxygen and pH. *Biotechnology and Bioengineering*, 100(3), 430-438.

Kopsahelis, N., Nisiotou, A., Kourkoutas, Y., Panas, P., Nychas, G. J. E. and Kanellaki, M. (2009). Molecular characterization and molasses fermentation performance of a wild yeast strain operating in an extremely wide temperature range. *Bioresource Technology*, 100(20), 4854-4862.

Kotze, M. J. and Badenhorst, C. (2005). Chronic disease risk management: combining genetic testing with medical and nutrition therapy. *Genetics in Family Practice*, 47(4), 43-44.

Krantz-Rulcker, C., Stenberg, M., Winquist, F. and Lundstrom, I. (2001). Electronic tongues for environmental monitoring based on sensor arrays and pattern recognition: a review. *Analytica Chimica Acta* 426(2), 217-226.

Krommenhoek, E. E., Gardeniers, J. G. E., Bomer, J. G., Li, X., Ottens, M., van Dedem, G. W. K., Van Leeuwen, M., van Gulik, W. M., van der Wielen, L. A. M., Heijnen, J. J. and van den Berg, A. (2007). Integrated electrochemical sensor array for on-line monitoring of yeast fermentations. *Analytical Chemistry*, 79(15), 5567-5573.

Krommenhoek, E. E., van Leeuwen, M., Gardeniers, H., van Gulik, W. M., van den Berg, A., Li, X. N., Ottens, M., van der Wielen, L. A. M. and Heijnen, J. J. (2008). Lab-scale fermentation tests of microchip with integrated electrochemical sensors for pH,

temperature, dissolved oxygen and viable biomass concentration. *Biotechnology and Bioengineering*, 99(4), 884-892.

Kuwana, E. and Sevick-Muraca, E. M. (2003). Fluorescence lifetime spectroscopy for pH sensing in scattering media. *Analytical Chemistry*, 75(16), 4325-4329.

LaFratta, C. N. and Walt, D. R. (2008). Very high density sensing arrays. *Chemical Reviews*, 108(2), 614-637.

Lakowicz, J. R. (2006). Principles of fluorescence spectroscopy. 3rd ed. Springer, New York.

Lakowicz, J. R., Dattelbaum, J. D. and Gryczynski, I. (1999). Intensity measurements in scattering media. *Sensors and Actuators B-Chemical*, 60(1), 1-7.

Lakowicz, J. R. and Maliwal, B. (1993). Optical sensing of glucose using phase-modulation fluorimetry. *Analytica Chimica Acta*, 271(1), 155-164.

Lange, U., Roznyatouskaya, N. V. and Mirsky, V. M. (2008). Conducting polymers in chemical sensors and arrays. *Analytica Chimica Acta*, 614(1), 1-26.

Langner, M. and Hui, S. W. (1993). Merocyanine interaction with phosphatidylcholine bilayers. *Biochimica Et Biophysica Acta*, 1149(1), 175-179.

Lawrence, N. S., Beckett, E. L., Davis, J. and Compton, R. G. (2002). Advances in the voltammetric analysis of small biologically relevant compounds. *Analytical Biochemistry*, 303(1), 1-16.

Lee, E. D., Werner, T. C. and Seitz, W. R. (1987). Luminescence ratio indicators for oxygen. *Analytical Chemistry*, 59(2), 279-283.

Lee, G., Chu, K., Conroy, L., Fix, L., Lui, G. and Truesdell, C. (2007). A study of biophotonics: market segments, size and growth. *Optik & Photonik*(2), 30-35.

Lee, R. J., Wang, S., Turk, M. J. and Low, P. S. (1998). The effects of pH and intraliposomal buffer strength on the rate of liposome content release and intracellular drug delivery. *Bioscience Reports*, 18(2), 69-78.

Lee, S., They, B. L., Cote, G. L. and Pishko, M. V. (2008). Measurement of pH and dissolved oxygen within cell culture media using a hydrogel microarray sensor. *Sensors and Actuators B-Chemical*, 128(2), 388-398.

Lee, S. Y., Kim, H. U., Park, J. H., Park, J. M. and Kim, T. Y. (2009). Metabolic engineering of microorganisms: general strategies and drug production. *Drug Discovery Today*, 14(1-2), 78-88.

Li, B. B., Gao, Z. H., Zhou, X. Y., Ren, H. B., Xie, M., Fan, Y. J., Hu, J. F. and Jia, W. S. (2008). A confocal technique applicable to studies of cellular pH-related signaling in plants. *Journal of Integrative Plant Biology*, 50(6), 682-690.

- Liang, F., Pan, T. S. and Sevick-Muraca, E. M. (2005). Measurements of FRET in a glucose-sensitive affinity system with frequency-domain lifetime spectroscopy. *Photochemistry and Photobiology*, 81(6), 1386-1394.
- Lieberzeit, P. A. and Dickert, F. L. (2008). Rapid bioanalysis with chemical sensors: novel strategies for devices and artificial recognition membranes. *Analytical and Bioanalytical Chemistry*, 391(5), 1629-1639.
- Lieberzeit, P. A. and Dickert, F. L. (2009). Chemosensors in environmental monitoring: challenges in ruggedness and selectivity. *Analytical and Bioanalytical Chemistry*, 393(2), 467-472.
- Lin, H. J., Herman, P., Kang, J. S. and Lakowicz, J. R. (2001). Fluorescence lifetime characterization of novel low-pH probes. *Analytical Biochemistry*, 294(2), 118-125.
- Lin, H. J., Herman, P. and Lakowicz, J. R. (2003). Fluorescence lifetime-resolved pH imaging of living cells. *Cytometry Part A*, 52A(2), 77-89.
- Lin, H. J., Szmazinski, H. and Lakowicz, J. R. (1999). Lifetime-based pH sensors: Indicators for acidic environments. *Analytical Biochemistry*, 269(1), 162-167.
- Liu, J. X., Diwu, Z. J. and Leung, W. Y. (2001). Synthesis and photophysical properties of new fluorinated benzo[c]xanthene dyes as intracellular pH indicators. *Bioorganic & Medicinal Chemistry Letters*, 11(22), 2903-2905.
- Liu, W. T., Wu, J. H., Li, E. S. Y. and Selamat, E. S. (2005). Emission characteristics of fluorescent labels with respect to temperature changes and subsequent effects on DNA microchip studies. *Applied and Environmental Microbiology*, 71(10), 6453-6457.
- Lobanov, A. V., Borisov, I. A., Gordon, S. H., Greene, R. V., Leathers, T. D. and Reshetilov, A. N. (2001). Analysis of ethanol-glucose mixtures by two microbial sensors: application of chemometrics and artificial neural networks for data processing. *Biosensors & Bioelectronics*, 16(9-12), 1001-1007.
- Lopez-Feria, S., Cardenas, S. and Valcarcel, M. (2008). Simplifying chromatographic analysis of the volatile fraction of foods. *Trac-Trends in Analytical Chemistry*, 27(9), 794-803.
- Luo, W., Abbas, M. E., Zhu, L. H., Zhou, W. Y., Li, K. J., Tang, H. Q., Liu, S. S. and Li, W. Y. (2009). A simple fluorescent probe for the determination of dissolved oxygen based on the catalytic activation of oxygen by iron(II) chelates. *Analytica Chimica Acta*, 640(1-2), 63-67.
- Luong, J. H. T., Male, K. B. and Glennon, J. D. (2008). Biosensor technology: technology push versus market pull. *Biotechnology Advances*, 26(5), 492-500.
- Magg, T. and Albert, M. H. (2007). Tracking cell proliferation using the far red fluorescent dye SNARF-1. *Cytometry Part B-Clinical Cytometry*, 72B(6), 458-464.

- Malecha, M., Bessant, C. and Saini, S. (2002). Principal components analysis for the visualisation of multidimensional chemical data acquired by scanning Raman microspectroscopy. *Analyst*, 127(9), 1261-1266.
- Manconi, M., Isola, R., Falchi, A. M., Sinico, C. and Fadda, A. M. (2007). Intracellular distribution of fluorescent probes delivered by vesicles of different lipidic composition. *Colloids and Surfaces B-Biointerfaces*, 57(2), 143-151.
- Mano, J. F. (2008). Stimuli-responsive polymeric systems for biomedical applications. *Advanced Engineering Materials*, 10(6), 515-527.
- Marcotte, N. and Brouwer, A. M. (2005). Carboxy SNARE-4F as a fluorescent pH probe for ensemble and fluorescence correlation spectroscopies. *Journal of Physical Chemistry B*, 109(23), 11819-11828.
- McCarroll, M. E., Billiot, F. H. and Warner, I. M. (2001). Fluorescence anisotropy as a measure of chiral recognition. *Journal of the American Chemical Society*, 123(13), 3173-3174.
- McMeekin, T. A., Hill, C., Wagner, M., Dahl, A. and Ross, T. (2010). Ecophysiology of food-borne pathogens: Essential knowledge to improve food safety. *International Journal of Food Microbiology*, In Press, Corrected Proof.
- McShane, M. J., Russell, R. J., Pishko, M. V. and Cote, L. G. (2000). Glucose monitoring using implanted fluorescent microspheres. *Ieee Engineering in Medicine and Biology Magazine*, 19(6), 36-45.
- Maeda, H., Matsu-ura, S., Yamauchi, Y. and Ohmori, H. (2001). Resazurin as an electron acceptor in glucose oxidase-catalyzed oxidation of glucose. *Chemical & Pharmaceutical Bulletin*, 49(5), 622-625.
- Medlock, K., Harmer, H., Worsley, G., Horgan, A. and Pritchard, J. (2007). pH-sensitive holograms for continuous monitoring in plasma. *Analytical and Bioanalytical Chemistry*, 389(5), 1533-1539.
- Mehta, G., Mehta, K., Sud, D., Song, J. W., Bersano-Begey, T., Futai, N., Heo, Y. S., Mycek, M. A., Linderman, J. J. and Takayama, S. (2007). Quantitative measurement and control of oxygen levels in microfluidic poly(dimethylsiloxane) bioreactors during cell culture. *Biomedical Microdevices*, 9(2), 123-134.
- Mendelson, Y. (2000). Optical sensors. In: *The biomedical engineering handbook*. CRC Press, Boca Raton.
- Meuwis, M. A., Fillet, M., Chapelle, J. P., Malaise, M., Louis, E. and Merville, M. P. (2008). New biomarkers of Crohn's disease: serum biomarkers and development of diagnostic tools. *Expert Review of Molecular Diagnostics*, 8(3), 327-337.
- Miller, E. and Jozwik-Styczynska, D. (2007). The mechanism of pyrene fluorescence quenching by selective and nonselective quenchers during sol-gel transition. *Colloid and Polymer Science*, 285(14), 1561-1571.

Moczko, E., Meglinski, I. and Piletsky, S. (2008). Vanishing "tattoo" multi-sensor for biomedical diagnostics. In: *Conference on Biophotonics - Photonic Solution for Better Health Care*, Strasbourg, France, Apr 08-10, 2008. SPIE-Int. Soc. Opt. Eng, Bellingham, WA.

Moczko, E., Meglinski, I. V., Bessant, C. and Piletsky, S. A. (2009). Dyes assay for measuring physicochemical parameters. *Analytical Chemistry*, 81(6), 2311-2316.

Mordon, S., Maunoury, V., Devoisselle, J. M., Abbas, Y. and Coustaud, D. (1992). Characterization of tumorous and normal tissue using a pH-sensitive fluorescence indicator (5,6-carboxyfluorescein) in vivo. *Journal of Photochemistry and Photobiology B-Biology*, 13(3-4), 307-314.

Moschou, E. A., Sharma, B. V., Deo, S. K. and Daunert, S. (2004). Fluorescence glucose detection: advances toward the ideal in vivo biosensor. *Journal of Fluorescence*, 14(5), 535-547.

Nagl, S., Schaeferling, M. and Wolfbeis, O. S. (2005). Fluorescence analysis in microarray technology. *Microchimica Acta*, 151(1-2), 1-21.

Nagl, S., Stich, M. I. J., Schaeferling, M. and Wolfbeis, O. S. (2009). Method for simultaneous luminescence sensing of two species using optical probes of different decay time, and its application to an enzymatic reaction at varying temperature. *Analytical and Bioanalytical Chemistry*, 393(4), 1199-1207.

Nagl, S. and Wolfbeis, O. S. (2007). Optical multiple chemical sensing: status and current challenges. *Analyst*, 132(6), 507-511.

Natrajan, V. K. and Christensen, K. T. (2009). Two-color laser-induced fluorescent thermometry for microfluidic systems. *Measurement Science & Technology*, 20(1), 11.

Neish, A. S. (2009). Microbes in Gastrointestinal Health and Disease. *Gastroenterology*, 136(1), 65-80.

Nitin, N., Carlson, A. L., Muldoon, T., El-Naggar, A. K., Gillenwater, A. and Richards-Kortum, R. (2009). Molecular imaging of glucose uptake in oral neoplasia following topical application of fluorescently labeled deoxy-glucose. *International Journal of Cancer*, 124(11), 2634-2642.

O'Neil, R. G., Wu, L. and Mullani, N. (2005). Uptake of a fluorescent deoxyglucose analog (2-NBDG) in tumor cells. *Molecular Imaging and Biology*, 7(6), 388-392.

O'Riordan, T. C., Fitzgerald, K., Ponomarev, G. V., Mackrill, J., Hynes, J., Taylor, C. and Papkovsky, D. B. (2007). Sensing intracellular oxygen using near-infrared phosphorescent probes and live-cell fluorescence imaging. *American Journal of Physiology-Regulatory Integrative and Comparative Physiology*, 292(4), R1613-R1620.

Öberg, P. Å. (2003). Optical sensors in medical care. *Sensors Update*, 13(1), 201-232.

- Olivieri, A. C. (2008). Analytical advantages of multivariate data processing. One, two, three, infinity? *Analytical Chemistry*, 80(15), 5713-5720.
- Onganer, Y. and Quitevis, E. L. (1992). Effect of solvent on nonradiative processes in xanthene dyes: pyronin B in alcohols and alcohol-water mixtures. *Journal of Physical Chemistry*, 96(20), 7996-8001.
- Ordovas, J. M. and Shen, J. (2008). Gene-environment interactions and susceptibility to metabolic syndrome and other chronic diseases. *Journal of Periodontology*, 79(8), 1508-1513.
- Orsini, A. and D'Arnico, A. Chemical sensors and chemical sensor systems: Fundamentals limitations and new trends. In: *Conference of the NATO Advanced-Study-Institute on Advances in Sensing with Security Applications*, Ciocco, Italy, Jul, 2005. Springer.
- Orte, A., Crovetto, L., Talavera, E. M., Boens, N. and Alvarez-Pez, J. M. (2005). Absorption and emission study of 2',7'-difluorofluorescein and its excited-state buffer-mediated proton exchange reactions. *Journal of Physical Chemistry A*, 109(5), 734-747.
- Oter, O., Ertekin, K., Topkaya, D. and Alp, S. (2006). Emission-based optical carbon dioxide sensing with HPTS in green chemistry reagents: room-temperature ionic liquids. *Analytical and Bioanalytical Chemistry*, 386(5), 1225-1234.
- Otto, M. (2007). Chemometrics: statistics and computer application in analytical chemistry. Wiley-VCH, Chichester.
- Palacios, M. A., Nishiyabu, R., Marquez, M. and Anzenbacher, P. (2007). Supramolecular chemistry approach to the design of a high-resolution sensor array for multianion detection in water. *Journal of the American Chemical Society*, 129(24), 7538-7544.
- Pan, L. and Yang, S. X. (2007). A new intelligent electronic nose system for measuring and analysing livestock and poultry farm odours. *Environmental Monitoring and Assessment*, 135(1-3), 399-408.
- Paolesse, R., Lvova, L., Nardis, S., Di Natale, C., D'Amico, A. and Lo Castro, F. (2008). Chemical images by porphyrin arrays of sensors. *Microchimica Acta*, 163(1-2), 103-112.
- Papkovsky, D. B., Ponomarev, G. V., Trettnak, W. and Oleary, P. (1995). Phosphorescent complexes of porphyrin ketones: optical properties and application to oxygen sensing. *Analytical Chemistry*, 67(22), 4112-4117.
- Pearce, T. C., Schiffman, S. S., Nagle, H. T. and Gardner, J. W. (2003). Handbook of machine olfaction: electronic nose technology. Wiley-VCH, Weinheim.
- Penn, D. J., Oberzaucher, E., Grammer, K., Fischer, G., Soini, H. A., Wiesler, D., Novotny, M. V., Dixon, S. J., Xu, Y. and Brereton, R. G. (2007). Individual and gender

fingerprints in human body odour. *Journal of the Royal Society Interface*, 4(13), 331-340.

Pereira, L. and Plonski, G. A. (2009). Shedding light on technological development in Brazil. *Technovation*, 29(6-7), 451-464.

Perez-Guisado, J., Munoz-Serrano, A. and Alonso-Moraga, A. (2008). Spanish Ketogenic Mediterranean diet: a healthy cardiovascular diet for weight loss. *Nutrition Journal* 7(30), 1-7.

Pickup, J. C., Hussain, F., Evans, N. D., Rolinski, O. J. and Birch, D. J. S. (2005). Fluorescence-based glucose sensors. *Biosensors & Bioelectronics*, 20(12), 2555-2565.

Piletsky, S., Moczko, E. and Meglinski, I. (2002). Optical multisensor. C. University. UK.

Pioggia, G., Di Francesco, F., Marchetti, A., Ferro, A., Leardi, R. and Ahluwalia, A. (2007). A composite sensor array impedentiometric electronic tongue part II. Discrimination of basic tastes. *Biosensors & Bioelectronics*, 22(11), 2624-2628.

Pioggia, G., Ferro, M. and Di Francesco, F. (2007). Towards a real-time transduction and classification of chemoresistive sensor array signals. *Ieee Sensors Journal*, 7(1-2), 237-244.

Pioggia, G., Ferro, M., Di Francesco, F., Ahluwalia, A. and De Rossi, D. (2008). Assessment of bioinspired models for pattern recognition in biomimetic systems. *Bioinspiration & Biomimetics*, 3(1), 11.

Potyrailo, R. A. and Hieftje, G. M. (1998). Oxygen detection by fluorescence quenching of tetraphenylporphyrin immobilized in the original cladding of an optical fiber. *Analytica Chimica Acta*, 370(1), 1-8.

Pravdova, V., Pravda, M. and Guilbault, G. G. (2002). Role of chemometrics for electrochemical sensors. *Analytical Letters*, 35(15), 2389-2419.

Price, C. P. (2001). Microarrays: The reincarnation of multiplexing in laboratory medicine, but now more relevant? *Clinical Chemistry*, 47(8), 1345-1346.

Prüss-Üstün, A., Bos, R., Gore, F. and Bartram, J. (2008). Safer water, better health: costs, benefits and sustainability of interventions to protect and promote health. Geneva, World Health Organization.

Rahman, M. A., Kumar, P., Park, D. S. and Shim, Y. B. (2008). Electrochemical sensors based on organic conjugated polymers. *Sensors*, 8(1), 118-141.

Rajesh, Ahuja, T. and Kumar, D. (2009). Recent progress in the development of nano-structured conducting polymers/nanocomposites for sensor applications. *Sensors and Actuators B-Chemical*, 136(1), 275-286.

- Raykov, T. and Marcoulides, G. A. (2008). An introduction to applied multivariate analysis. CRC Press, New York.
- Reiff, C. and Kelly, D. (2010). Inflammatory bowel disease, gut bacteria and probiotic therapy. *International Journal of Medical Microbiology*, 300(1), 25-33.
- Rencher, A. C. (2002). Principal component analysis. In: *Methods of multivariate analysis*. John Wiley & Sons Inc, New York.
- Ribou, A. C., Vigo, J. and Salmon, J. M. (2004). Lifetime of fluorescent pyrene butyric acid probe in single living cells for measurement of oxygen fluctuation. *Photochemistry and Photobiology*, 80(2), 274-280.
- Ricchelli, F., Gobbo, S., Jori, G., Salet, C. and Moreno, G. (1995). Temperature-induced changes in fluorescence properties as a probe of porphyrin microenvironment in lipid membranes. 2. The partition of hematoporphyrin and protoporphyrin in mitochondria. *European Journal of Biochemistry*, 233(1), 165-170.
- Ricchelli, F., Gobbo, S., Moreno, G., Salet, C., Brancaloni, L. and Mazzini, A. (1998). Photophysical properties of porphyrin planar aggregates in liposomes. *European Journal of Biochemistry*, 253(3), 760-765.
- Rochon, P., Jourdain, M., Mangalaboyi, J., Fourrier, F., Soulie-Begu, S., Buys, B., Dehlin, G., Lesage, J. C., Chambrin, M. C. and Mordon, S. (2007). Evaluation of BCECF fluorescence ratio imaging to properly measure gastric intramucosal pH variations in vivo. *Journal of Biomedical Optics*, 12(6), 7.
- Rock, F., Barsan, N. and Weimar, U. (2008). Electronic nose: Current status and future trends. *Chemical Reviews*, 108(2), 705-725.
- Rock, F., Gurlo, A. and Weimar, U. (2005). Multisensor system for characterization of packaging emissions: prediction of total solvent amount and odor scores. *Analytical Chemistry*, 77(9), 2762-2769.
- Rodriguez-Mozaz, S., de Alda, M. J. L. and Barcelo, D. (2006). Biosensors as useful tools for environmental analysis and monitoring. *Analytical and Bioanalytical Chemistry*, 386(4), 1025-1041.
- Rogers, K. R. (1995). Biosensors for environmental applications. *Biosensors & Bioelectronics*, 10(6-7), 533-541.
- Rudnitskaya, A. and Legin, A. (2008). Sensor systems, electronic tongues and electronic noses, for the monitoring of biotechnological processes. *Journal of Industrial Microbiology & Biotechnology*, 35(5), 443-451.
- Russell, D. A., Pottier, R. H. and Valenzano, D. P. (1995). In vivo spectroscopic properties of the fluorescent pH indicator biscarboxyethyl carboxyfluorescein. *Journal of Photochemistry and Photobiology B-Biology*, 29(1), 17-22.

- Russell, R. J., Pishko, M. V., Gefrides, C. C., McShane, M. J. and Cote, G. L. (1999). A fluorescence-based glucose biosensor using concanavalin A and dextran encapsulated in a poly(ethylene glycol) hydrogel. *Analytical Chemistry*, 71(15), 3126-3132.
- Sabnis, R. W. (2008). Handbook of acid-base indicators. Taylor & Francis, San Francisco.
- Sakakibara, J. and Adrian, R. J. (1999). Whole field measurement of temperature in water using two-color laser induced fluorescence. *Experiments in Fluids*, 26(1-2), 7-15.
- Salimi, A., Noorbakhsh, A., Mamkhezri, H. and Ghavami, R. (2007). Electrocatalytic reduction of H₂O₂ and oxygen on the surface of thionin incorporated onto MWCNTs modified glassy carbon electrode: Application to glucose detection. *Electroanalysis*, 19(10), 1100-1108.
- Samarasinghe, S. (2007). Neural networks for applied sciences and engineering. Taylor & Francis, Boca Raton.
- Sanders, R., Draaijer, A., Gerritsen, H. C., Hout, P. M. and Levine, Y. K. (1995). Quantitative pH imaging in cells using confocal fluorescence lifetime imaging microscopy. *Analytical Biochemistry*, 227(2), 302-308.
- Sato, K. and Anzai, J. (2006). Fluorometric determination of sugars using fluorescein-labeled concanavalin A-glycogen conjugates. *Analytical and Bioanalytical Chemistry*, 384(6), 1297-1301.
- Schmalzlin, E., van Dongen, J. T., Klimant, I., Marmodee, B., Steup, M., Fisahn, J., Geigenberger, P. and Lohmannsroben, H. G. (2005). An optical multifrequency phase-modulation method using microbeads for measuring intracellular oxygen concentrations in plants. *Biophysical Journal*, 89(2), 1339-1345.
- Scholz, M. (2006). Approaches to analyse and interpret biological profile data. *Ph.D. thesis*, Max-Planck-Institut, Potsdam University, Potsdam.
- Schroder, C. R., Polerecky, L. and Klimant, I. (2007). Time-resolved pH/pO₂ mapping with luminescent hybrid sensors. *Analytical Chemistry*, 79(1), 60-70.
- Schroder, C. R., Weidgans, B. M. and Klimant, I. (2005). pH fluorosensors for use in marine systems. *Analyst*, 130(6), 907-916.
- Scott, S. M., James, D. and Ali, Z. (2006). Data analysis for electronic nose systems. *Microchimica Acta*, 156(3-4), 183-207.
- Seidel, M. and Niessner, R. (2008). Automated analytical microarrays: a critical review. *Analytical and Bioanalytical Chemistry*, 391(5), 1521-1544.
- Setford, S. J. and Saini, S. (2000). High-sensitivity chromatographic detector incorporating three-dimensional charge coupled device fluorimetry. *Journal of Chromatography A*, 867(1-2), 93-104.

- Sharma, A. and Quantrill, N. S. M. (1994). Measurement of glucose using fluorescence quenching. *Spectrochimica Acta Part a-Molecular and Biomolecular Spectroscopy*, 50(6), 1179-1193.
- Shearer, A. E. H., Neetoo, H. S. and Chen, H. Q. (2009). Effect of growth and recovery temperatures on pressure resistance of *Listeria monocytogenes*. *International Journal of Food Microbiology*, 136(3), 359-363.
- Shepard, J. R. E., Danin-Poleg, Y., Kashi, Y. and Walt, D. R. (2005). Array-based binary analysis for bacterial typing. *Analytical Chemistry*, 77(1), 319-326.
- Sikurova, L. and Cunderlikova, B. (1997). pH dependence of merocyanine 540 absorption and fluorescence spectra. *Spectrochimica Acta Part a-Molecular and Biomolecular Spectroscopy*, 53(2), 293-297.
- Singer, V. L. (1998). Fluorophore characteristics: making intelligent choices in application-specific dye selection. In: *Eighth International Symposium on Human Identification*, Scottsdale, AZ, Sept 17-20, 1997. Promega Corporation.
- Siripatrawan, U. (2008). Rapid differentiation between *E. coli* and *Salmonella Typhimurium* using metal oxide sensors integrated with pattern recognition. *Sensors and Actuators B-Chemical*, 133(2), 414-419.
- Sjoback, R., Nygren, J. and Kubista, M. (1995). Absorption and fluorescence properties of fluorescein. *Spectrochimica Acta Part a-Molecular and Biomolecular Spectroscopy*, 51(6), L7-L21.
- Slivka, M. A., Chu, C. C. and Zhang, Y. L. (2001). Laser confocal microscopic study of pH profiles of synthetic absorbable fibers upon in vitro hydrolytic degradation. *Journal of Materials Science-Materials in Medicine*, 12(3), 241-247.
- Song, A., Parus, S. and Kopelman, R. (1997). High-performance fiber optic pH microsensors for practical physiological measurements using a dual-emission sensitive dye. *Analytical Chemistry*, 69(5), 863-867.
- Spaepen, S., Vanderleyden, J. and Okon, Y., Plant Growth-Promoting Actions of Rhizobacteria. In *Plant Innate Immunity*, 2009; Vol. 51, pp 283-320.
- Srivastava, A. K. and Dravid, V. P. (2006). On the performance evaluation of hybrid and mono-class sensor arrays in selective detection of VOCs: A comparative study. *Sensors and Actuators B-Chemical*, 117(1), 244-252.
- Stanier, R. Y., Ingraham, J. L., Wheelis, M. L. and Painter, P. R. (1987). The methods of microbiology. In: *General Microbiology* 5th ed. Macmillan Education Ltd, London.
- Starly, B. and Choubey, A. (2008). Enabling sensor technologies for the quantitative evaluation of engineered tissue. *Annals of Biomedical Engineering*, 36(1), 30-40.

Steen, W. A. and Stork, C. L. (2008). Using multivariate analyses to compare subsets of electrodes and potentials within an electrode array for predicting sugar concentrations in mixed solutions. *Journal of Electroanalytical Chemistry*, 624(1-2), 186-196.

Tanev, S., Wilson, B. C., Tuchin, V. V. and Matthews, D. (2008). Biophotonics. *Advances in Optical Technologies*, 1-2.

Thete, A. R., Henkel, T., Gockeritz, R., Endlich, M., Kohler, J. M. and Gross, G. A. (2009). A hydrogel based fluorescent micro array used for the characterization of liquid analytes. *Analytica Chimica Acta*, 633(1), 81-89.

Thomas, J. A., Buchsbaum, R. N., Zimniak, A. and Racker, E. (1979). Intracellular pH measurements in Ehrlich ascites tumor cells utilizing spectroscopic probes generated in situ. *Biochemistry*, 18(11), 2210-2218.

Thompson, T., Fawell, F., Kunikane, S., Jackson, D., Appleyard, S., Callan, P., Bartram, J. and Kingston, P. (2008). Chemical safety of drinking-water: Assessing priorities for risk management. Geneva.

Toko, K. (1998). A taste sensor. *Measurement Science & Technology*, 9(12), 1919-1936.

Turner, R. M., Muscatello, D. J., Zheng, W., Willmore, A. and Arendts, G. (2007). An outbreak of cardiovascular syndromes requiring urgent medical treatment and its association with environmental factors: an ecological study. *Environmental Health*, 6, 13.

Twomey, K., Truemper, A. and Murphy, K. (2006). A portable sensing system for electronic tongue operations. *Sensors*, 6(11), 1679-1696.

Tzoneva, R., Seifert, B., Albrecht, W., Richau, K., Groth, T. and Lendlein, A. (2008). Hemocompatibility of poly(ether imide) membranes functionalized with carboxylic groups. *Journal of Materials Science-Materials in Medicine*, 19(10), 3203-3210.

Underhill, D. and Braun, J. (2008). Current understanding of fungal microflora in inflammatory bowel disease pathogenesis. *Inflammatory Bowel Diseases*, 14(8), 1147-1153.

Unger, I. M., Motavalli, P. P. and Muzika, R. M. (2009). Changes in soil chemical properties with flooding: a field laboratory approach. *Agriculture Ecosystems & Environment*, 131(1-2), 105-110.

Underhill, D. and Braun, J. (2008). Current understanding of fungal microflora in inflammatory bowel disease pathogenesis. *Inflammatory Bowel Diseases*, 14(8), 1147-1153.

Valeur, B. (2001). Molecular fluorescence: principles and applications Wiley-VCH, Weinheim.

- Vasylevska, G. S., Borisov, S. M., Krause, C. and Wolfbeis, O. S. (2006). Indicator-loaded permeation-selective microbeads for use in fiber optic simultaneous sensing of pH and dissolved oxygen. *Chemistry of Materials*, 18(19), 4609-4616.
- Vecer, J., Holoubek, A. and Sigler, K. (2001). Fluorescence behavior of the pH-sensitive probe carboxy SNARF-1 in suspension of liposomes. *Photochemistry and Photobiology*, 74(1), 8-13.
- Vlasov, Y. and Legin, A. Non-selective chemical sensors in analytical chemistry: from "electronic nose" to "electronic tongue". In: *International Congress on Analytical Chemistry*, Moscow, Russia, Jun 15-21, 1997.
- Vlasov, Y. G., Legin, A. V. and Rudnitskaya, A. M. (2008). Electronic tongue: Chemical sensor systems for analysis of aquatic media. *Russian Journal of General Chemistry*, 78(12), 2532-2544.
- Vojinovic, V., Cabral, J. M. S. and Fonseca, L. P. (2006). Real-time bioprocess monitoring Part I: In situ sensors. *Sensors and Actuators B-Chemical*, 114(2), 1083-1091.
- Vollmer, A. P. (2005). Development of an integrated microfluidic platform for oxygen sensing and delivery. *MSc thesis*, Department of Mechanical Engineering, Massachusetts Institute of Technology, Cambridge, MA.
- Wanekaya, A. K., Chen, W. and Mulchandani, A. (2008). Recent biosensing developments in environmental security. *Journal of Environmental Monitoring*, 10(6), 703-712.
- Wang, Y., Xu, H., Zhang, J. M. and Li, G. (2008). Electrochemical sensors for clinic analysis. *Sensors*, 8(4), 2043-2081.
- Wang, Z., Palacios, M. A. and Anzenbacher, P. (2008). Fluorescence sensor array for metal ion detection based on various coordination chemistries: General performance and potential application. *Analytical Chemistry*, 80(19), 7451-7459.
- Weidgans, B. M., Krause, C., Klimant, I. and Wolfbeis, O. S. (2004). Fluorescent pH sensors with negligible sensitivity to ionic strength. *Analyst*, 129(7), 645-650.
- WHO (2008). Primary health care - now more than ever. D. Hopkins. Geneva, Switzerland, World Health Organization.
- Wijmenga, C. (2005). Expressing the differences between Crohn disease and ulcerative colitis. *Plos Medicine*, 2(8), 719-720.
- Winqvist, F., Holmin, S., Krantz-Rulcker, C., Wide, P. and Lundstrom, I. (2000). A hybrid electronic tongue. *Analytica Chimica Acta*, 406(2), 147-157.
- Winqvist, F. (2008). Voltammetric electronic tongues - basic principles and applications. *Microchimica Acta*, 163(1-2), 3-10.

Wolfbeis, O. S. (1985). Fluorescent optical sensors in analytical chemistry. *Trac-Trends in Analytical Chemistry*, 4(7), 184-188.

Wolfbeis, O. S. (2005). Materials for fluorescence-based optical chemical sensors. *Journal of Materials Chemistry*, 15(27-28), 2657-2669.

Wolfbeis, O. S. (2008). Sensor paints. *Advanced Materials*, 20(19), 3759-3763.

Wolfbeis, O. S. (2008). Fiber-optic chemical sensors and biosensors. *Analytical Chemistry*, 80(12), 4269-4283.

Wu, M. H., Lin, J. L., Wang, J. B., Cui, Z. F. and Cui, Z. (2009). Development of high throughput optical sensor array for on-line pH monitoring in micro-scale cell culture environment. *Biomedical Microdevices*, 11(1), 265-273.

Xu, X., Liu, C., Jia, J., Liu, B., Yang, X. and Dong, S. (2008). A simple and inexpensive method for fabrication of ultramicroelectrode array and its application for the detection of dissolved oxygen. *Electroanalysis*, 20(7), 797-802.

Yamada, K., Saito, M., Matsuoka, H. and Inagaki, N. (2007). A real-time method of imaging glucose uptake in single, living mammalian cells. *Nature Protocols*, 2(3), 753-762.

Yassine, M., Salmon, J. M., Vigo, J. and Viallet, P. (1997). C-SNARF-1 as a pH fluoroprobe: discrepancies between conventional and intracellular data do not result from protein interactions. *Journal of Photochemistry and Photobiology B-Biology*, 37(1-2), 18-25.

Yuen, Y. C. and Andrew, W. W. (2009). Application of a temperature-dependent fluorescent dye (rhodamine B) to the measurement of radiofrequency radiation-induced temperature changes in biological samples. *Bioelectromagnetics*, 9999(9999), 1-8.

Zhu, Q. Z., Aller, R. C. and Fan, Y. Z. (2005). High-performance planar pH fluorosensor for two-dimensional pH measurements in marine sediment and water. *Environmental Science & Technology*, 39(22), 8906-8911.

Phenomenex (2009). Try Phenex Syringe Filters. Accessed Feb 2009 from http://www.phenomenex.com/products/brands/view2.aspx?id=11545&ekmense1=10_submenu_75_link_14.

The World Bank (2009). World Bank - country classification. Accessed Jun 2009 from <http://go.worldbank.org/K2CKM78CC0>.

Appendix A: Matlab pseudo-codes

A.1. Illustration, adding and subtracting 3D fluorescent spectra

```
% Clear variables and close figures
% Import SPC file
% Plot and colour 3D surface
    % Set properties (pixels)
    % Replace pixel numbers with wavelength values
    % Label axes
% Plot intensity image
    % Flipped intensity matrix vertically
    % Set properties (pixels)
    % Replace pixel numbers with wavelength values
    % Label axes
% Choose the next step of procedure to add, subtract or finish
    % Use 'while' loop and 'if' loops
    while (condition = ADD OR SUBSTRACT) do
        if (condition statemen = ADD)
            % Select next SPC file
            % Import SPC file
            % Add selected SPC file
            % Display summarised 3D and intensity plot
        elseif (condition statemen = SUBSTRACT)
            % Select next SPC file
            % Import SPC file
            % Substract selected SPC file
            % Display subtracted plot
        end
    if (condition statemen = FINISH)
        % Ask if import backgroaund SPC file (Yes / No)
        if (condition statemen = No)
            % No file is imported
        break
    end
```

```

        if (condition statemen = Yes)
            % Select background SPC file
            % Import background SPC file
            % Subtract selected SPC file
            % Display summarised 3D and intensity plot
        end
    end
end
end

```

pause

A.2. ANN design and simulation for four parameters

```

% Clear variables and close figures
% LOAD and SPLIT data into training and test sets
% NORMALISE training and test sets
% CHOOSE the parameter you want to simulate
% Use SWITCH LOOP for different user entries
switch user_entry (condition statement)
    case 'condition statement 1'
        % load variables for pH simulation
    case 'condition statement 2'
        % load variables for temperature simulation
    case 'condition statement 3'
        % load variables for dissolved DO simulation
    case 'condition statement 4'
        % load variables for pH simulation
    otherwise
        % diplay unknown parameter
End

if (condition statement = 1 OR condition statement = 2 OR condition statement = 3 OR
condition statement = 4)
    % DEFINE the number of training cycles (j) and neurons in hidden layer (i)
    for j = 'epoch'

```

```

for i = 'neurons'
    % CREATE the model network
    % set transfer functions and training function
    % set training parameters (number of epochs for each run, epochs between
    displays, performance goal, initial momentum)
    % TRAIN and TEST the network (simulate target parameter)
    % CALCULATE mean square error (MSE) and standard deviation (STD)
    % PLOT the network outputs and error bars
    % Perform REGRESSION analysis
    % SAVE results
    close
end
end
else
    % do not perform simulation; end program
end
% ASK to run again (Yes / Nn)
if (Yes)
    % RUN again
else
    % do not ask again; end program
end
end
end

```

Appendix B: Code of practice and content forms

B.1. Code of practice (COP)

Cranfield Health

(Updated February 2008)

CODE OF PRACTICE

Handling of Clinical / Biological Samples

This code of practice describes how to safely handle and dispose of clinical / biological samples including blood, urine and faeces and must be strictly observed. **It is your responsibility to ensure that that you do not endanger the health of your co-workers.** If you do not understand anything, ask for help / advice from the Biological Safety Officer (BSO), Mr R E Ashby.

GENERAL

1. All biological samples must be viewed and treated as being a possible source of infection and therefore a biohazard until evidence is obtained to the contrary.
2. **Before** receiving **any** biological / clinical samples, a risk assessment **must** be completed, outlining the source, tissue type and details of the proposed study.
3. Do not accept any samples known to be infected with HIV, Hepatitis B, Hepatitis C, Tuberculosis or MRSA.
4. Samples can only be accepted if they are received in clearly labelled sealed tubes / vials. If in doubt about any samples do not bring them into Cranfield Health.

HANDLING OF SAMPLES

5. Only competent trained personnel should handle biological / clinical samples. All personnel handling human specimens must be immunised against Hepatitis B (details are available from the Medical Centre).
6. Laboratory coats, disposable gloves (free from holes) and eye protection **must** be worn at all times when handling samples.

7. Clinical / biological samples must only be handled in P2 designated laboratories and the appropriate laboratory practices described in the Code of Practice for Microbiological Safety adopted (e.g no mouth pipetting, eating, drinking, or pencil chewing in the laboratory).
8. All manipulations should be carried out, as far as possible, within a contained area of the bench e.g. on a plastic tray. This will contain any spillages and minimise any inadvertent contamination of the environment. All surfaces must be thoroughly cleaned with 1% Virkon after use, allowing 15 minutes contact time, prior to finally washing with water.
9. Extreme care must be employed if hypodermic needles are required during sample handling. Any needles must be disposed of in a Sharps Bin which will be sent as Hazardous Waste when full.

AEROSOLS AND SAFETY CABINETS

10. Activities likely to cause the production of aerosols, e.g. homogenisation of samples, must be carried out within a Class 1 Biological Safety Cabinet. The safety cabinet must be cleaned with 1% Virkon (as described in Section 8) after every use.

ACCIDENTS AND SPILLAGES

11. All accidents / incidents, however minor, must be reported to the Laboratory Manager, Mr R E Ashby who will record the nature of the injury / incident and the perceived risk of infection.
12. All spillages must be disinfected / inactivated using an excess of 2% Virkon (contact time must be 15 minutes) prior to washing with excess water (see SOP 1056)

DISPOSAL

13. Treatment of liquid biological waste and dirty glassware / pipettes should be as described in SOP 1057 for the disinfection of mammalian cell culture items.
14. Solid clinical samples, tissues and any disposables must be placed in a supported autoclave bag and at the end of the day autoclaved. It is the responsibility of the operator to ensure that an adequate process is given (see appropriate SOP ?).

B.2. Ethics approval form



National Research Ethics Service

Bedfordshire Research Ethics Committee

Ambulance Training Centre
Via Location Code Q7
QE11 Hospital
Howlands
Welwyn Garden City
Hertfordshire
AL7 4HQ

Telephone: 01707 362583
Facsimile: 01707 394475

03 August 2007

Dr Claire Turner
Senior Research Fellow
Cranfield University
Silsoe
Bedford
MK45 4DT

Dear Dr Turner

Full title of study: Abnormal sulphur metabolism in the pathogenesis of gastrointestinal disease
REC reference number: 07/Q1205/39
SSA reference number: 07/H0309/48

Thank you for your application to conduct the above research as local Principal Investigator for Cranfield University. We can confirm that the application was received on 03 August 2007.

An assessment of the suitability of the local Principal Investigator, site and facilities will be made by this Committee. We will notify the main Research Ethics Committee Leeds (West) Research Ethics Committee within 25 days of receiving your application whether or not there is any objection to the research being conducted locally.

It is the responsibility of the main REC to confirm the favourable opinion for each research site, taking account of the advice from site-specific assessors. The main REC will notify the decision to the Chief Investigator for the study and provide a list of approved sites (on form SF1). It is the responsibility of the Chief Investigator to notify the local Principal Investigator at each site.

It is your responsibility to ensure you have final approval from the R&D office for the relevant NHS care organisation before commencing any research procedures.

Yours sincerely

Sue Oliver
Assistant Administrator

Email: su.oliver@nhs.net

This Research Ethics Committee is an advisory committee to East of England Strategic Health Authority
*The National Research Ethics Service (NRES) represents the NRES Directorate within
the National Patient Safety Agency and Research Ethics Committees in England*



National Research Ethics Service

Leeds (West) Research Ethics Committee

A/B Floor, Old Site
Leeds General Infirmary
Great George Street
Leeds
LS1 3EX

Telephone: 0113 392 6788
Facsimile: 0113 392 2863

14 August 2007

Professor John Hunter
Consultant Physician
Addenbrooke's Hospital
Hills Road
Cambridge
CB2 2QQ

Dear Professor Hunter

Full title of study: Abnormal sulphur metabolism in the pathogenesis of gastrointestinal disease
REC reference number: 07/Q1205/39

The REC gave a favourable ethical opinion to this study on 24 April 2007.

Further notification(s) have been received from local site assessor(s) following site-specific assessment. On behalf of the Committee, I am pleased to confirm the extension of the favourable opinion to the new site(s). I attach an updated version of the site approval form, listing all sites with a favourable ethical opinion to conduct the research.

R&D approval

The Chief Investigator or sponsor should inform the local Principal Investigator at each site of the favourable opinion by sending a copy of this letter and the attached form. The research should not commence at any NHS site until approval from the R&D office for the relevant NHS care organisation has been confirmed.

Statement of compliance

The Committee is constituted in accordance with the Governance Arrangements for Research Ethics Committees (July 2001) and complies fully with the Standard Operating Procedures for Research Ethics Committees in the UK.

07/Q1205/39

Please quote this number on all correspondence

Yours sincerely

Miss Anna Fawlk
Assistant Administrator

Email: anna.fawlk@leedsth.nhs.uk

This Research Ethics Committee is an advisory committee to Yorkshire and The Humber Strategic Health Authority
The National Research Ethics Service (NRES) represents the NRES Directorate within
the National Patient Safety Agency and Research Ethics Committees in Eng and

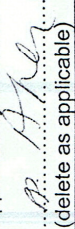
Leeds (West) Research Ethics Committee

LIST OF SITES WITH A FAVOURABLE ETHICAL OPINION

For all studies requiring site-specific assessment, this form is issued by the main REC to the Chief Investigator and sponsor with the favourable opinion letter and following subsequent notifications from site assessors. For issue 2 onwards, all sites with a favourable opinion are listed, adding the new sites approved.

REC reference number:	07/Q1205/39	Issue number:	4	Date of issue:	14 August 2007
Chief Investigator:	Professor John Hunter				
Full title of study:	Abnormal sulphur metabolism in the pathogenesis of gastrointestinal disease				
This study was given a favourable ethical opinion by Leeds (West) Research Ethics Committee on 24 April 2007. The favourable opinion is extended to each of the sites listed below. The research may commence at each NHS site when management approval from the relevant NHS care organisation has been confirmed.					
Principal Investigator	Post	Research site	Site assessor	Date of favourable opinion for this site	Notes ⁽¹⁾
Prof John Hunter	Consultant Physician	Addenbrookes Hospital	Cambridgeshire 2 Research Ethics Committee	04/07/2007	
Dr Rosemary Waring	Reader in Human Toxicology	University of Birmingham Edgbaston Birmingham B15 2TT	South Birmingham Research Ethics Committee	01/06/2007	
Dr Claire Turner	Senior Research Fellow	Cranfield University Silsoe Beds MK45 4DT	Bedfordshire Research Ethics Committee	14/08/2007	

Approved by the Chair on behalf of the REC:

 (delete as applicable) (Signature of Chair/Co-ordinator)

..... CARLA SAVINA (Name)

(1) The notes column may be used by the main REC to record the early closure or withdrawal of a site (where notified by the Chief Investigator or sponsor), the suspension of termination of the favourable opinion for an individual site, or any other relevant development. The date should be recorded.

B.3. Information and consent forms

B.3.1. Information form

ABNORMAL SULPHUR METABOLISM IN THE PATHOGENESIS OF GASTROINTESTINAL DISEASE vs 2 26/03/07

You are being invited to take part in a research study. Before you decide, it is important for you to understand why the research is being done and what it will involve. Please take time to read the following information carefully. Talk to others about the study if you wish.

- Part 1 tells you the purpose of this study and what will happen to you if you take part.
- Part 2 gives you more detailed information about the conduct of the study.

Ask us if there is anything that is not clear or if you would like more information

Part 1

What is the purpose of the study?

Although many people suffer from ulcerative colitis, Crohn's disease and irritable bowel, the causes are still unknown. Mucins are proteins which protect the gastrointestinal tract and contain sulphate. Bacteria in the gut can remove sulphate from mucin, making the gut leakier and more inflamed. The sulphate is converted to hydrogen sulphide which is poisonous. Normally, it is rapidly converted to non-toxic compounds. We think that all three of these diseases are caused by disruption of this process; mucin breakdown may be too fast, hydrogen sulphide may not be removed fast enough or mucin synthesis may be faulty. We aim to find the precise fault points in the three diseases, looking at bacterial strains, individual metabolism and genetic differences in patients and controls. We will use complex computer techniques to integrate all our data. This information will help to identify individuals 'at risk' of suffering from these diseases and may provide improved treatments.

Why have I been chosen?

1. Because the health professionals involved in your care believe that you are suffering from one of the conditions in which we are interested, that is to say, Inflammatory Bowel Disease, or another bowel disorder which produces similar symptoms.
2. We are also seeking healthy volunteers who may provide specimens for the purposes of comparison.

Do I have to take part?

Taking part in this study is entirely voluntary. If you have been approached as a healthy control, be reassured that should you wish not to take part in this study, there are many other people we can ask. If you have been approached as a patient, your future care will not be compromised if you decide not to take part.

What will happen to me if I take part? What do I have to do?

We need to ask you a few questions about your health and any medicines you may be taking. Then the nurse will arrange to collect a number of samples. You will be asked to blow into a plastic balloon to fill it up with your breath. She will also take a 20ml sample of blood and will give you a plastic bottle into which you will be asked to pass a specimen of urine. You will also be given a plastic container in which we would like to you provide a small quantity of your next bowel motion.

The breath and the urine will be analysed to see which chemicals are present which contain sulphur. The blood will be used to measure the activity of enzymes involved in sulphur metabolism and also for DNA studies to see if the genetic makeup of people with gastrointestinal diseases, is in any way different. The stools will be analysed to see if they contain bacteria which produce a toxic chemical - hydrogen sulphide.

These samples will not reveal any information about you other than that required for this research and all samples will be destroyed after the research has been completed.

What are any possible disadvantages and risks of taking part?

We do not know of any.

What are the possible benefits of taking part?

These tests are completely new, and will not be used by the doctors looking after you to help in the management of your case, because we are still investigating their potential value. You personally will receive no benefit from taking part other than of knowing you may have helped in the understanding of these diseases.

'What will happen if I don't want to carry on with the study?'

You may choose to withdraw from the study at any stage. Your data will have been identified by an individual number which will also be used to identify the samples. If you decide that you wish your data to be withdrawn from the study, you should inform one of the research team who will ensure that all information collected under your number is destroyed. None of the data will be identified by your name, which is known only to the research team at Addenbrooke's.

Will my taking part in the study be kept confidential?

Yes. All the information about your participation in this study will be kept confidential. (see above for clarification).

Contact details

You may phone Mrs Catherine Price on 01223 586739

Please feel free to ask the research team if you have any further questions.

Part 2

Who has reviewed the Study?

The study has been reviewed and approved by the Leeds (West) Research Ethical Committee.

What happens if new relevant information becomes available during the study?

The study will still be completed in case the further information generated by this study further helps our understanding of the diseases concerned

What if there is a problem?

If you have a complaint, you may address it to the director of the Gastroenterology Department, Dr Miles Parkes, Box 133, Addenbrooke's Hospital, Cambridge CB2 2QQ.

What if I come to any harm?

It is unlikely that you will come to any harm providing these samples, although sometimes taking a blood sample can leave a small bruise on the arm. However, if anything went wrong, you would be protected by the usual indemnity arrangements of the National Health Service.

Will my taking part in the study be kept confidential?

Yes, no-one other than the team collecting your samples will know that you have taken part. Your GP will not be informed, as at this early stage, the information derived from the tests will not be of any help to him and we shall not in any way change your treatment.

All data will be stored anonymously under the terms and conditions of the Data Protection Act 1998. Data will be stored in locked cupboard and kept in line with Addenbrooke's NHS Trust 'Data Retention and Destruction Policy' with a retention period of 30yrs in line with the Dept of Health Code of Practice Management

Who is organising and paying for the study?

The study is part of the continuing research program of the Department of Gastroenterology at Addenbrooke's Hospital. The analysis on the specimens which we collect will be performed in the school of Biosciences at the University of Birmingham and at the Dept of Analytical Science and Informatics at the University of Cranfield.

The costs of this study are covered by a grant from the Wellcome Trust - the largest private body funding research in the UK. No individual payments are made to any of the staff taking part.

How will the results of the study be publicised?

In peer-reviewed internationally read medical journals.

THANK YOU FOR YOUR INTEREST

B.3.3. Questionnaire

QUESTIONNAIRE Version 1 31/1/07

Project: ABNORMAL SULPHUR METABOLISM IN THE PATHOGENESIS OF
GASTROINTESTINAL DISEASE

Participant number:

Today's date:

Time of sample:

PLEASE ANSWER THE FOLLOWING QUESTIONS:

DOB:

APPROX WEIGHT:

APPROX HEIGHT

Do you/have or have you ever had?

Condition	YES	NO	If yes, what - details
Asthma			
Diabetes			
Metabolic Disorder			
Any other long term medical condition			

DO YOU FEEL WELL TODAY?

If not what is wrong (eg: cold, sore throat, headache etc)

BEFORE YOU SUPPLY THIS URINE SAMPLE HOW LONG AGO WAS IT THAT YOU:

1. Ate a standard meal (breakfast, lunch or dinner) – HOURS

What did you eat?

1. Had a drink (tea, orange juice etc) – HOURS

What did you drink?

If tea or coffee how much sugar did you have?

2. Had an alcoholic drink (beer, wine etc) – HOURS, DAYS

Not within the past month

Never

What and how much

3. Had a cigarette to smoke – HOURS , DAYS

Not within the past month

Never

4. Do you use artificial sweeteners as a matter of choice in your food or drink products?

ALWAYS

INDIFFERENT

ACTIVELY AVOID

5. When was the last time you exercised? – HOURS, DAYS

What did you do?

6. If you can remember, please record overleaf what you ate or drank over the last 24hours

9. What medication are you taking?

Appendix C: Human skin properties

Skin is one of the most important parts of the human body (Boon *et al.*, 2006; Freinkel *et al.*, 2001). Problems with the skin can affect people of all ages. Complaints include not only skin diseases, but also appearance and general skin conditions. Healthy and attractive skin is important for most people, because it is one of the main components of the image they present to the outside world. Therefore, it is desirable for it to be physically resilient (i.e. stretch and shrinkage), and highly active metabolically. Weak and unhealthy skin can be a sign of the abnormal state of the body. To prevent many of these problems it is important to diagnose the medical condition of the skin and find its possible meaning. Therefore, monitoring skin properties is important for various cosmetic and clinical applications. Utilising modern technology could be an opportunity for fast and possibly low cost monitoring of the skin, which could test the validity, safety and efficiency of pharmaceutical and cosmetic products. Because many types of human skin are presented, the real-time, painless diagnosis and therapeutic monitoring of skin of particular patients and the interaction with products should be studied. In order to obtain a better description of the process involved, the structure and optical properties of the skin must be taken into account.

C.1. The structure and functions of the skin

The human skin is a multilayered and complex organ which covers and shapes the body. The skin consists of three main layers: epidermis, dermis and hypodermis (see Figure C.1). Each of these layers has its own structural and functional importance (Boon *et al.*, 2006; Freinkel *et al.*, 2001).

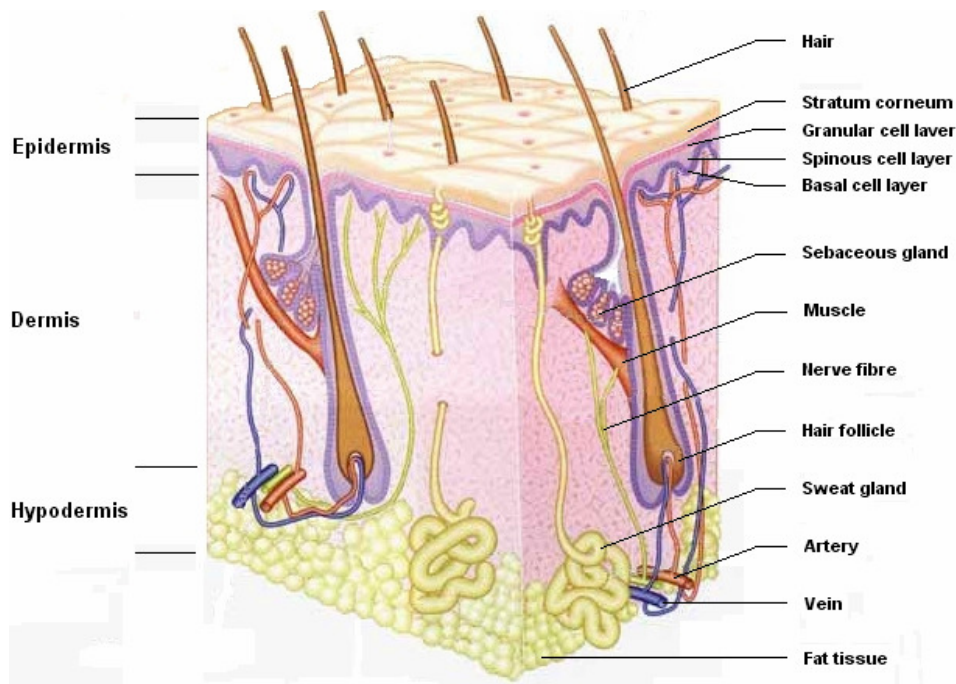


Figure C.1: Three-dimensional, schematic drawing of the skin structure; thin hairy skin of the forearm. Adopted from (Procter & Gamble, P&G, 2006).

The epidermis (thickness approximations for a selected set of body sites are given in Table D.1(Whitton *et al.*, 1973); the most exterior layer includes four other layers that are arranged from the surface as follows: corneus (stratum corneum), grainy (stratum granulosum), spiny (stratum spinosum) and basic (stratum basale), see Figure C.2. Additionally, in the thick skin, between stratum corneum and stratum granulosum, lies fifth layer; stratum lucidum. The epidermis is mainly composed of keratinocytes and melanocytes, Langerhans cells, Merkel cells, and unmyelinated axons. The epidermis does not contain blood vessels and it is nourished by diffusion from the underlying dermis. It is responsible for waterproofing, skin colour, and serves as a protective barrier to infections.

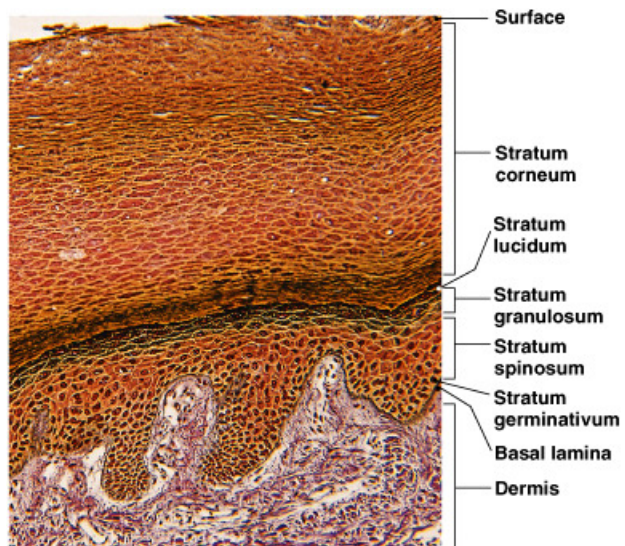


Figure C.2: Layer structure of the epidermis.

The epidermis does not contain blood vessels and it is nourished by diffusion from the underlying dermis. It is responsible for waterproofing, skin colour, and serves as a protective barrier to infections.

Table C.1: Mean values for full epidermal thickness.

Body Site	Mean Thickness (μm)
Palm	429.0
Fingertip	369.0
Back of hand	84.5
Forearm	60.9
Upper arm	43.9
Thoracic region	37.6
Abdomen	46.6
Upper back	43.4
Lower back	43.2
Thigh	54.3
Calf	74.9
Forehead	50.3
Cheek	38.8

The dermis (1-4 mm thick), so called true skin, consists of two main dermal layers: upper (stratum papillare) located under the epidermis and real dermis (stratum reticulare), see Figure C.3 (Saddik, E., 2006).

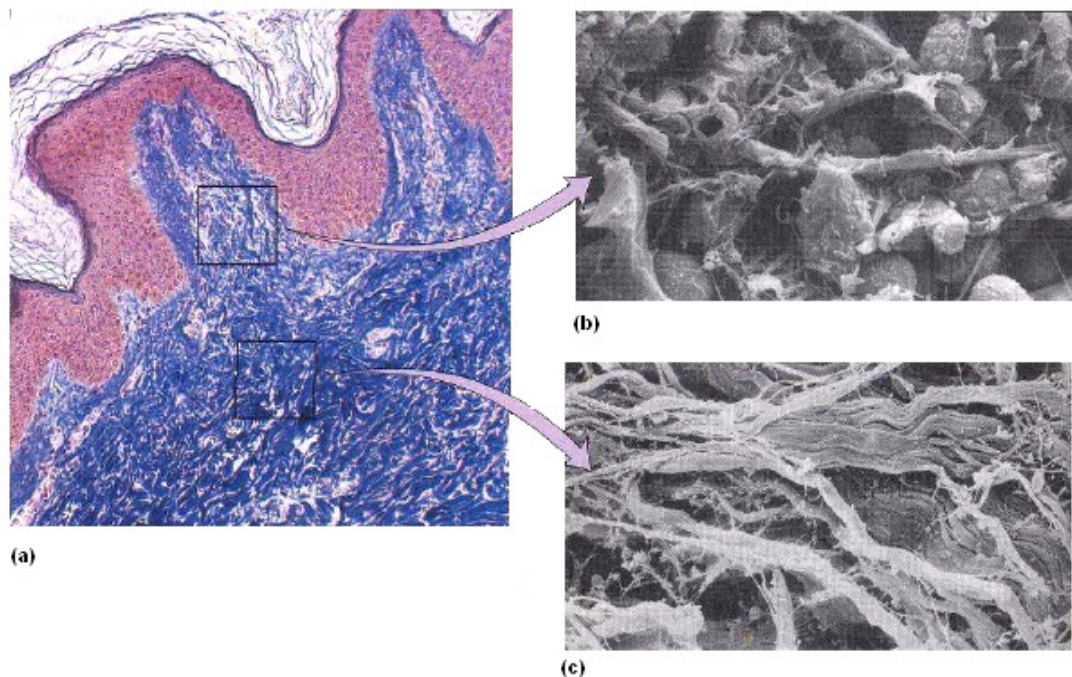


Figure C.3: Structure of the dermis: a) layers of the dermis, b) the papillary layer, made of loose tissue, forms dermal papillae, c) the reticular layer, dense irregular connective tissue.

The dermis is less cellular than the epidermis, and its main component is the network of collagen and elastin fibers, crucial to skin tensile strength and elasticity. The dermis also consists of eccrine and apocrine glands, hair follicles, veins, nerves, and components of

extra cellular matrix eg. proteins and sugars. It interacts with the epidermis to repair and remodel the skin.

The most interior layer is *the hypodermis* (1-6 mm thick) also called *superficial fascia* (Saddik, E., 2006) (Figure C.4). The blood vessels, nerves, lymph vessels, and hair follicles also cross through this layer. The hypodermis is considered as a thermal insulator and is the reserve energy supply for the body. This layer, together with the epidermis and the dermis, also protects internal organs from injury.

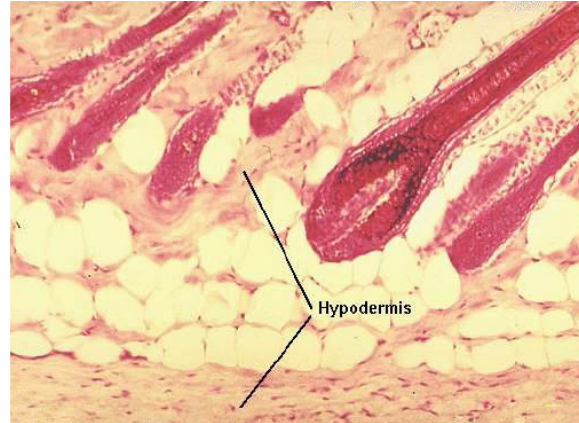


Figure C.4: Structure of the hypodermis.

C.2. Optical properties of the skin

In the skin are different types of *chromophores* - molecules or substances able to absorb light. The structure of the skin and chromophores play a major role in signal distribution across the tissue. Therefore, they strongly affect the clinical diagnostic measurements when a signal returns from the skin and is analysed.

Novel technologies for skin diagnosis are based on optical measurements. The impact on the process and the result are down to two main phenomena, which are light absorption and skin scattering (Lim, 1993). However, most of the applicable radiation does not return according to rules of regular reflectance (Anderson *et al.*, 1982). The classic optical pathway in the skin is shown in Figure C.5.

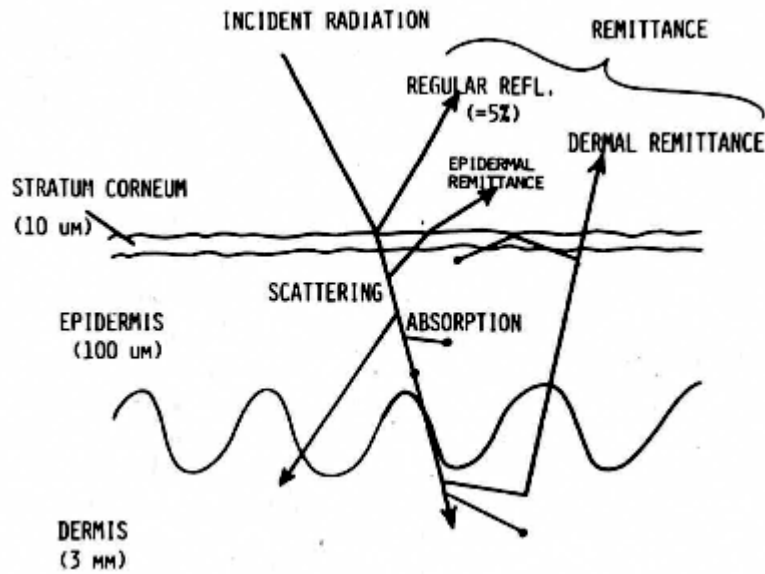


Figure C.5: Schematic drawing of optical pathway in the skin.

The regular reflectance includes only a small fraction of the incident beam. The rest of the radiation can be absorbed (taken up by other atoms or molecules), scattered (different direction of light propagation) or re-emitted as multi-scatter radiation (backwards light scatter) on any of the skin layer. Many studies of the optical properties of the human skin have been reported (Anderson *et al.*, 1982; Bigio *et al.*, 1997; Gillies *et al.*, 2000; Zeng *et al.*, 1997), but there is still a high level of research activity that can be directed towards the development of novel technologies for optical skin diagnostics (Bos *et al.*, 2004; Meglinski *et al.*, 2002).

The first task of every optical diagnostic is to account for the loss of signal because of interaction with the numerous chromophores in human skin (Young, 1997). The main skin chromophores are summarised in Table C.2.

Shorter wavelength light is absorbed mainly by aromatic amino acids (proteins), nucleic acids or urocanic acid. Melanin and hemoglobin absorb strongly in the ultraviolet (UV: 330-400 nm) and visible (VIS: 400-700 nm) range of the spectrum. During the infrared (IR: 700-1600) region the strongest absorbers are water and deoxyhemoglobin (Kollias *et al.*, 2000).

Table C.2: Main chromophores found in human skin. Adopted form (Kollias *et al.*, 2000).

The principal chromophores of skin^a

Skin chromophore	Spectral range of absorption	Fluorescence	Principal absorption maxima (nm)
Oxyhemoglobin	UV-VIS	NO	412, 542, 577
Deoxyhemoglobin	UV-VIS	NO	430, 555, 760
Melanin	UV-VIS	NO	Monotonic increase to short wavelengths
Water	IR-long VIS	NO	760, 900, 1250, 1400, etc.
Porphyryns	VIS	Yes	Ex: ~405; Em: 600
Bilirubin	VIS	NO	460
NAD/NADH	UV	Yes	Ex: ~350; Em: 460
DNA/RNA	UV	NO	260
Tryptophan	UV	Yes	Ex: 295; Em: 340-350
Urocanic acid	UV	NO	280
Collagen x-links	UV	Yes	Ex: 335, 370; Em: 380, 460
Elastin x-links	UV-VIS	Yes	Ex: 420, 460; Em: 500, 540
Keratin (dry), horn	UV	Yes	Ex: 370; Em: 460

^a NO: not observable; Ex: excitation wavelength; Em: emission wavelength.

The second important fact concerning optical skin properties and the application of non-invasive techniques is *the depth of the light penetration*. This parameter describes how deep the light can penetrate the skin (Anderson *et al.*, 1982; Churmakov *et al.*, 2003) (Table C.3). As the wavelength of the incident light becomes longer, the light reaches deeper into the skin. In human skin, the near-infrared spectral range, (NIR 600–1600 nm) has been defined as a good region for light penetration (Öberg, 2003; Richards-Kortum *et al.*, 1996). This part of the spectrum is called the ‘diagnostic window’ (or the ‘therapeutic window’), the most practical region for medical diagnosis of the skin.

Table C.3: The relationship between depth of penetration of incident light and wavelength in the case of caucasian skin.

Wavelength / nm	Depth / μm
400	90
450	150
500	230
600	550
700	750

C.3. Reference

Anderson, R. R. and Parrish, J. A. (1982). Optical properties of human skin. In: *The science of photomedicine* Plenum Press, New York.

Bigio, I. J. and Mourant, J. R. (1997). Ultraviolet and visible spectroscopies for tissue diagnostics: fluorescence spectroscopy and elastic-scattering spectroscopy. *Physics in Medicine and Biology*, 42(5), 803-814.

Boon, N. A., Colledge, N. R., Walker, B. R. and Hunter, J. A. A. (2006). Davidson's principles and practice of medicine. 20th ed. Churchill Livingstone, Edinburgh.

Briganti, S. and Picardo, M. (2003). Antioxidant activity, lipid peroxidation and skin diseases. What's new. *Journal of the European Academy of Dermatology and Venereology*, 17(6), 663-669.

Buraczewska, I. and Loden, M. (2005). Treatment of surfactant-damaged skin in humans with creams of different pH values. *Pharmacology*, 73(1), 1-7.

Churmakov, D. Y., Meglinski, I. V., Piletsky, S. A. and Greenhalgh, D. A. (2003). Analysis of skin tissues spatial fluorescence distribution by the Monte Carlo simulation. *Journal of Physics D-Applied Physics*, 36(14), 1722-1728.

Freinkel, R. K. and Woodley, D. (2001). The biology of the skin. The Parthenon Publishing Group, New York.

Gillies, R., Zonios, G., Anderson, R. R. and Kollias, N. (2000). Fluorescence excitation spectroscopy provides information about human skin in vivo. *Journal of Investigative Dermatology*, 115(4), 704-707.

Kollias, N., Zonios, G. and Stamatas, G. N. Fluorescence spectroscopy of skin. In: *Conference on Shedding New Light on Disease - Optical Diagnostics for the New Millennium*, Winnipeg, Canada, Jun 25-30, 2000. Elsevier Science Bv.

Lee, S. H., Jeong, S. K. and Ahn, S. K. (2006). An update of the defensive barrier function of skin. *Yonsei Medical Journal*, 47(3), 293-306.

Lim, H. W. (1993). Clinical photomedicine. CRC Press, New York.

Martinez-Pla, J. J., Martin-Biosca, Y., Sagrado, S., Villanueva-Camanas, R. M. and Medina-Hernandez, M. J. Evaluation of the pH effect of formulations on the skin permeability of drugs by biopartitioning micellar chromatography. In: *3rd European Workshop on Waste Water Cluster*, Almeria, SPAIN, Nov 19-21, 2003.

Meglinski, I. V. and Matcher, S. J. (2002). Quantitative assessment of skin layers absorption and skin reflectance spectra simulation in the visible and near-infrared spectral regions. *Physiological Measurement*, 23(4), 741-753.

Öberg, P. Å. (2003). Optical sensors in medical care. *Sensors Update*, 13(1), 201-232.

Richards-Kortum, R. and Sevick-Muraca, E. (1996). Quantitative optical spectroscopy for tissue diagnosis. *Annual Review of Physical Chemistry*, 47, 555-606.

Whitton, J. T. and Everall, J. D. (1973). Thickness of epidermis. *British Journal of Dermatology*, 89(5), 467-476.

Young, A. R. (1997). Chromophores in human skin. *Physics in Medicine and Biology*, 42(5), 789-802.

Zeng, H. S., MacAulay, C., McLean, D. I. and Palcic, B. (1997). Reconstruction of in vivo skin autofluorescence spectrum from microscopic properties by Monte Carlo simulation. *Journal of Photochemistry and Photobiology B-Biology*, 38(2-3), 234-240.

Ziosi, P., Besco, E., Vertuani, S., Solaroli, N. and Manfredini, S. (2006). A non-invasive method for the in vivo determination of skin antioxidant capacity (IAC-S(R)). *Skin Research and Technology*, 12(4), 303-308.

Procter & Gamble (2006). Procter & Gamble Haircare Research Centre. Accessed Oct 2006 from <http://www.pg.com/science>.

Saddik, E. (2006). The Skin. Accessed Oct 2006 from www.site.uottawa.ca/~elsaddik/abedweb/teaching/elg5124/Skin.

Appendix D: List of publications and awards

D.1. Publications

Moczko, E., Cautchi, M., Turner, C., Meglinski, I., and Piletsky, S., Optical assay for biotechnology and clinical diagnosis (submission on June 2010).

Moczko, E., Meglinski, I.V., Bessant, C., and Piletsky, S.A., Dyes assay for measuring physicochemical parameters, *Analytical Chemistry*, 2009, 81 (6), 2311–2316.

Moczko, E., Meglinski, I., and Piletsky, S., Vanishing 'tattoo' multi-sensor for biomedical diagnostics in: *Advanced Biomedical and Clinical Diagnostic Systems VI*, Edited by T. Vo-Dinh, W.S. Grundfest, D.A. Benaron, and G.E. Cohn, *Proc. SPIE*, 2008, 6848, 68480K.

Moczko, E., Meglinski, I., and Piletsky, S.A., Vanishing 'tattoo' multi-sensor for biomedical diagnostics in: *Biophotonics: Photonic Solutions for Better Health Care*, Edited by J. Popp, W. Drexler, V.V. Tuchin, D.L. Matthews, *Proc. SPIE*, 2008, 6991, 69911V.

D.2. Patent

Piletsky, S., Meglinski, I., Moczko, E., Optical monitoring method, WO2009044177, April 4 2009.

D.3. Oral presentations

Moczko, E., Meglinski, I., and Piletsky, S., Dye array for monitoring of physico-chemical parameters, *Cranfield Health Postgraduate Conference*, Cranfield, UK, 18 September, 2008.

Moczko, E., Meglinski, I., and Piletsky, S., Vanishing tattoo multisensor for biomedical diagnostics, *BIOS 2008, SPIE Photonics West*, San Jose, California, USA, January 2008.

D.4. Posters

Moczko, E., Chianella, I., Meglinski, I., and Piletsky, S., Optical Multisensor for Chemical, Biochemical and Physico-Chemical Examination, *Bioanalytical Sensors Graduate Research Seminar*, Smithfield, RI, USA, June 28-29, 2008.

Moczko, E., Meglinski, I., and Piletsky, S., Vanishing ‘tattoo’ multi-sensor for biomedical diagnostics, *Photonics Europe 2008, SPIE*, Strasbourg, France, 7-11 April, 2008.

Moczko, E., Meglinski, I., Piletsky, S., and Barr, H., Vanishing “tattoo” Sensors for express clinical diagnostics, *Cranfield Health Partnership Conference*, Cranfield, UK, March, 2007.

Moczko, E., Meglinski, I., and Piletsky, S., Vanishing tattoo for a non-invasive biomedical diagnosis, *7th Silsoe Postgraduate Conference*, Cranfield University, Silsoe, UK, June 2006.

D.5. Awards

Scientific scholarship – Vice-Chancellor initiative, Cranfield University, UK (2005 - 2008).

Third prize at the Cranfield Health Postgraduate Conference, Cranfield University, UK (2008).

First prize at the Cranfield Health Partnership Conference, Cranfield University, UK (2007).